

Enhancement of Mixing in a Rectangular Jet by Mechanical Tabs

W.H. Brown and K.K. Ahuja
*Georgia Tech Research Institute
Georgia Institute of Technology
Atlanta, Georgia*

April 1990

Prepared for
Lewis Research Center
Under Grant NAG3-1062



National Aeronautics and
Space Administration

Date for general release March 1994

(NASA-CR-185207) ENHANCEMENT OF
MIXING IN A RECTANGULAR JET BY
MECHANICAL TABS (Georgia Inst. of
Tech.) 86 p

N94-32872

Unclass

FOREWORD

This report was prepared by the Georgia Tech Research Institute (GTRI), a Unit of Georgia Institute of Technology, Atlanta, Georgia, for NASA Lewis Research Center, Cleveland, Ohio, under grant NAG3-1062, entitled "Jet Mixing Enhancement by Mechanical Tabs."

The NASA Project Manager was Mr. M. Vanco. Dr. K. K. Ahuja was the GTRI Program Manager, and the principal investigator of this program was Mr. W. H. Brown. The authors are grateful to Mr. John Manes, a Georgia Tech co-op, for his assistance in the acquisition of data for this program.

TABLE OF CONTENTS

<u>Section</u>		<u>Page</u>
	SUMMARY.....	v
1	INTRODUCTION.....	1
2	TEST FACILITIES AND EXPERIMENTAL PROCEDURES.....	3
2.1	Heated Air Supply.....	3
2.2	Rectangular Nozzle and Tabs.....	3
2.3	Nomenclature, Coordinate System, and Traverse Paths.....	9
2.3.1	Nomenclature.....	9
2.3.2	Coordinate System and Traverse Paths.....	9
2.4	Test Conditions.....	12
2.4.1	Baseline.....	12
2.4.2	Mixing Modification.....	12
2.5	Test Procedures.....	12
2.6	Probe.....	14
3	MIXING MODIFICATION IN RECTANGULAR JETS BY MECHANICAL TABS.....	17
3.1	Introduction.....	17
3.2	Results.....	17
3.2.1	Nomenclature for Figures.....	17
3.2.2	Flow Development for Selected Configurations...	18
3.2.3	Effect of Tab Size "D".....	18
3.2.4	Effect of the Six Tab Configuration.....	18
3.2.5	Effect of the Full Nozzle Height Tab.....	40
3.2.6	Complete Data.....	40
4	CONCLUDING REMARKS.....	42
	REFERENCES.....	43
APPENDIX A	LIST OF SYMBOLS.....	44
APPENDIX B	DATA PLOTS.....	45

SUMMARY

This effort was conducted to obtain additional test data/configurations required to better understand the effects of tab length and width on jet mixing enhancement for a rectangular nozzle. The configurations tested were: a 6-tab configuration defined by NASA, a full height tab configuration, and 2-tab configurations with selected tab lengths and widths. Additional test data were also required for all candidate configurations to better interpret the data.

This report presents test data from this effort. On the basis of these data, the following general observations were noted:

1. The 6-tab rectangular nozzle configuration provided a lower peak velocity than either the 2-tab or 4-tab configuration.
2. The rectangular nozzle with a full height tab had about the same peak velocity as the 2-tab configuration; however, the full height tab configuration had a somewhat lower centerline velocity.

SECTION 1

INTRODUCTION

In studies by Ahuja and Brown (Reference 1) and Bradbury and Khadem (Reference 2), mechanical tabs placed at the lip of a round nozzle with cold or heated flow enhanced the jet mixing considerably. The jet flow velocity is reduced significantly, and for heated jets, the temperature of the jet is also reduced noticeably. Based on the results from Reference 1, two tabs appear to provide the best overall result.

In a subsequent study by Brown and Ahuja, the effects of tabs on mixing enhancement were obtained for a rectangular nozzle with an aspect ratio of four (Reference 3). A total of eight tab configurations were studied. The results of this effort showed that tab size and tab arrangement are significant factors in the determination of mixing enhancement. The general results are summarized below.

1. With the exception of one configuration with tabs parallel to the major axis of the rectangular jet, all configurations produced velocity profiles that showed that the centerline velocity of the jet is indeed reduced by the mechanical tabs.
2. In general, configurations with tabs aligned along the minor axis appear to be better performers than those with tabs aligned along the major axis of the rectangular jet. Tabs along the minor axis provided velocity profiles that were depressed around the centerline. Tabs aligned along the major axis produced a bulge in the middle of the velocity profile. This observation led to a configuration that was an attempt to improve the performance of the horizontal (major axis) tab configuration by using the vertical (minor axis) centerline tabs to counter the tendency of the profile to bulge in the middle. The resultant mixing with tabs aligned along the major axis was no better than that of the baseline nozzle.
3. Data from many of the configurations indicated that the tabs pinch the jet in one direction and cause it to expand in another.

Analysis of the Reference 3 test data indicated that additional test data/configurations were required to understand the effects of tab length and width on jet mixing enhancement. A configuration with tab length and width of two candidate configurations was selected. Also, a configuration of six tabs was defined by NASA to exploit the jet profile spreading of the four-tab configuration while retaining the centerline depression of two tabs on the minor axis of the jet. Additional test data at $X/D_e = 4$ were required for all candidate configurations to better interpret the

data.

This report presents the test data from this additional effort. The data are a supplement to Reference 3.

The test facilities and the experimental procedures used for the present study were identical to those used in Reference 3, but for the sake of completion, a short description is presented in the next section. Data derived from this study are described in Section 3.

Two appendices are included with this report. Appendix A provides a list of symbols. Appendix B contains the data plots obtained in the present study.

SECTION 2

TEST FACILITIES AND EXPERIMENTAL PROCEDURES

The experiments described here were carried out in GTRI's Jet Flow Facility where the majority of the aerodynamic data of the previously published studies on jet mixing enhancement by acoustic excitation was obtained. A detailed description of this facility can be found in References 3, 4, 5, 6, and 7. A general cross-sectional view of the plenum section is shown in Figure 2.1. The acoustic excitation source shown in the figure was present but was not used in this program.

2.1 HEATED AIR SUPPLY

In essence, the flow in this facility is heated by a through-flow propane burner up to 1,000 K and pressure ratios exceeding 4. The flow from the burner enters through a 10-inch (25.4 cm) diameter plenum that is followed by a contraction to a 4-inch (10.16 cm) diameter acoustic source section. The test nozzles are mounted on the end of the 4-inch (10.16) diameter section. For the 2-inch (5.08 cm) equivalent diameter nozzles used for most of the work reported herein, the plenum-to-nozzle area ratio was 25. The air was not heated for the tests reported here, even though the unheated air passed through the burners.

2.2 RECTANGULAR NOZZLE AND TABS

A rectangular nozzle having an aspect ratio (AR) of 4 was used in this study. This nozzle mounts directly on the end of the 4-inch (10.16 cm) diameter duct section. The nozzle translates, over 7 inches (17.78 cm) of length, from this 4-inch diameter circular cross-section to a 3.54 inch (8.99 cm) by 0.866 inch (2.2 cm) rectangular section having the equivalent area of a 2-inch (5.08 cm) diameter circular nozzle as shown in Figure 2.2. The area equivalency of the rectangular nozzle and the circular nozzle permits easy comparison of their flow characteristics.

Basically, four sides of a circular section were machined off at the proper angles and replaced by 1/4-inch thick plates that were trimmed to fit. The nozzle was completed by machining a sharp lip on the exit.

The designs of the tabs are shown in Figure 2.3.

Various tab configurations that were tested in this program are shown in Figure 2.4, and the exact tab sizes for each configuration are shown in Figure 2.5.

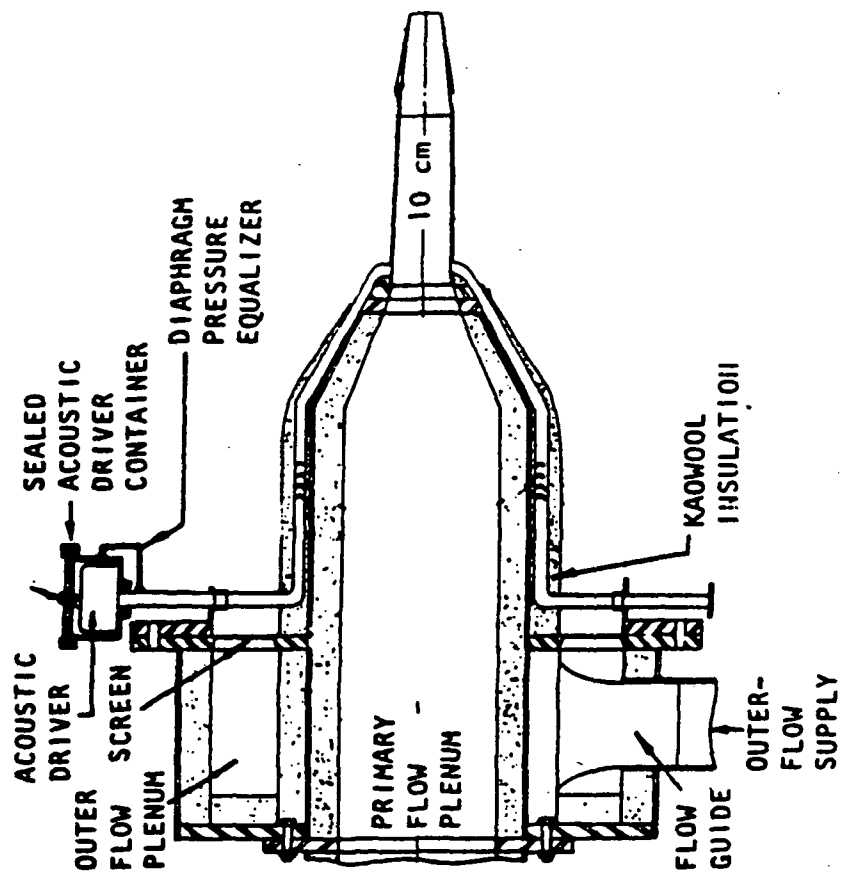


Figure 2.1 Jet Flow Plenum Assembly

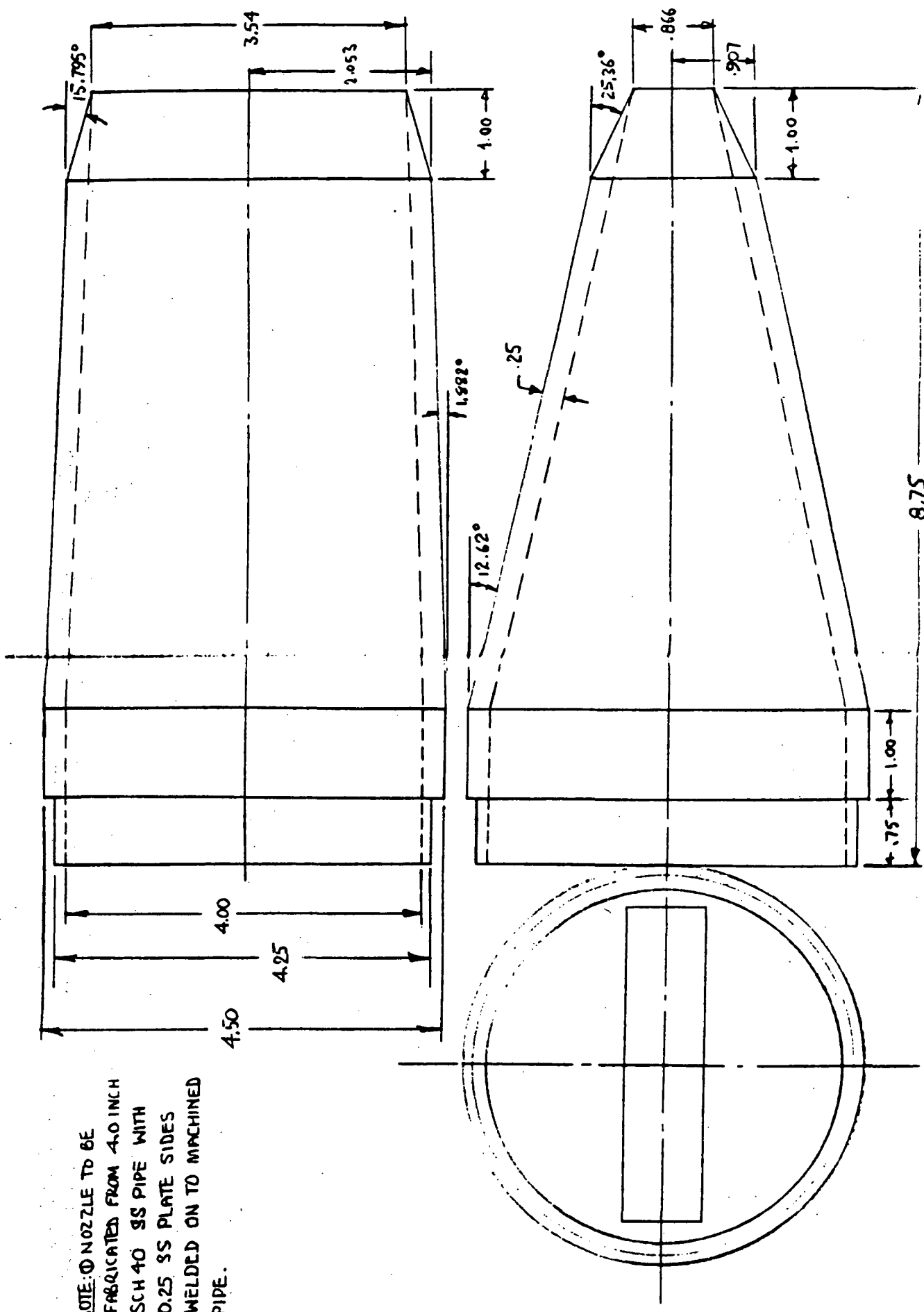


Figure 2.2 Rectangular Nozzle Design

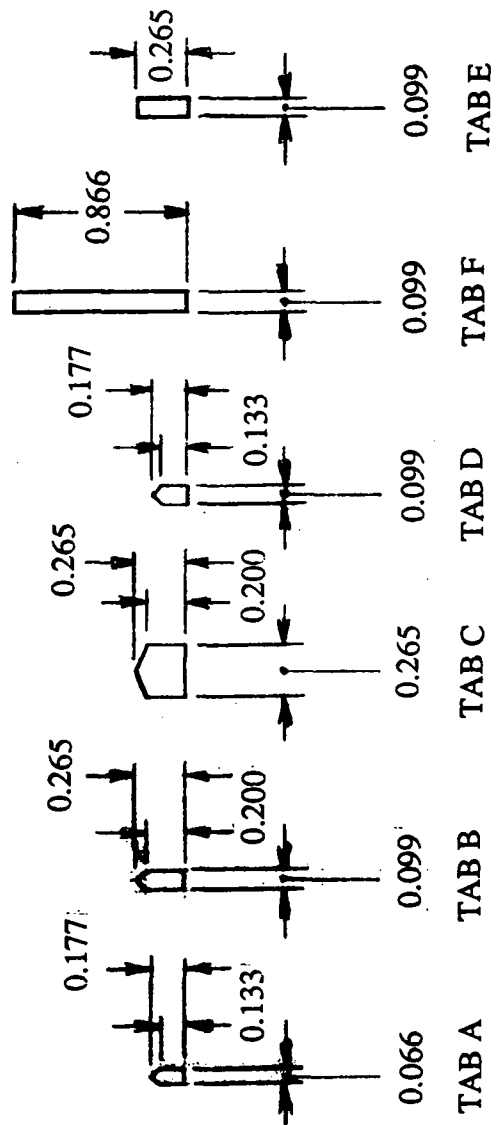
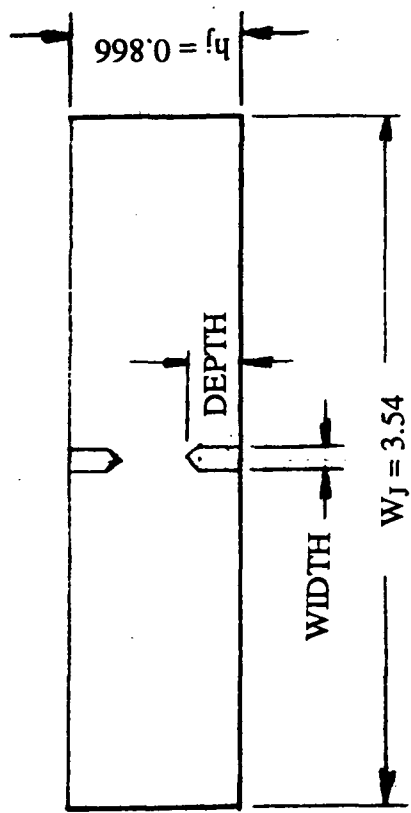
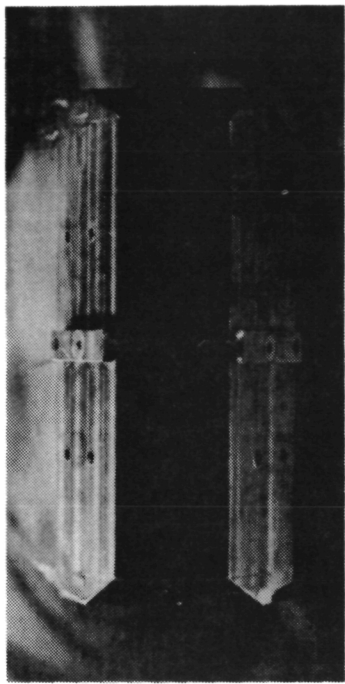
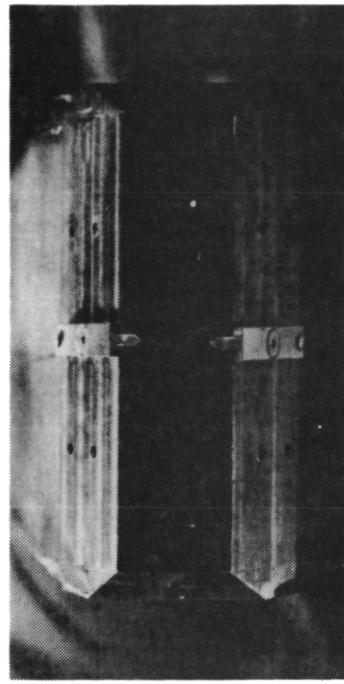


Figure 2.3. Details of tabs (all dimensions in inches).

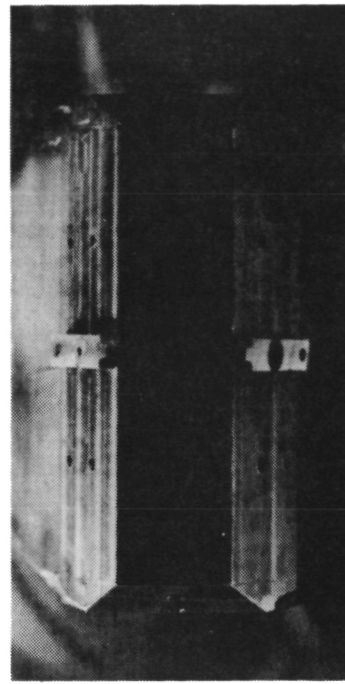
ORIGINAL PAGE
BLACK AND WHITE PHOTOGRAPH



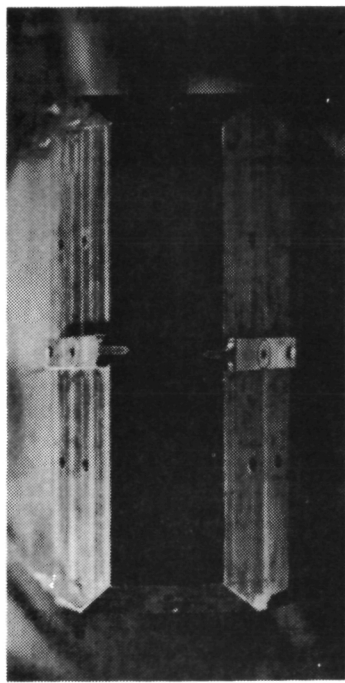
I-A



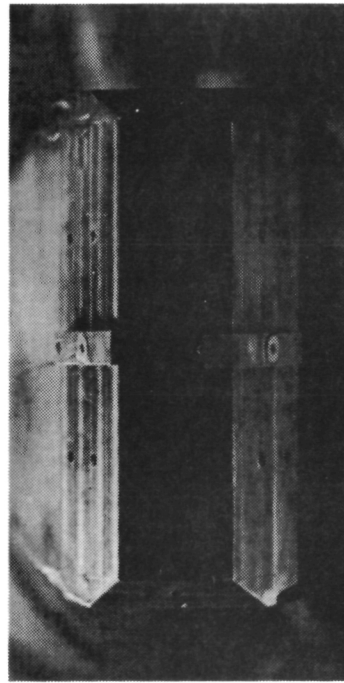
I-B



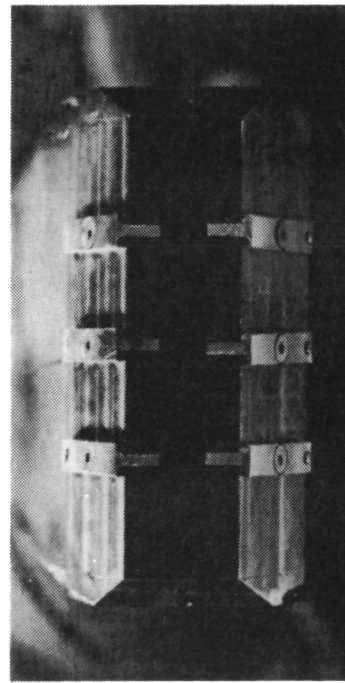
I-C



I-D



I-E



I-F

Figure 2.4. Tab configurations.

CONFIGURATION	TAB DIMENSIONS	
	WIDTH	DEPTH
I-A	0.066	0.177
I-B	0.099	0.265
I-C	0.265	0.265
I-D	0.099	0.177
E	0.099	0.265
F	0.099	0.866

Figure 2.5. Tab dimensions used in various configurations.

It should be noted that the sizes of tabs designated -A were scaled versions of those used in Reference 1 where a 2-inch (5.08 cm) diameter circular nozzle was used.

The tabs for the rectangular nozzle I-A configuration were scaled using the same ratios of tab dimension to nozzle dimension as those for the circular nozzle, but nozzle height was used in place of nozzle diameter for tabs.

The -B tabs are 1.5 times the -A sizes. Configuration I-C has tabs that have both length and width equal to the length of the I-B tabs.

Configuration I-D has two tabs on the minor axis of the nozzle. The tabs have the same width as the I-B tabs and the same length as the I-A tabs.

Configuration E has six tabs, one pair on the minor axis and two more pairs parallel to the minor axis so as to divide the nozzle exit into four equal areas. See Figure 2.4.

Configuration F has a single tab of the same width as the I-B tab, and it completely spans the nozzle along the minor axis as shown in Figure 2.4.

2.3 NOMENCLATURE, COORDINATE SYSTEM, AND TRAVERSE PATHS

This section presents nomenclature, the coordinate system, and the traverse paths used in Figures 2.6 and 2.7, respectively.

2.3.1 NOMENCLATURE

The terminology and symbols used in this report are given in Appendix A, List of Symbols.

2.3.2 COORDINATE SYSTEM AND TRAVERSE PATHS

The orthogonal coordinate system has its origin at the center of the nozzle exit plane. The X-coordinate is positive in the downstream direction, the Y-coordinate is positive to the left of the jet axis looking downstream, and the Z-coordinate is positive upwards as shown in Figure 2.6.

Horizontal traverses were made through the axis of the jet and parallel to the major axis of the rectangular nozzle as shown in Figure 2.7.

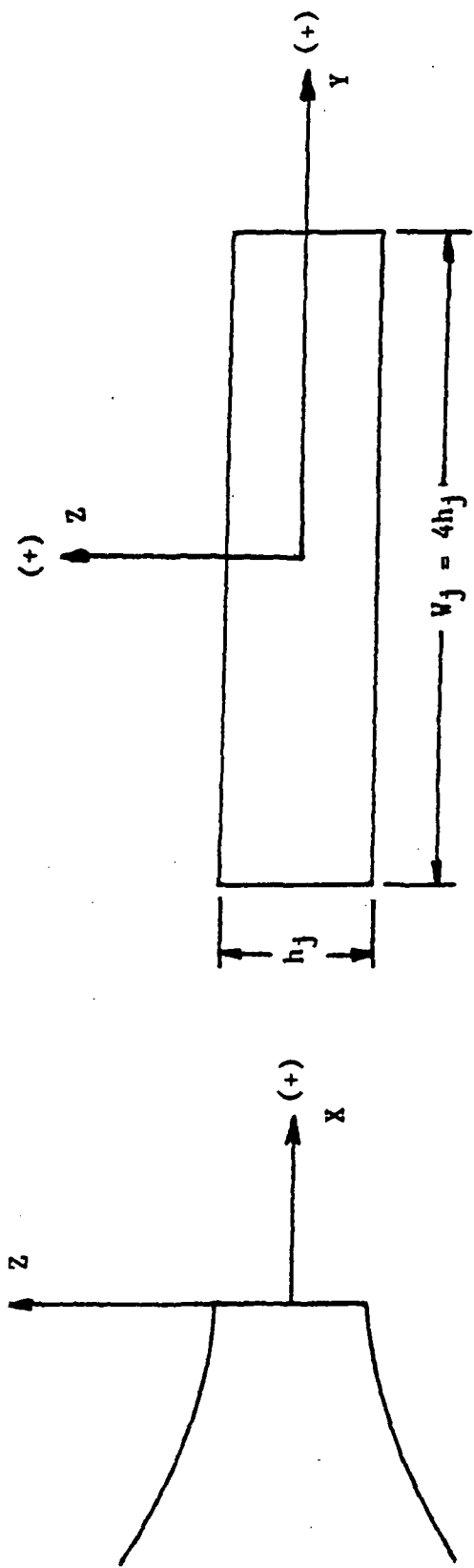


Figure 2.6. Coordinate system.

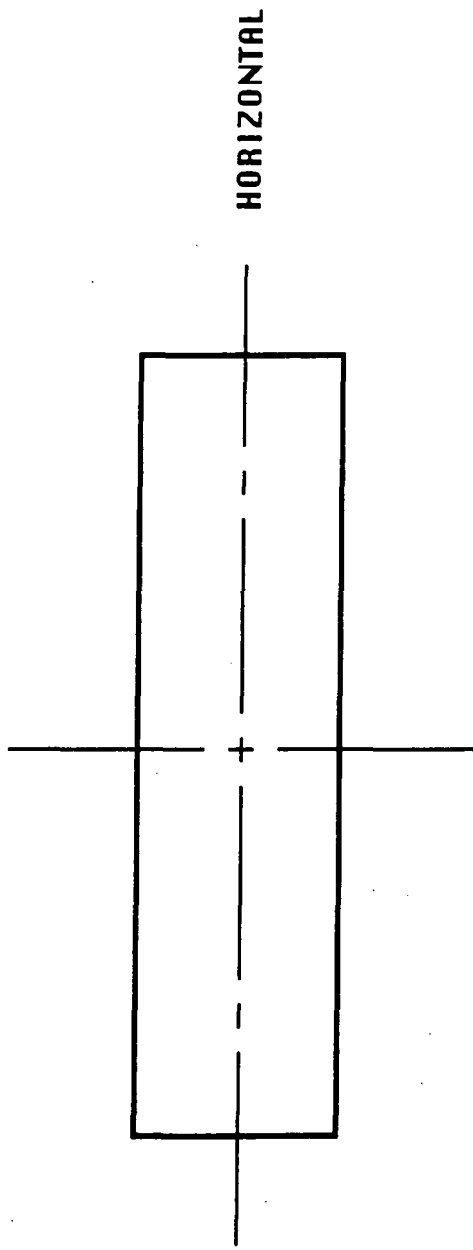


Figure 2.7. Traverse path.

2.4 TEST CONDITIONS

All tests were conducted with an unheated jet of Mach number (M_j) of 0.8 at various axial positions in terms of equivalent jet diameters (D_e) of $X/D_e = 1, 2, 3, 4, 5, 7, 9$, or 11 . Mach numbers for purposes of setting test conditions were calculated from the plenum-to-ambient pressure ratio and assume a fully expanded jet with $\gamma = 1.4$.

2.4.1 BASELINE

A new set of measurements was made with the baseline nozzle to establish a set of velocity profiles to which similar profiles for the various tab configurations could be compared and to provide evidence of the reproducibility of results from the previous program. The nominal conditions and corresponding run numbers are given in Figure 2.8 along with the mixing modification run numbers.

2.4.2 MIXING MODIFICATION

The majority of the runs that were made to evaluate the mixing modification produced by various tab configurations were made by operating the unheated jet at conditions corresponding to fully expanded jet exit Mach number of 0.8 and measuring the horizontal Mach number profiles at the desired X/D_e locations. Conditions and run numbers for these tests are given in Figure 2.8.

2.5 TEST PROCEDURES

The data acquisition process was automated so that the probability of human error was reduced as much as possible. Only the setting of plenum pressure was directly controlled by the operator; probe movement and transducer readings were under computer control by means of previously established command files.

The sequence of actions that constituted a run were as follows:

1. Find the center of the flow for the baseline configuration at the X/D_e location of the desired profile.
2. Verify that the command file will execute the desired traverse of the probe.
3. Execute the command file to begin the test run.
4. Take a transducer zero reading before the test.
5. Set the plenum conditions for the test.
6. Initiate the traverse and data acquisition.

X/DE	Tj/To	Mj	TAB	DATA SET
1	1	0.8	0	TAB610F
	1	0.8	C	TAB611F
2	1	0.8	0	TAB620F
	1	0.8	A	TAB621F
	1	0.8	C	TAB622F
	1	0.8	D	TAB623F
	1	0.8	E	TAB624F
3	1	0.8	0	TAB630F
	1	0.8	A	TAB631F
	1	0.8	B	TAB632F
	1	0.8	C	TAB633F
	1	0.8	D	TAB634F
	1	0.8	E	TAB635F
4	1	0.8	0	TAB640F
	1	0.8	A	TAB641F
	1	0.8	B	TAB642F
	1	0.8	C	TAB643F
	1	0.8	D	TAB644F
5	1	0.8	0	TAB650F
	1	0.8	A	TAB651F
	1	0.8	C	TAB652F
	1	0.8	D	TAB653F
	1	0.8	E	TAB654F
7	1	0.8	0	TAB670F
	1	0.8	D	TAB671F
	1	0.8	E	TAB672F
	1	0.8	A	TAB673F
9	1	0.8	0	TAB690F
	1	0.8	D	TAB691F
	1	0.8	E	TAB692F
	1	0.8	F	TAB693F
11	1	0.8	0	TAB600F
	1	0.8	A	TAB601F
	1	0.8	D	TAB602F
	1	0.8	E	TAB603F

Figure 2.8. Baseline and mixing modification for unheated subsonic jets.

7. Measure pressures and temperatures.
8. Take a transducer zero reading after the test.
9. Identify the data set (file name and comments).
10. Reduce the data.

The location of the center of the jet is found by making short horizontal and vertical traverses in the vicinity of the jet center and adjusting the traverse zeroes to the profile peaks. The peaks are located by folding the left side of the profile over the right side and shifting the axis left or right to obtain the best match of the folded and unfolded profiles. For profiles that are not symmetrical, the region close to the peak was favored. Figure 2.9 shows a typical plot used to locate the center of the jet. In this example, the Z-axis had to be offset 3 mm downward ($\Delta Z = -3$) to achieve symmetry. This new position became the new Z-zero for the runs that followed at that X/De position. In this program, the axes were aligned on the center of the flow from the baseline configuration before any data runs were made. The axes were not offset to recenter a flow that might have been deflected by the tabs.

2.6 PROBE

The probe used in this study was a Kiel probe with a miniature 1/16 inch diameter sensing head on a 1/8-inch diameter stem (United Sensor model USD-C-6) to which a miniature thermocouple with a 0.020-inch OD sheath (Omega SCASS-020E-6) was added for temperature measurements. This probe is shown in Figure 2-10.

The Kiel probe was selected because it is insensitive to flow direction changes over a wide range of pitch and yaw. This is advantageous in highly turbulent flows such as those in the near wake of the tabs and in the shear layer of the jet.

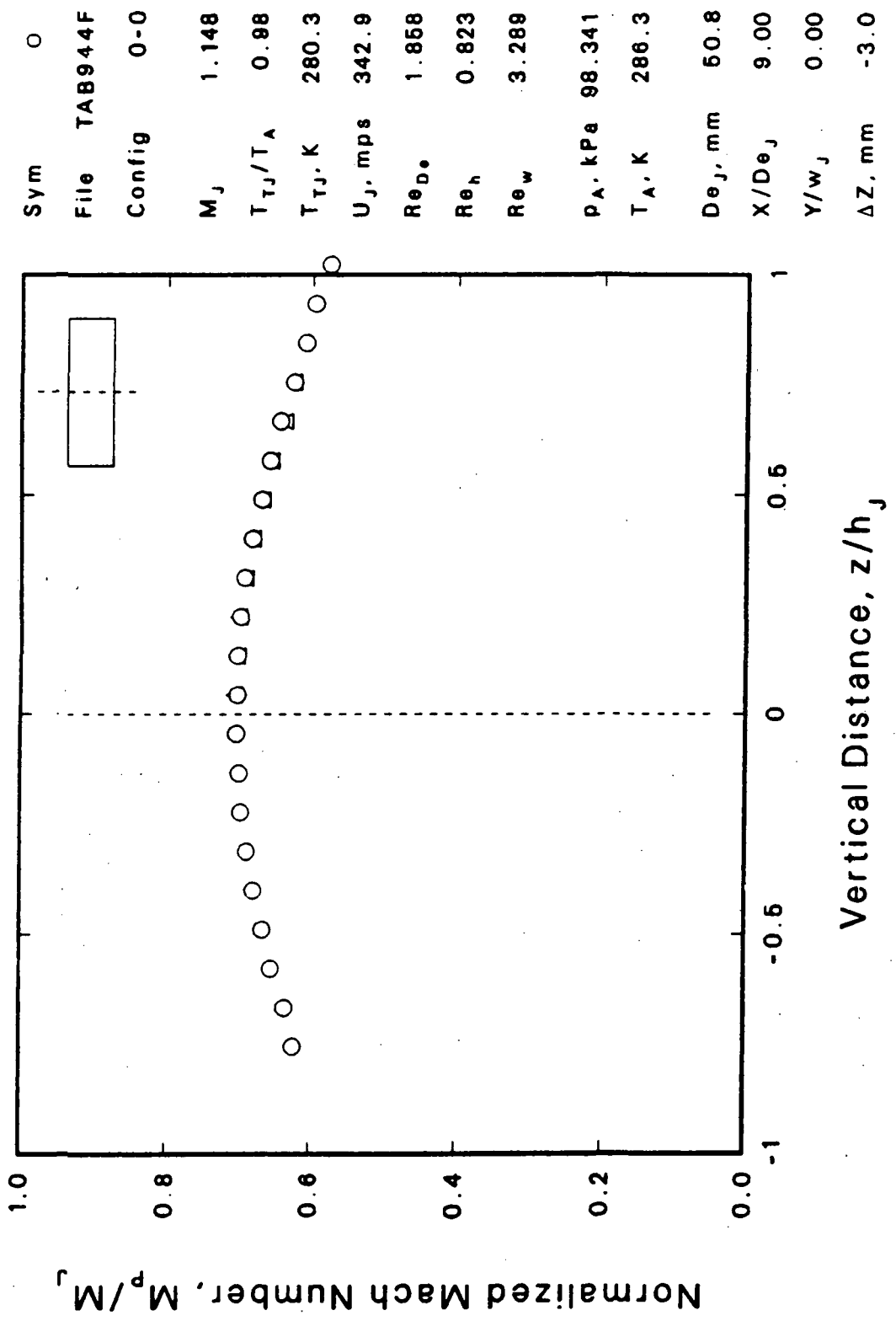
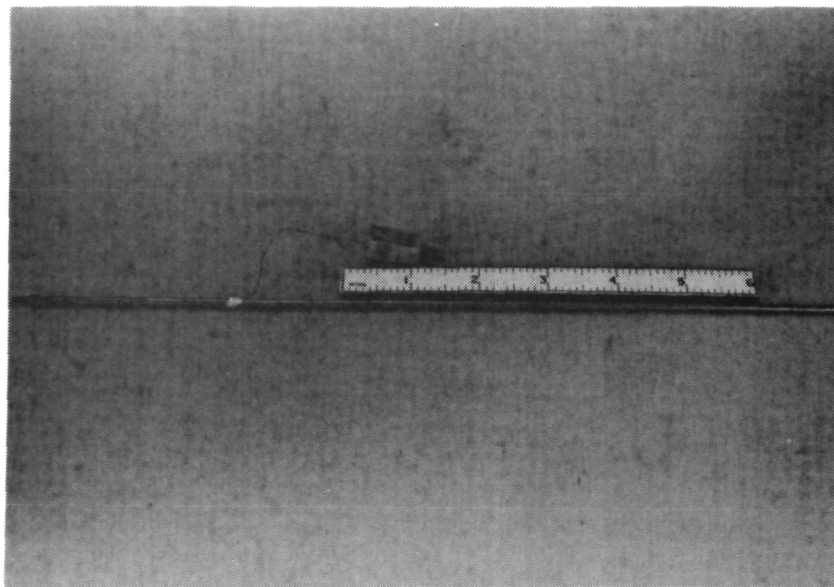


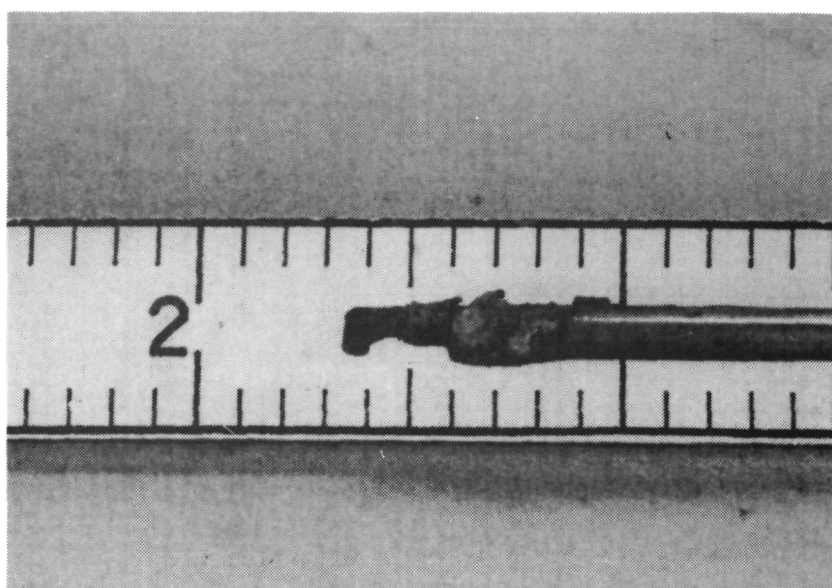
Figure 2.9. Sample plot showing method of locating flow centerline.

ORIGINAL PAGE
BLACK AND WHITE PHOTOGRAPH



OVERALL

ORIGINAL PAGE IS
OF POOR QUALITY



HEAD

Figure 2.10. Kiel probe with thermocouple.

SECTION 3

MIXING MODIFICATION IN RECTANGULAR JETS BY MECHANICAL TABS

3.1 INTRODUCTION

Effects of mechanical tabs on the flow development of a rectangular jet are presented in this section. Three new tab configurations were tested.

All data with and without the tabs for the various configurations are presented in plotted form in Appendix B. The data from those configurations that provided noticeably beneficial effect of the mechanical tabs are presented herein.

3.2 RESULTS

The evaluation of mixing modification in rectangular jets by mechanical tabs was accomplished by comparing the Mach number profiles generated by various tab arrangements to those generated by the nozzle alone. Data from this program along with selected data from Reference 3 were used for these evaluations. The results of this process are described in subsections 3.2.2 through 3.2.5.

3.2.1 NOMENCLATURE FOR FIGURES

The basic nomenclature used in the figures is defined in Appendix A. This subsection presents additional comments to further clarify the definition and use of some of the parameter ratios that appear on the right hand side of the figures.

M_j is the fully expanded jet Mach number based on the plenum total pressure and ambient pressure.

T_{TJ} and T_A are plenum total temperature and ambient temperature, respectively.

U_j is the velocity corresponding to M_j .

The Reynolds numbers are derived from conditions in the fully expanded jet and are based on equivalent jet diameter (D_{eJ}), nozzle height or minor axis length (h), and nozzle width or major axis length (w) as indicated by the subscript. D_{eJ} for the nozzle tested here was 2 inches.

P_A is the ambient pressure.

X/D_{eJ} is the X location of the measurement plane in terms of jet equivalent diameters. X is positive measured downstream from the nozzle exit.

Z/h_J is the vertical offset of a horizontal or diagonal profile. If Z/h_J is zero, the traverse was made through the center of the baseline jet. If it is non-zero, the jet was not centered and the traverse was made at the indicated height in order to pass through the center of the baseline jet on the Z axis. Z is positive above the center of the nozzle exit.

Y/w_J is the horizontal offset of a vertical profile. Y is positive to the right of the nozzle center as viewed from downstream. If Y/w_J is nonzero, the jet was not centered and the traverse was made at the indicated value in order to pass through the center of the baseline jet on the Y axis.

ΔY is the horizontal offset required to center the peak of a horizontal or diagonal profile; ΔZ is the vertical offset required to center a vertical profile. These offsets, used in Reference 3 only to center the plots, were not employed in this program. The plots are centered to facilitate the comparison of peak levels and profile shapes.

3.2.2 FLOW DEVELOPMENT FOR SELECTED CONFIGURATIONS

Axial development of the horizontal mach number profile is shown for configurations I-A, I-C, I-D, and E in Figures 3.1 through 3.9.

3.2.3 EFFECT OF TAB SIZE "D"

In Figures 3.10 through 3.15, the mixing performance of the "D" tab is seen to fall between that of the tab "A" that has the same depth of penetration and tab "B" that has the same width.

3.2.4 EFFECT OF THE SIX TAB CONFIGURATION

Configuration "E" has six tabs identical in size to those of I-B but with blunt ends. As shown in Figures 3.16 through 3.20, this configuration reduces peak velocity levels relative to I-B as early as $X/D_e = 3$. However, centerline velocity levels remain higher than those of I-B at all X/D_e .

The comparison at $X/D_e = 9$ of configuration "E" with I-B and VII-B, which is the corresponding four tab configuration, is shown in Figure 3.21. The six tab configuration has a lower peak velocity level than either the two tab or the four tab configuration and is slightly broader.

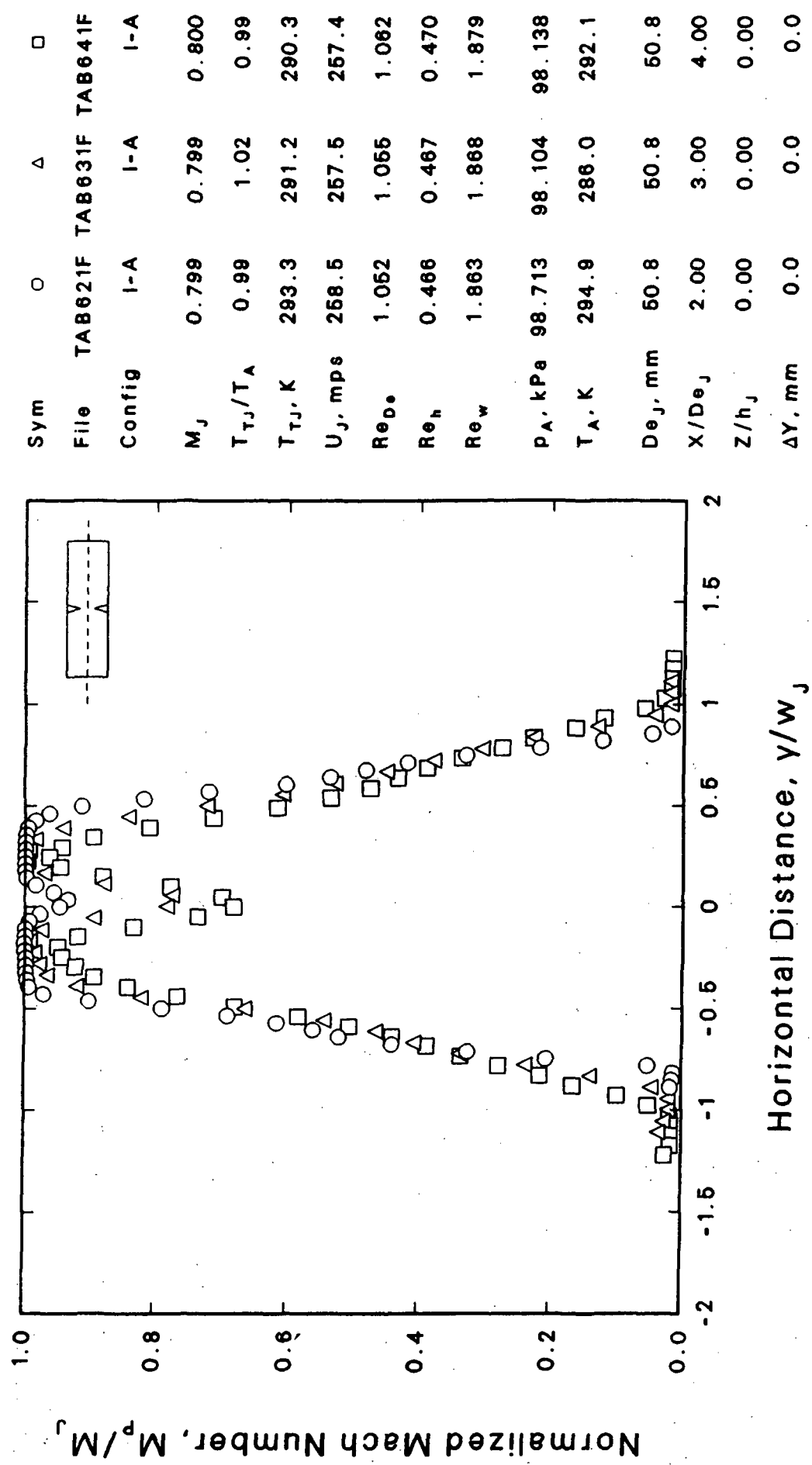


Figure 3.1 Effect of Axial Distance on Mach Number Profile
Tab A, $M_j = 0.8$, $T_j/T_0 = 1$, $X/De = 2, 3$, and 4

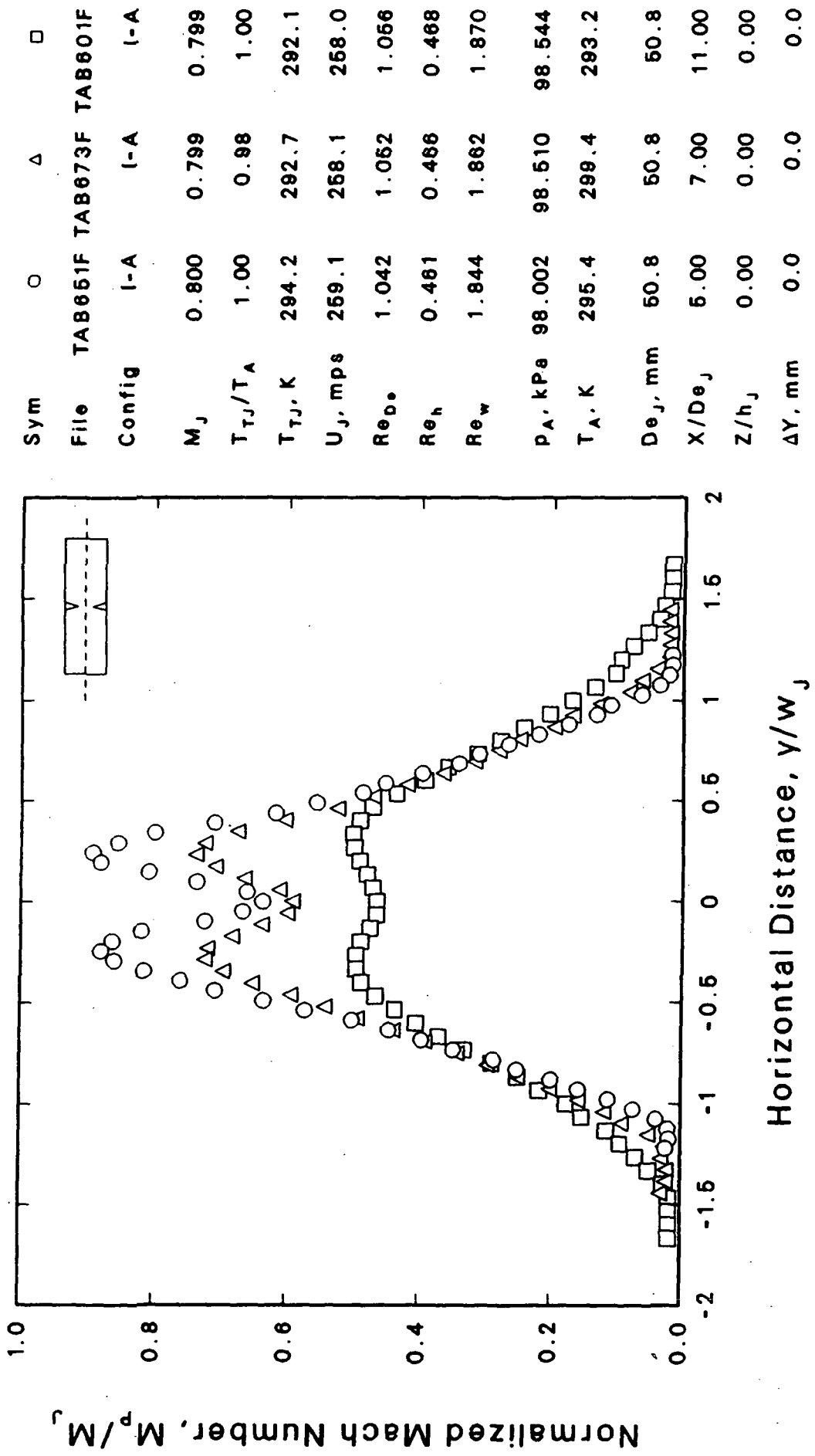


Figure 3.2 Effect of Axial Distance on Mach Number Profile
Tab A, $M_J = 0.8$, $T_J/T_0 = 1$, $X/D_{eJ} = 5, 7, \& 11$

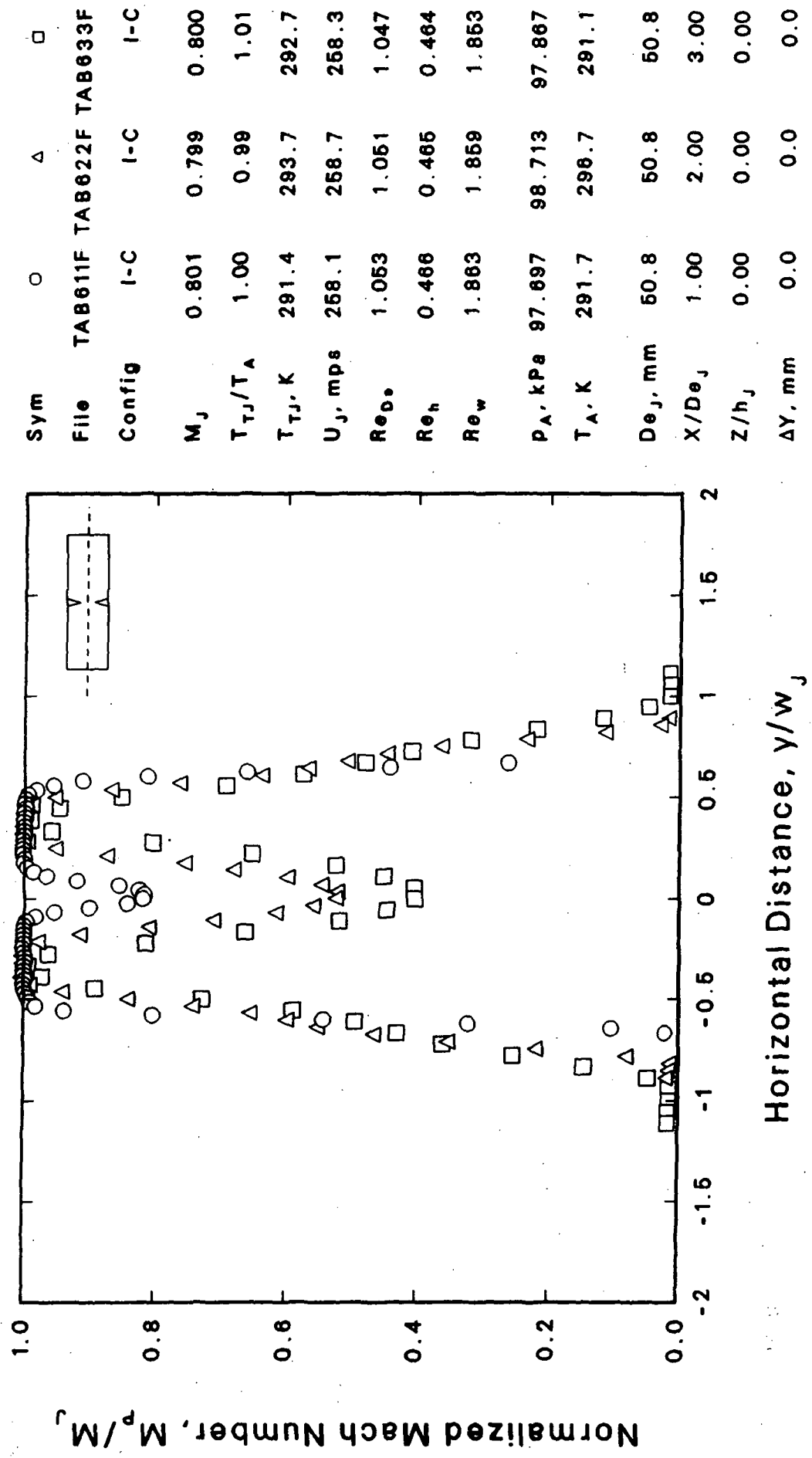


Figure 3.3 Effect of Axial Distance on Mach Number Profile
Tab C, $M_J = 0.8$, $T_{TJ}/T_0 = 1$, $X/D_{ej} = 1, 2$, and 3

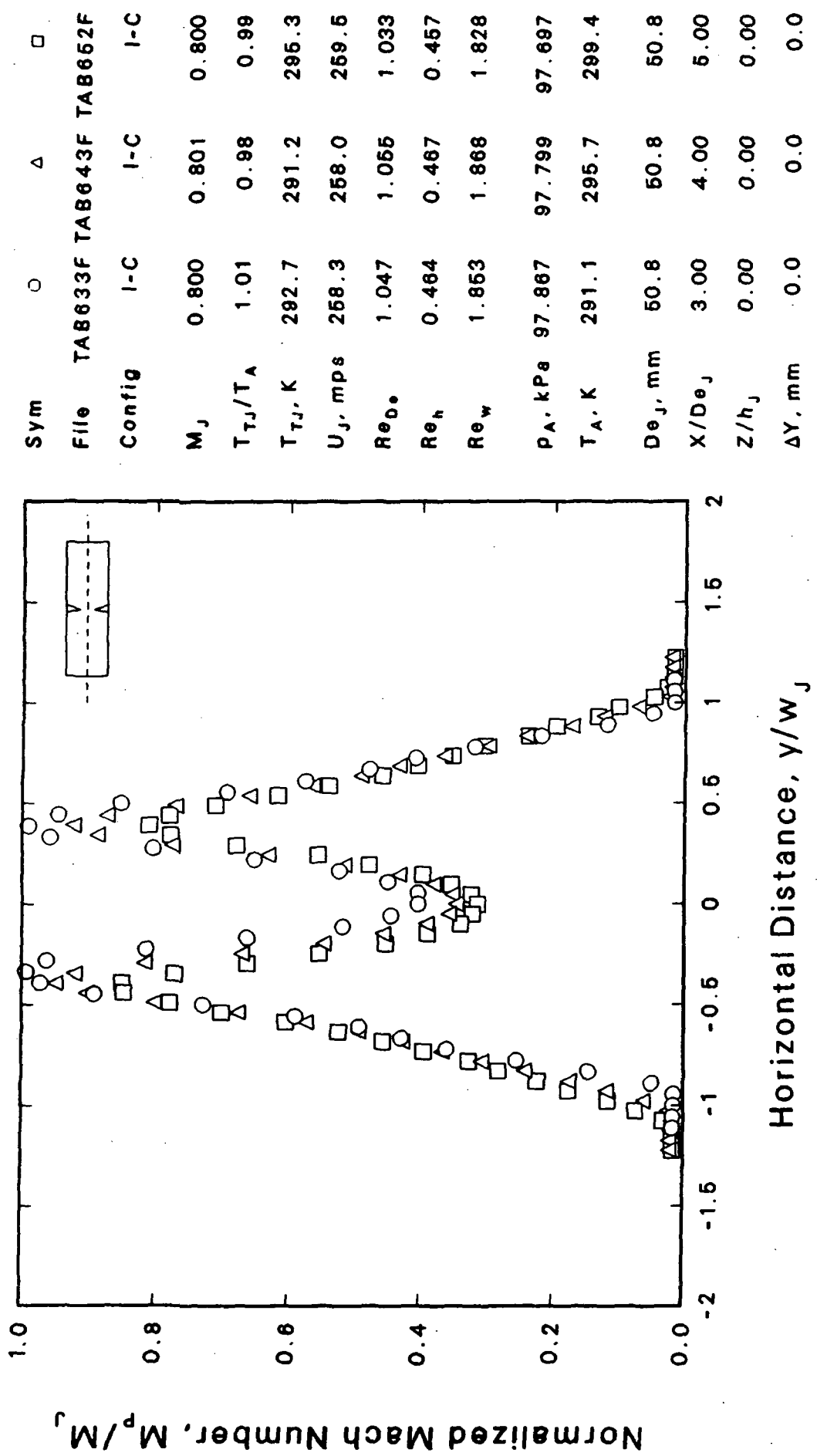


Figure 3.4 Effect of Axial Distance on Mach Number Profile
Tab C, $M_J = 0.8$, $T_J/T_0 = 1$, $X/D_e = 3, 4$, and 5

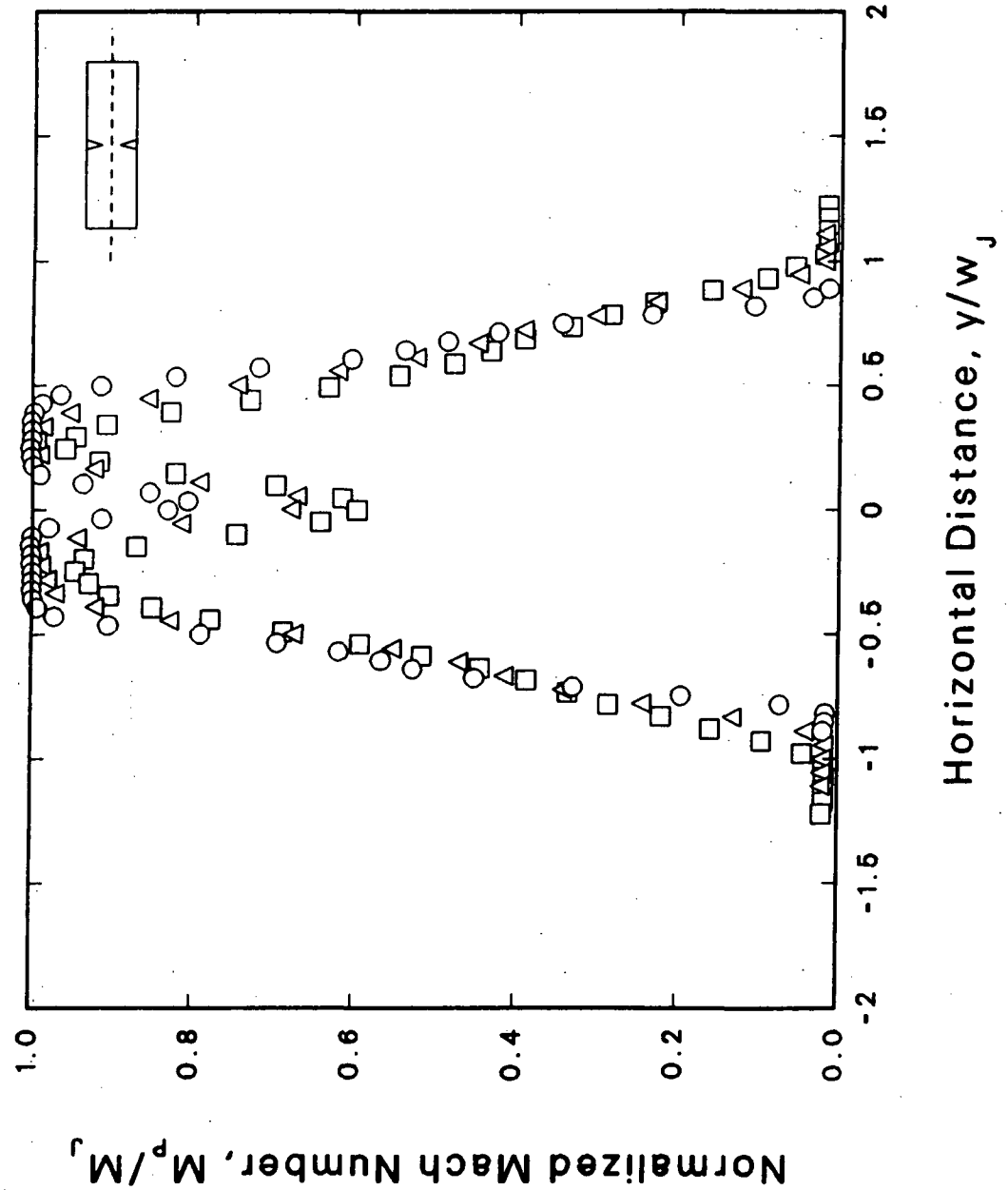


Figure 3.5 Effect of Axial Distance on Mach Number Profile Tab D, $M_J = 0.8$, $T_J/T_0 = 1$, $X/D\theta = 2$, 3, and 4

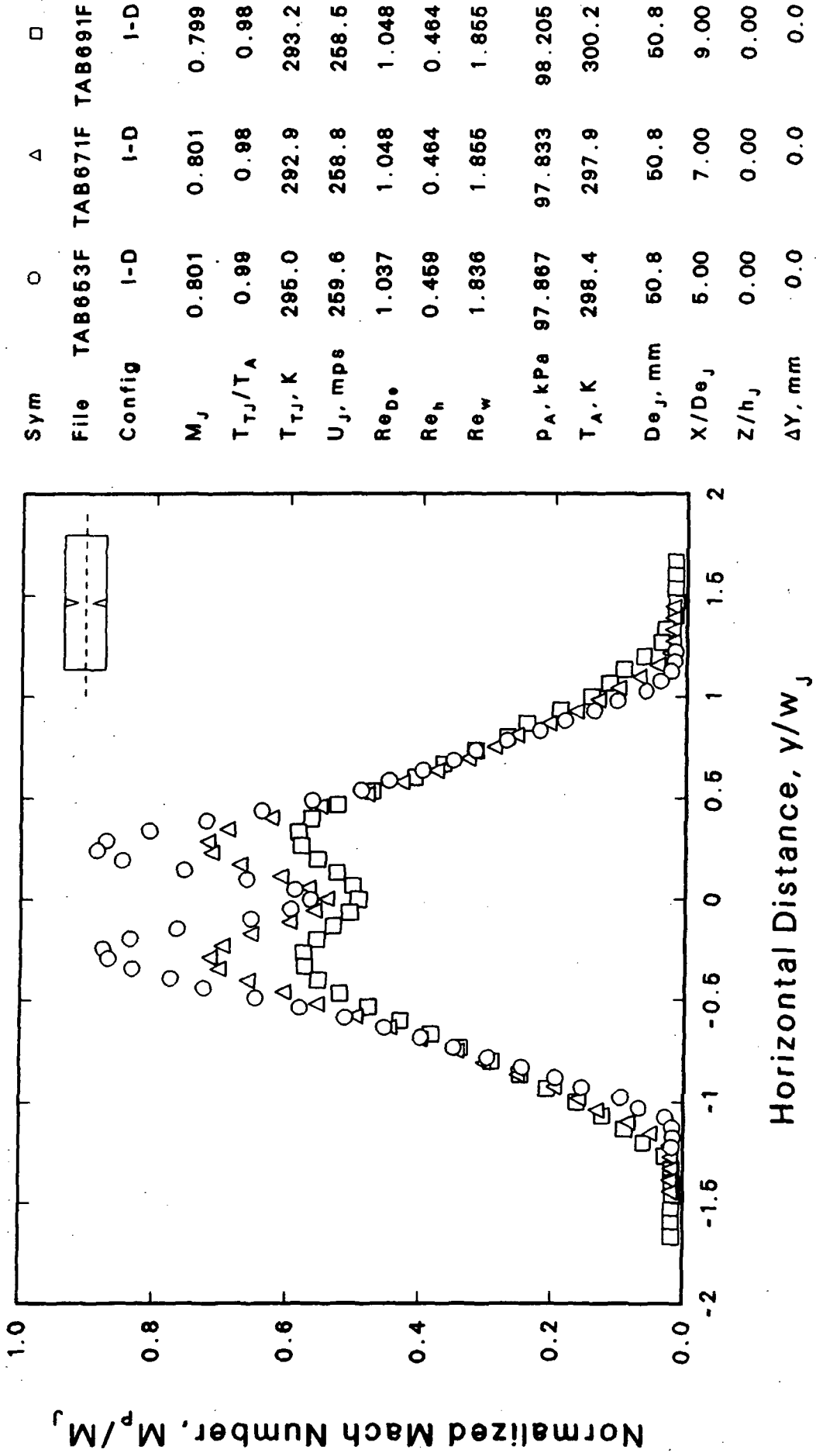


Figure 3.6 Effect of Axial Distance on Mach Number Profile
Tab D, $M_j = 0.8$, $T_j/T_0 = 1$, $X/De = 5, 7$, and 9

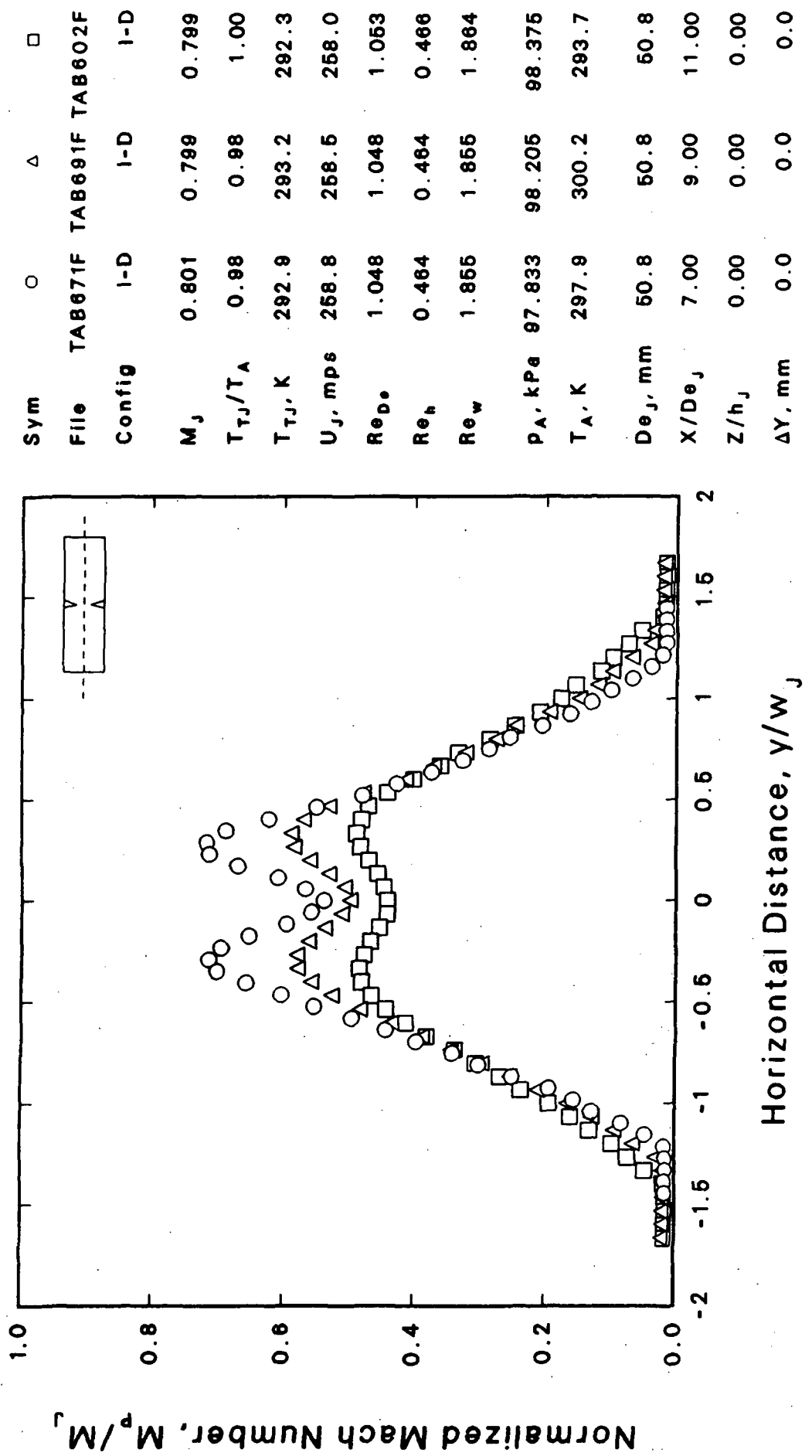


Figure 3.7 Effect of Axial Distance on Mach Number Profile
Tab D, $M_j = 0.8$, $T_j/T_0 = 1$, $X/D\theta = 7, 9$, and 11

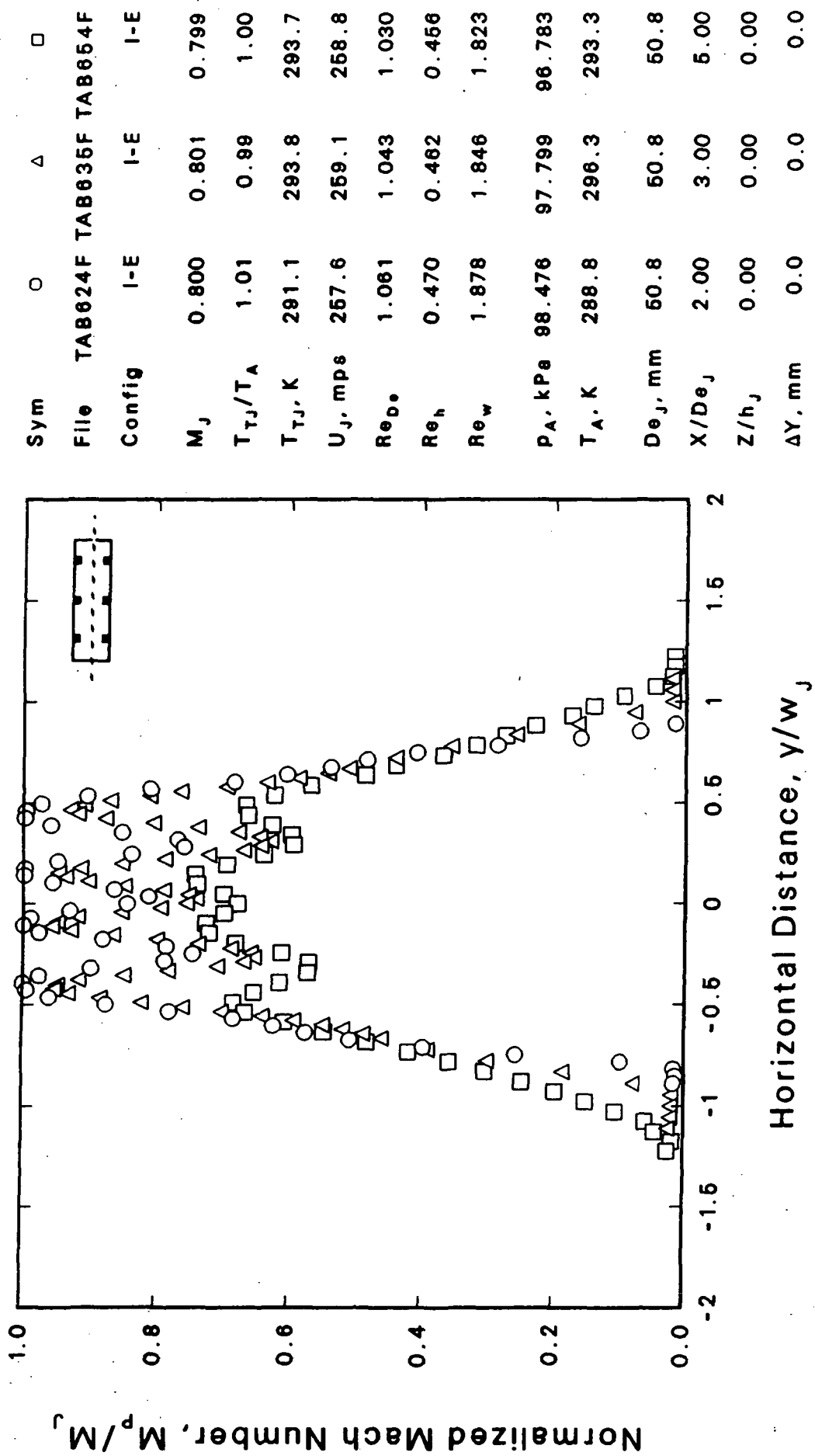


Figure 3.8 Effect of Axial Distance on Mach Number Profile
 Tab E, $M_j = 0.8$, $T_j/T_0 = 1$, $X/De = 2, 3, 5$

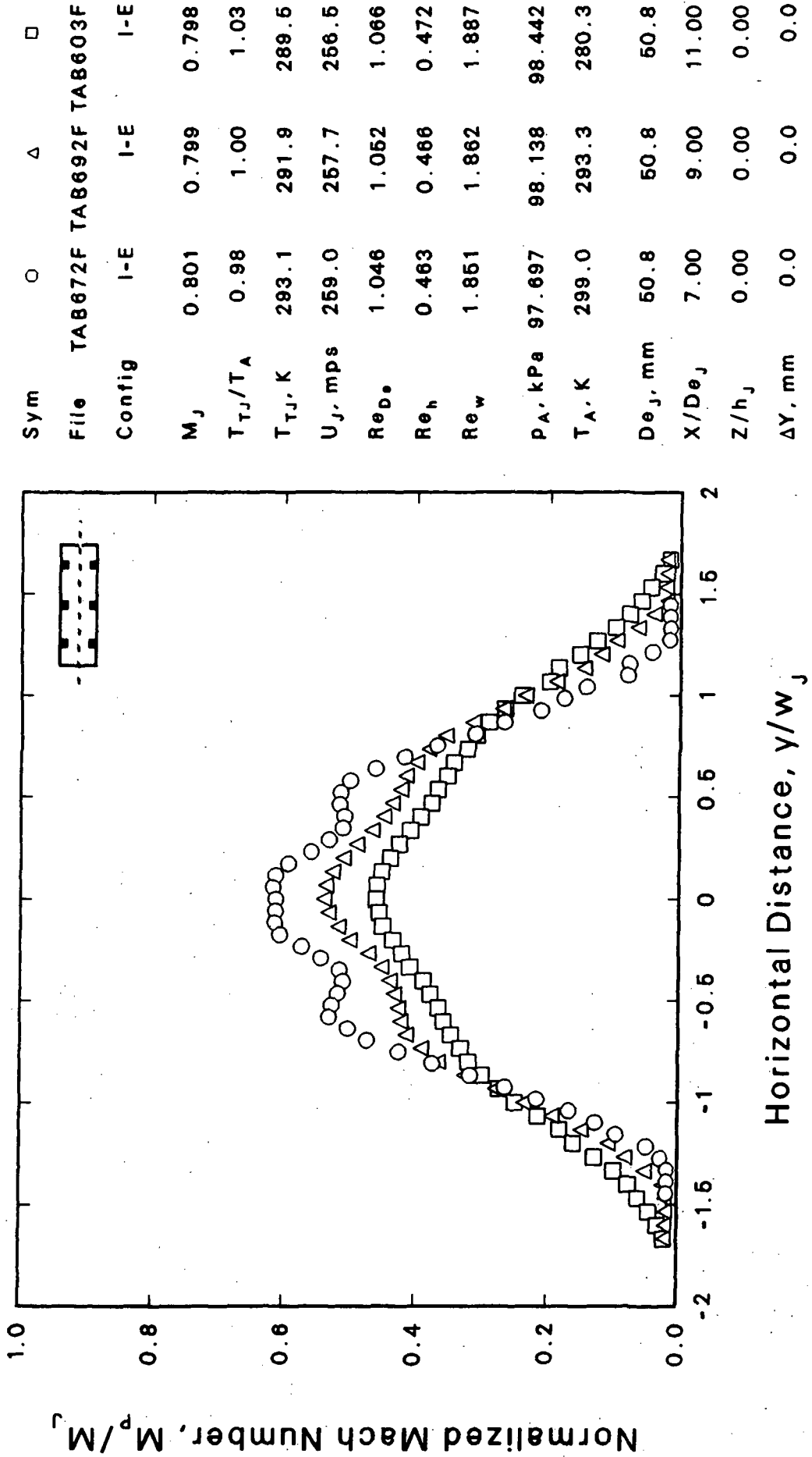


Figure 3.9 Effect of Axial Distance on Mach Number Profile
 Tab E, $M_J = 0.8$, $T_J/T_0 = 1$, $X/D_{eJ} = 7, 9, 11$

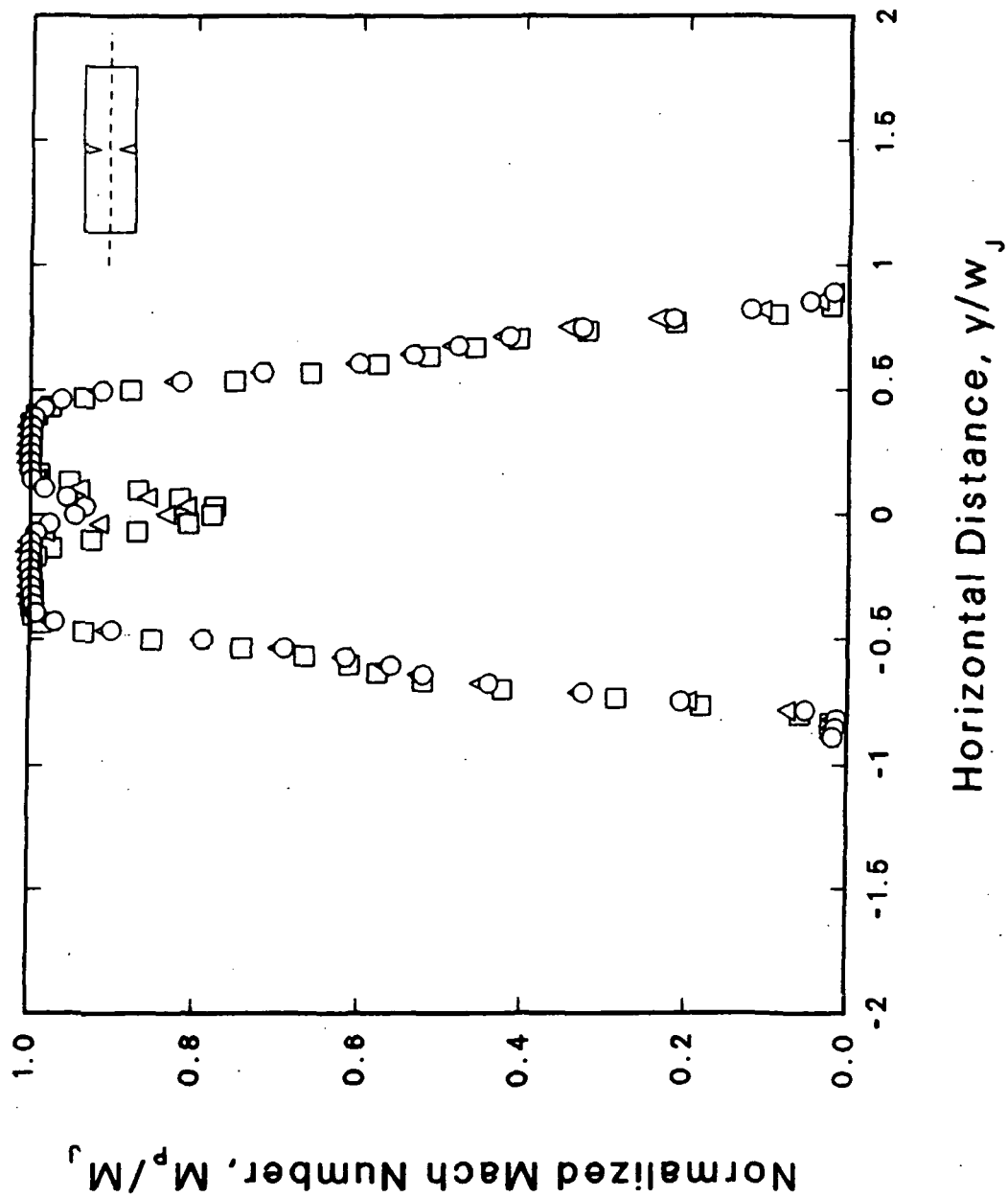


Figure 3.10 Effect of Tab Arrangement on Mach Number Profile
Tab D vs. A & B, $M_j = 0.8$, $T_j/T_0 = 1$, $X/D_e = 2$

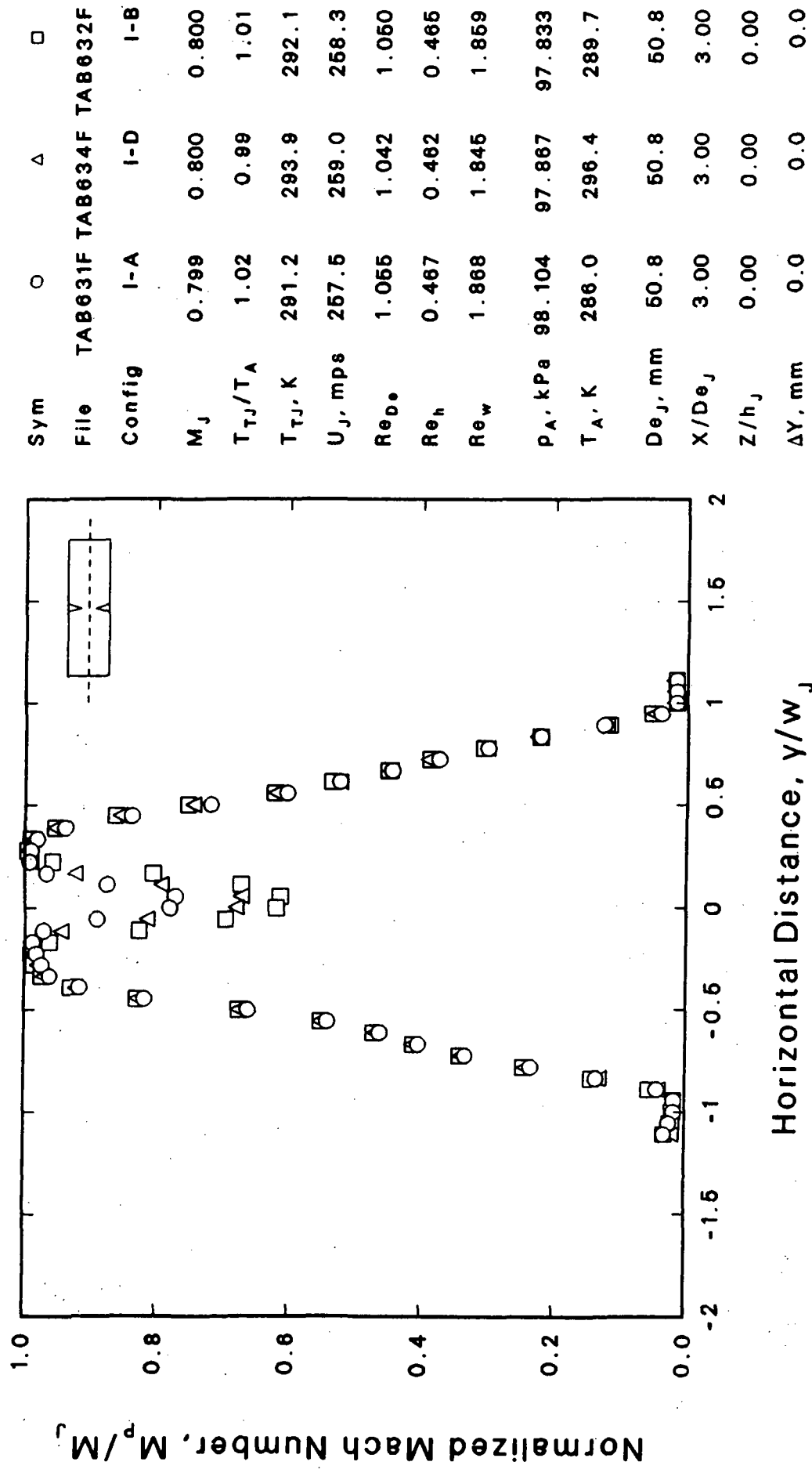


Figure 3.11 Effect of Tab Arrangement on Mach Number Profile Tab D vs. A & B, $M_j = 0.8$, $T_j/T_0 = 1$, $X/De = 3$.

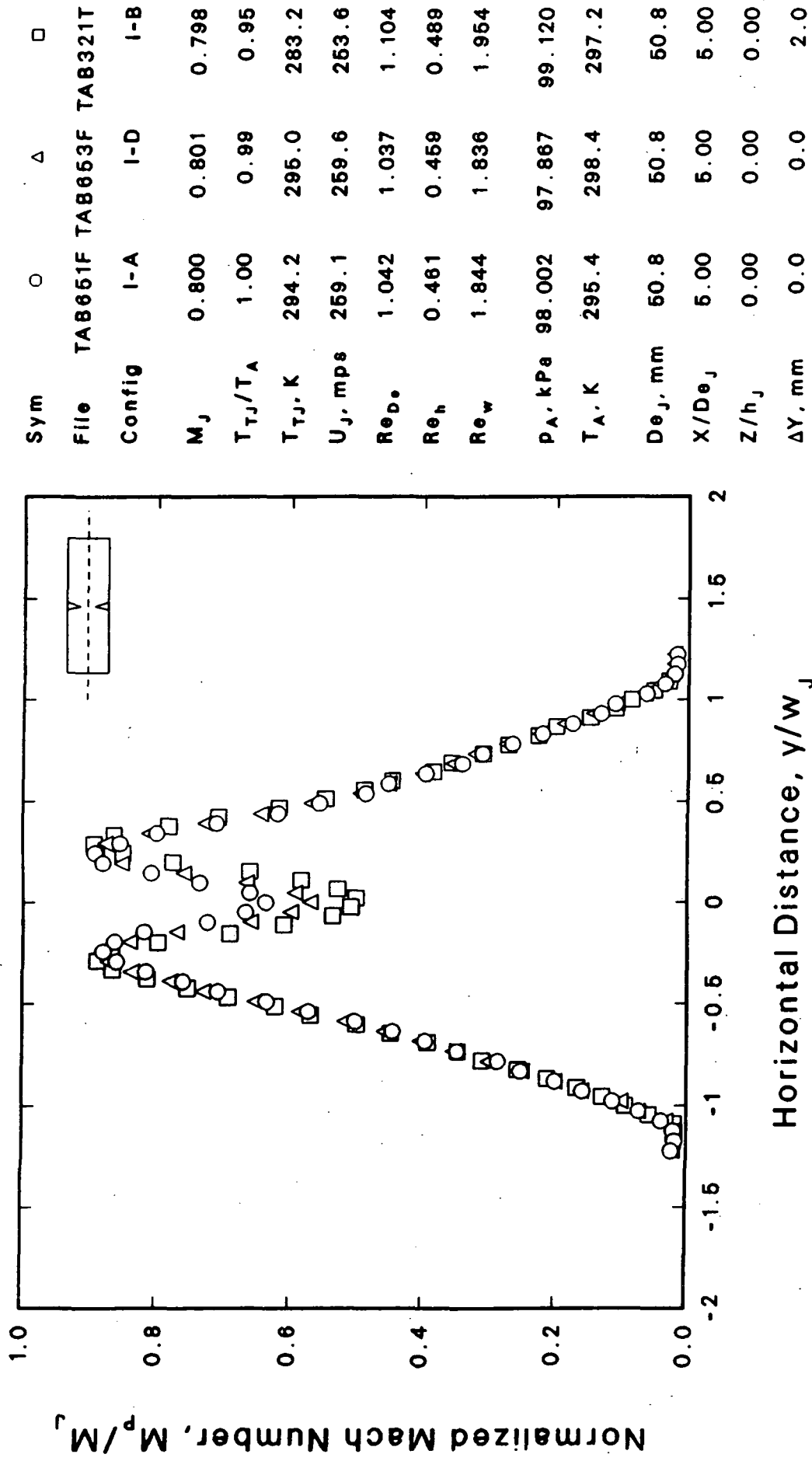


Figure 3.12 Effect of Tab Arrangement on Mach Number Profile
Tab D vs. A & B, $M_j = 0.8$, $T_j/T_0 = 1$, $X/De = 5$

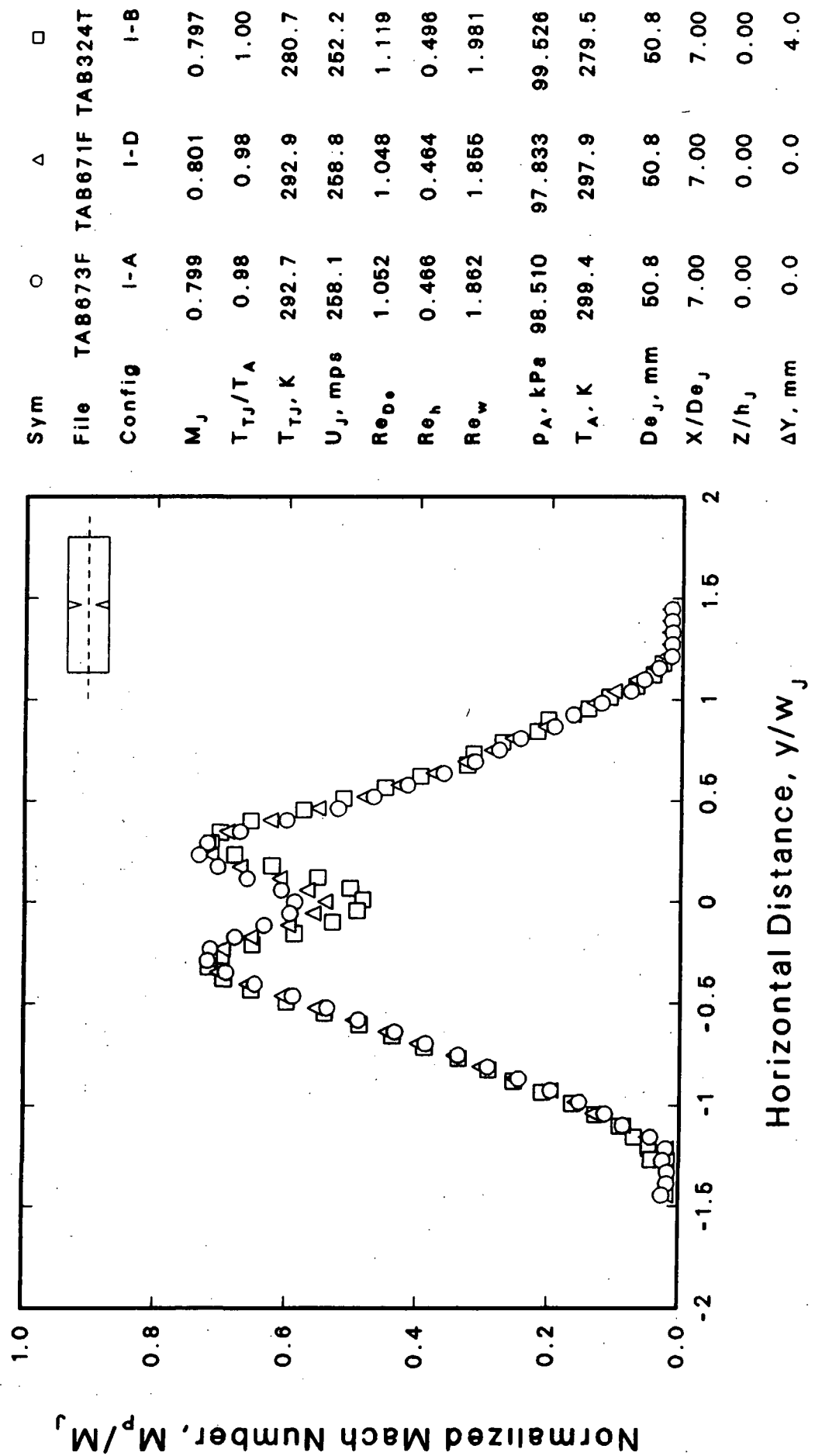


Figure 3.13 Effect of Tab Arrangement on Mach Number Profile Tab D vs. A & B, $M_j = 0.8$, $T_j/T_0 = 1$, $X/De = 7$

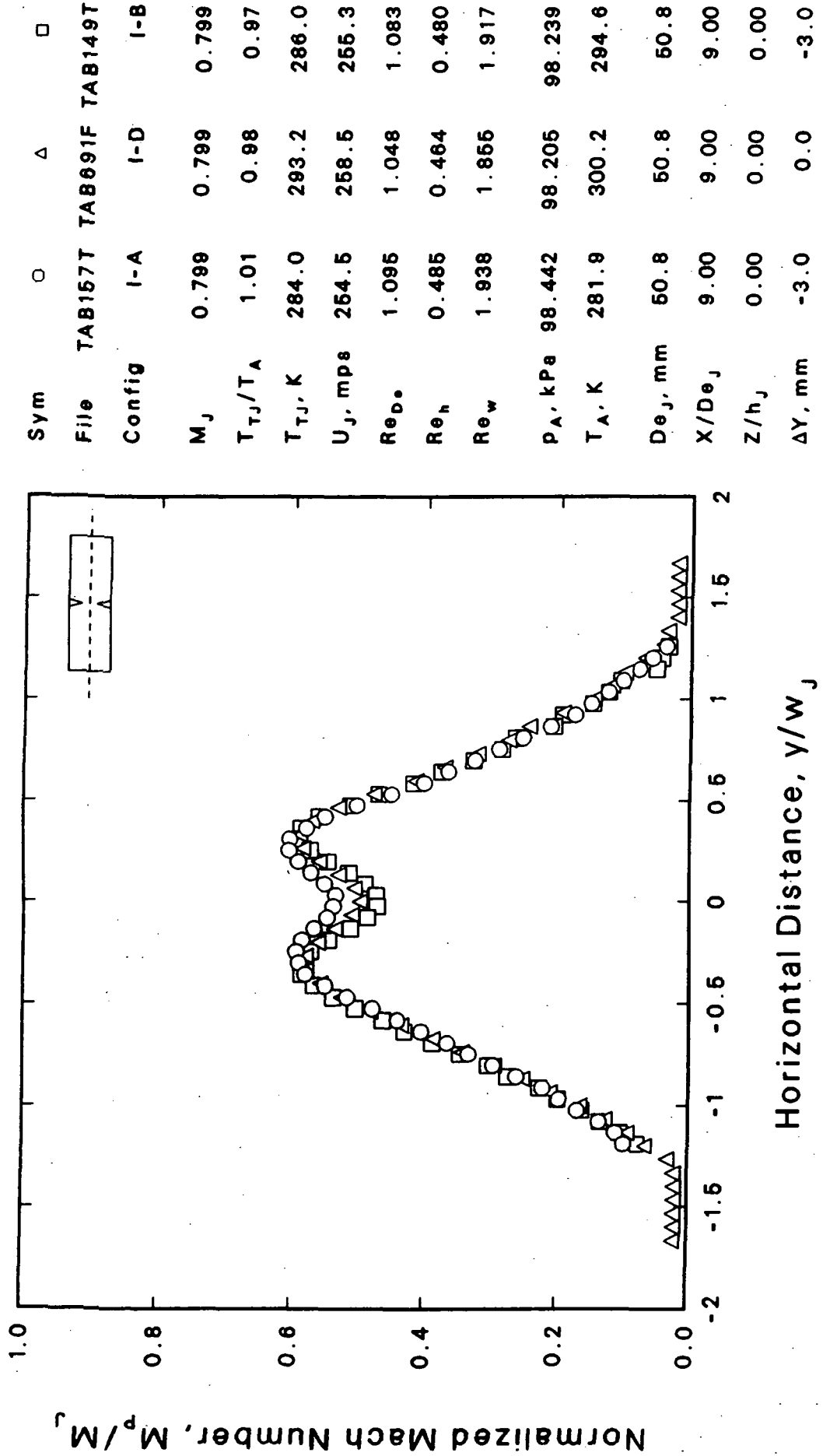


Figure 3.14 Effect of Tab Arrangement on Mach Number Profile
Tab D vs. A & B, $M_j = 0.8$, $T_j/T_0 = 1$, $X/D_{ej} = 9$

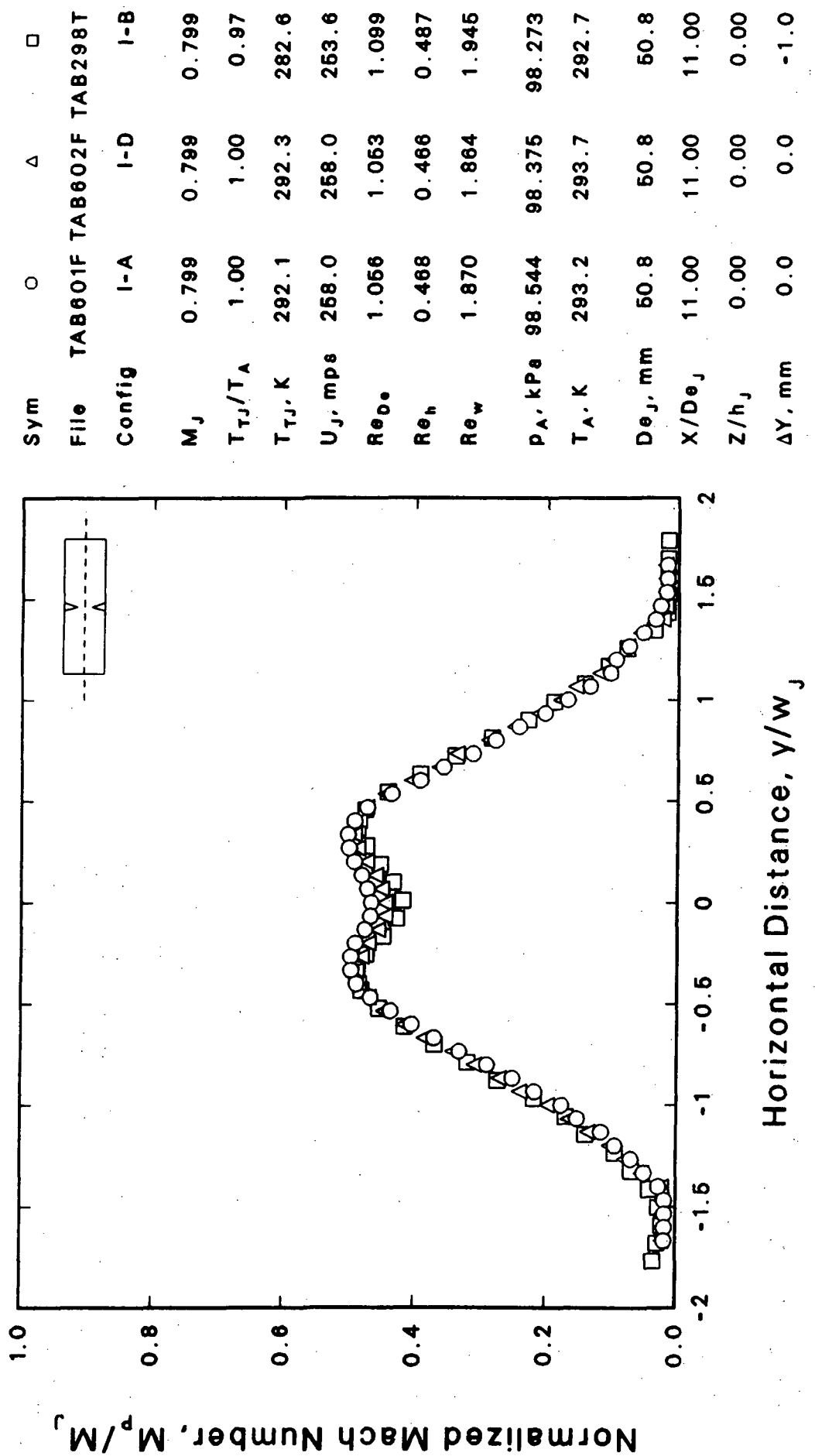


Figure 3.15 Effect of Tab Arrangement on Mach Number Profile Tab D vs. A & B, $M_j = 0.8$, $T_j/T_0 = 1$, $X/De = 11$



Sym

File TAB316T TAB624F

Config I-B I-E

M_J 0.798 0.800

T_{TJ}/T_A 0.98 1.01

T_{TJ}, K 281.9 291.1

U_J, mps 263.1 267.6

Re_D 1.104 1.061

Re_h 0.489 0.470

Re_w 1.964 1.878

p_A, kPa 98.510 98.476

T_A, K 294.5 288.8

D_{ej}, mm 50.8 50.8

X/De_j 2.00 2.00

Z/h_J 0.00 0.00

$\Delta Y, \text{mm}$ 0.0 0.0

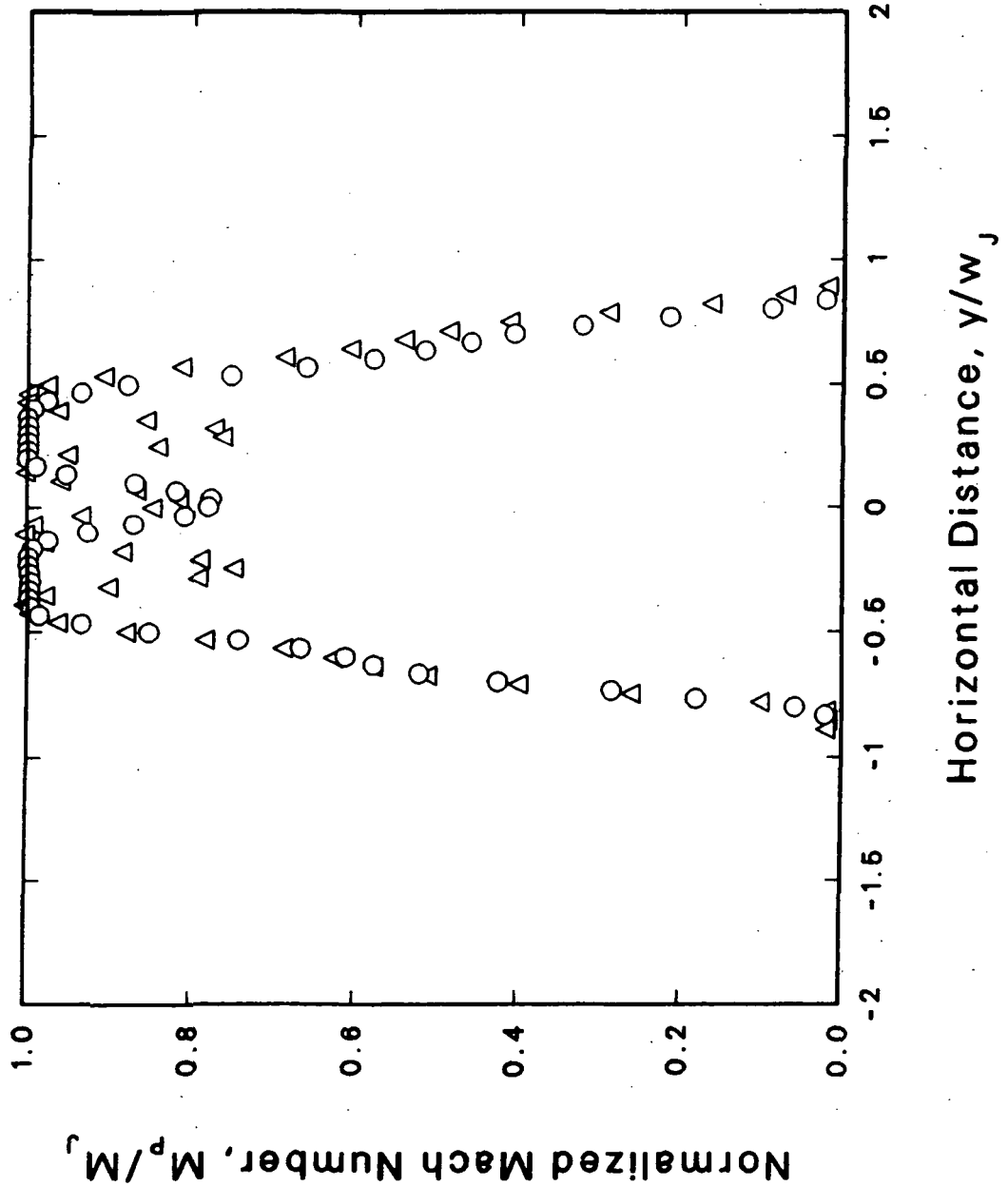


Figure 3.16 Effect of Tab Arrangement on Mach Number Profile Tab E vs. B, $M_J = 0.8$, $T_J/T_0 = 1$, $X/De = 2$

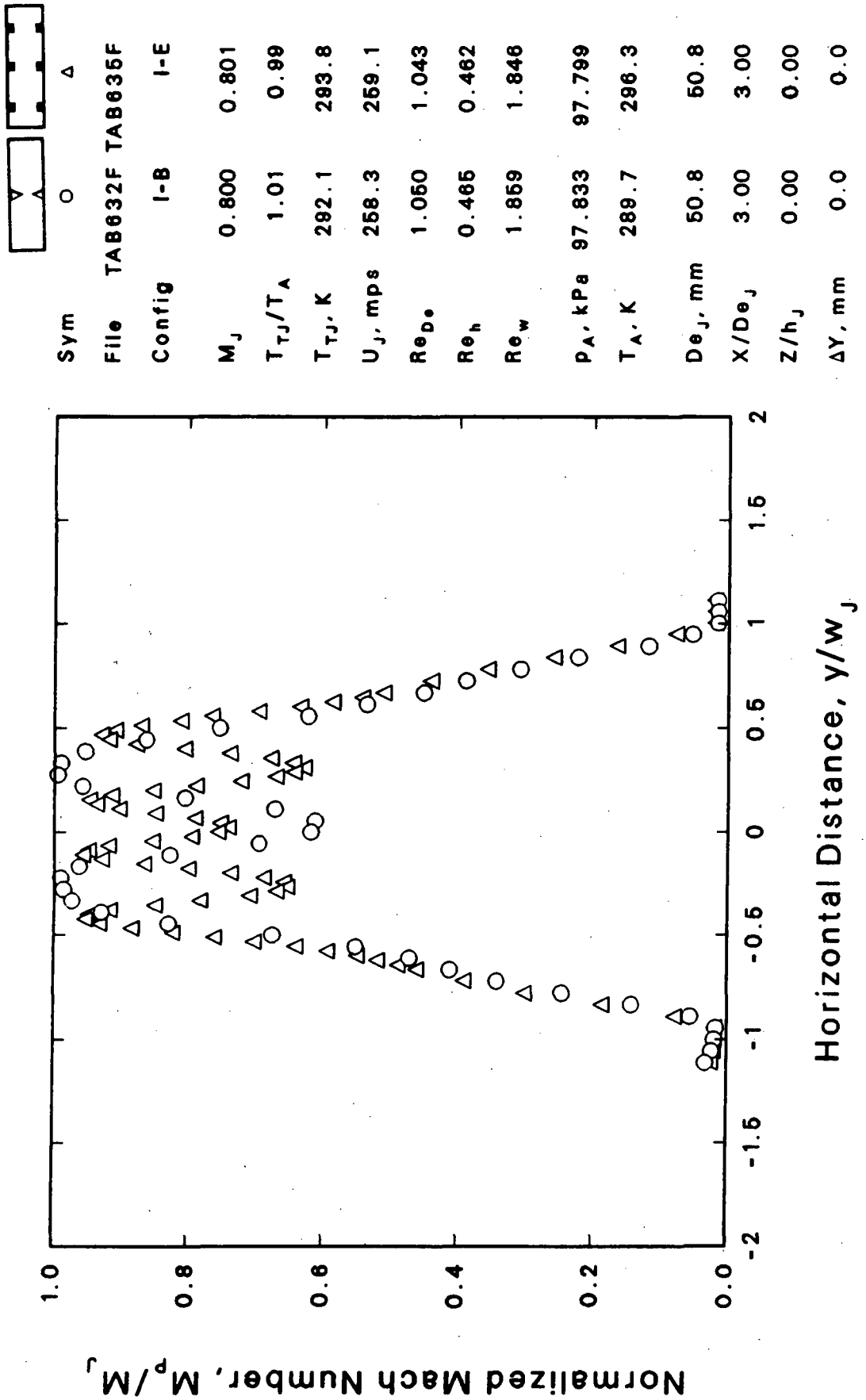
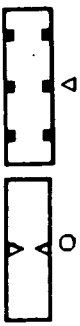


Figure 3.17 Effect of Tab Arrangement on Mach Number Profile
Tab E vs. B, $M_j = 0.8$, $T_j/T_0 = 1$, $X/De = 3$



Sym

File TAB321T TAB654F

Config I-B I-E

M_J 0.798 0.798

T_{TJ}/T_A 0.96 1.00

T_{TJ}, K 283.2 293.7

$U_J, \text{ mps}$ 263.6 268.8

Re_D 1.104 1.030

Re_h 0.489 0.466

Re_w 1.964 1.823

$p_A, \text{ kPa}$ 99.120 96.783

T_A, K 297.2 293.3

$D\epsilon_J, \text{ mm}$ 50.8 50.8

$X/D\epsilon_J$ 5.00 6.00

Z/h_J 0.00 0.00

$\Delta Y, \text{ mm}$ 2.0 0.0

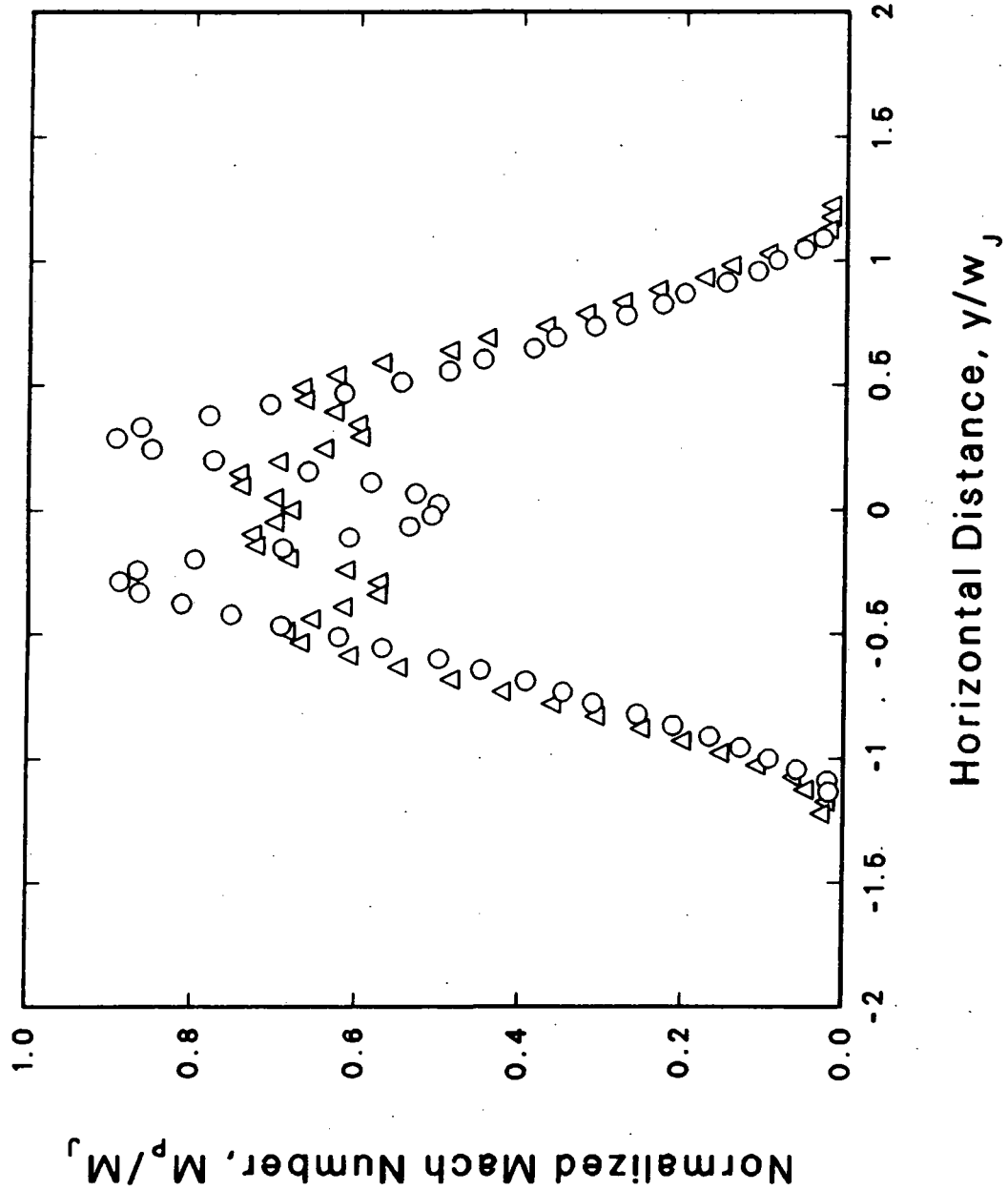


Figure 3.18 Effect of Tab Arrangement on Mach Number Profile
Tab E vs. B, $M_J = 0.8$, $T_j/T_0 = 1$, $X/D\epsilon = 5$

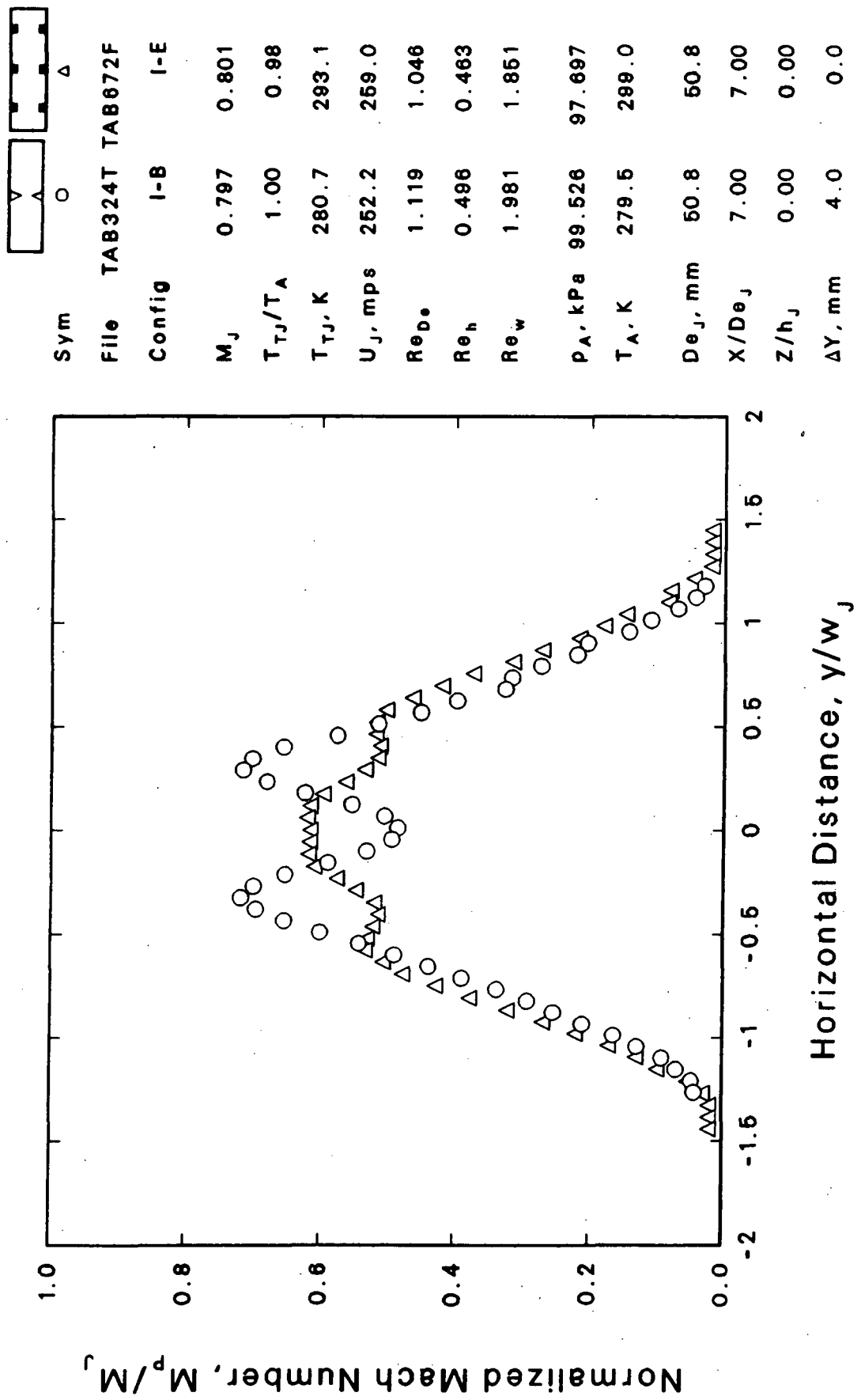


Figure 3.19 Effect of Tab Arrangement on Mach Number Profile Tab E vs. B, $M_j = 0.8$, $T_j/T_0 = 1$, $X/D_e = 7$

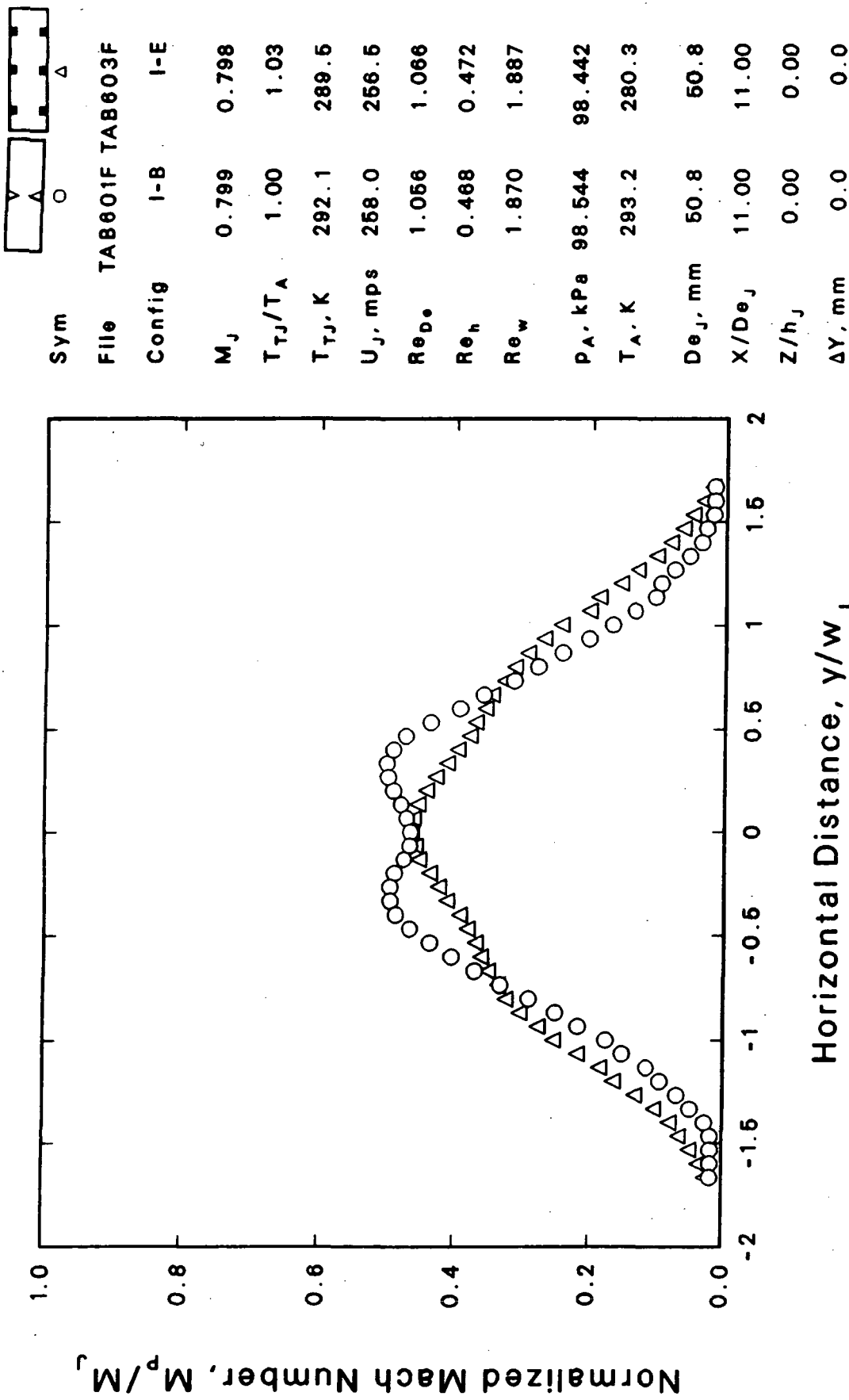


Figure 3.20 Effect of Tab Arrangement on Mach Number Profile
Tab E vs. B, $M_j = 0.8$, $T_j/T_0 = 1$, $X/De = 11$

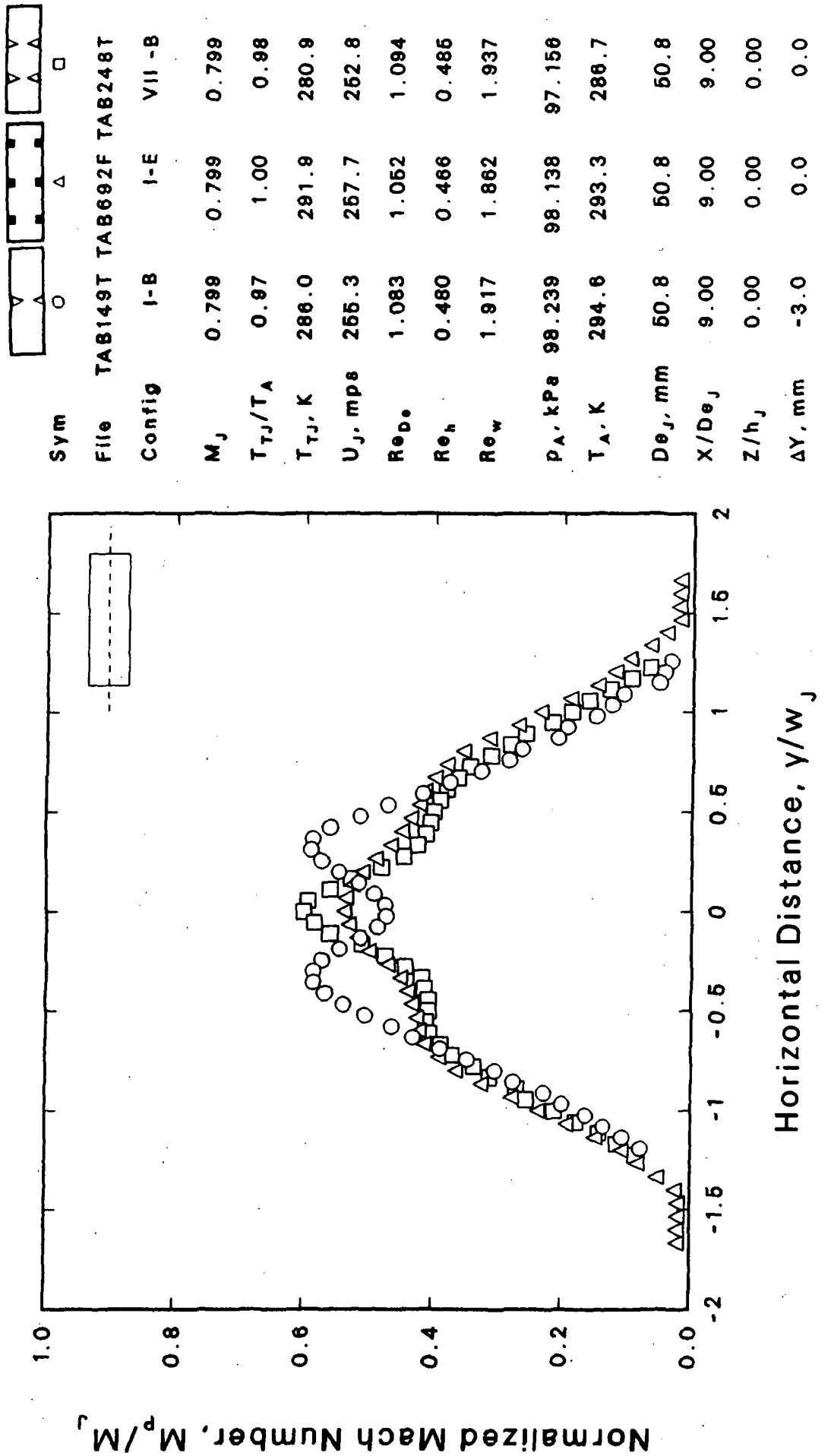


Figure 3.21 Effect of Tab Arrangement on Mach Number Profile Tab E vs. B, $M_j = 0.8$, $T_j/T_0 = 1$, $X/De = 9$

3.2.5 EFFECT OF THE FULL NOZZLE HEIGHT TAB

The full height tab "F" is compared with the baseline nozzle and with the two tab configuration of the same tab width (I-B) in Figure 3.22. Configurations I-B and "F" exhibit about the same peak velocity, but "F" has significantly lower centerline velocity.

3.2.6 COMPLETE DATA

All of the data profiles obtained in this effort are presented in Appendix B. Each plot shows the horizontal Mach number profile for one configuration at one axial location and the corresponding baseline profile for reference.

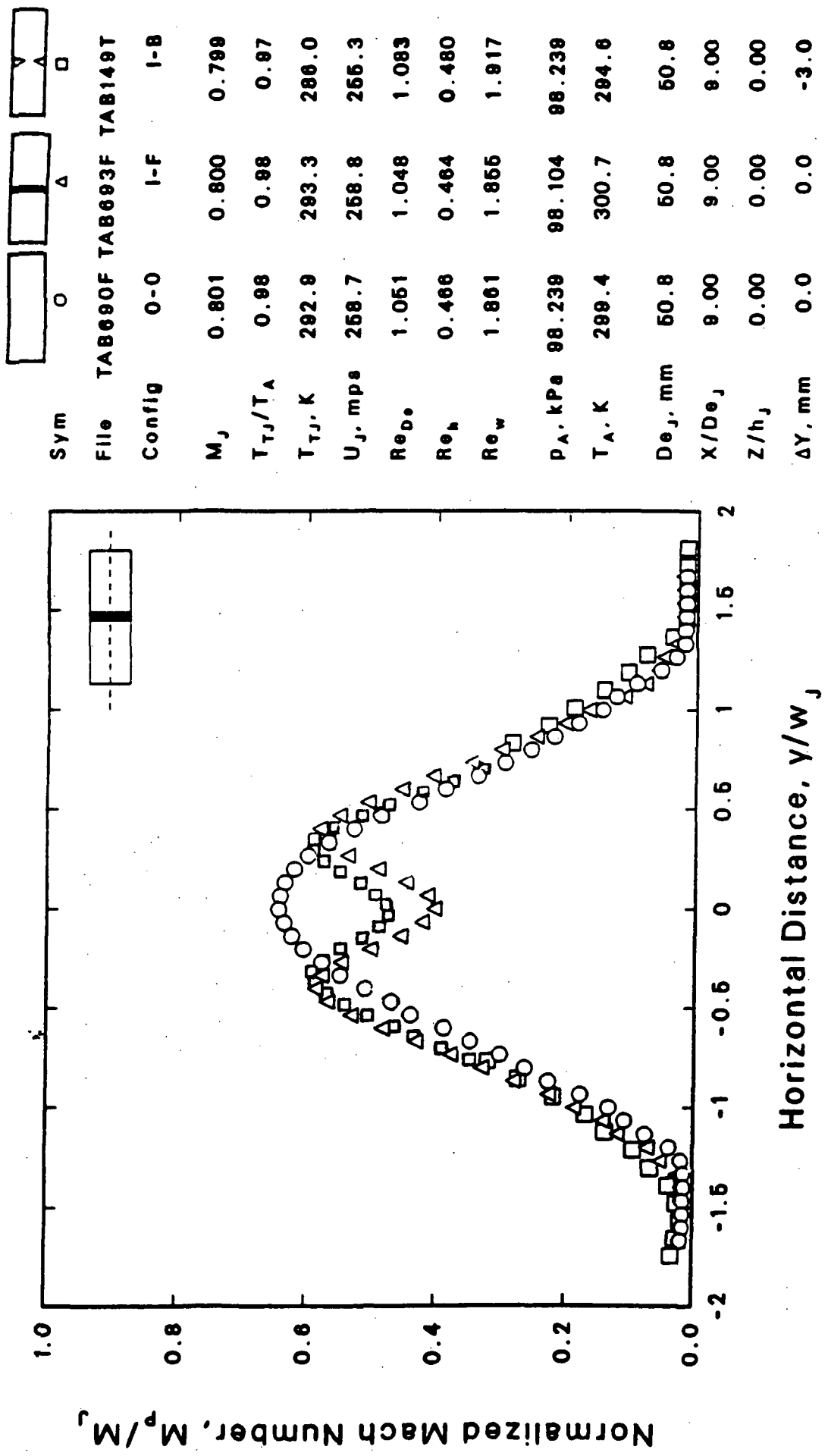


Figure 3.22 Effect of Tab Arrangement on Mach Number Profile Tab F vs. 0 & B, $M_J = 0.8$, $T_J/T_0 = 1$, $x/D_0 = 9$

SECTION 4

CONCLUDING REMARKS

This report provides additional test data required to better interpret Reference 3 test results. The following general observations were noted:

1. The 6-tab rectangular nozzle configuration provided a lower peak velocity than either the 2-tab or 4-tab configuration.
2. The rectangular nozzle with a full height tab had about the same peak velocity as the 2-tab configuration; however, the full height tab configuration had a somewhat lower centerline velocity

REFERENCES

1. Ahuja, K. K. and Brown, W. H.: Shear Flow Control by Mechanical Tabs, AIAA-89-0994, 1989.
2. Bradbury, L. J. S., and Khadem, A. H.: "The Distortion of a Jet by Tabs," *J. Fluid Mech.*, vol. 70, pt. 4, pp. 801-13, 1975.
3. Brown, W. H. and Ahuja, K. K.: "Shear Flow Control of Cold and Heated Rectangular Jets by Mechanical Tabs," Vol. I - Results and Discussion and Vol. II - Tabulated Data, NASA CR-182296 (Limited Distribution), 1989.
4. Ahuja, K. K.; Lepicovsky, J.; Tab, C.K.W.; Morris, P. J.; and Burrin, R. H.: Tone-Excited Jet -- Theory and Experiments. NASA CR-3538, 1982.
5. Lepicovsky, J.; Ahuja, K. K.; and Burrin, R. H.: Tone Excited Jets, Part III: Flow Measurements, *Journal of Sound and Vibration*, Vol. 102, No. 1, pp. 71-91, 1985.
6. Lepicovsky, J.; Ahuja, K. K.; Brown, W. H.; Salikuddin, M.; and Morris, P. J.: Acoustically Excited Heated Jets, Part I: Internal Excitation. NASA CR 4129, June 1988.
7. Lepicovsky, J.; Ahuja, K. K.; Brown, W. H.; and Burrin, R. H.: Coherent Large-Scale Structures in High Reynolds Number Supersonic Jets. NASA CR 3952, 1985.

APPENDIX A

LIST OF SYMBOLS

<u>Symbol</u>	<u>Meaning</u>
A, B, C, D, E, F	Tab size indicators
A	Nozzle exit area
d	Diagonal distance across rectangular nozzle
d_p	Tap depth
D	Diameter of round nozzles
D_e	Equivalent diameter = $(4A/\pi)^{**0.5}$
h	Height (smaller dimension) of rectangular nozzle
K	Degrees Kelvin
M	Mach number (fully expanded for supersonic)
P	Nozzle exit perimeter
Re	Reynolds number based on D, D_e , w, or h
T	Temperature
U	Velocity
w	Width (larger dimension) of rectangular nozzle
w_p	Tab width
X	Streamwise coordinate
Y	Horizontal coordinate
Z	Vertical coordinate
γ	Ratio of specific heats

Subscripts

A, 0	Ambient
D_e	Equivalent diameter
h	Height of rectangular nozzle
J	Jet exit conditions
S	Static
T	Total
w	Width of rectangular nozzle

APPENDIX B

DATA PLOTS

B.1 DATA ORGANIZATION

The plots in this appendix are arranged by axial position and then by tab configuration as shown in Figure B-1.

B.2 NOMENCLATURE FOR FIGURES

The basic nomenclature used in the figures is defined in Appendix A and described in Section 3.2.1.

X/DE	Tj/T ₀	M _j	TAB	DATA SET
1	1	0.8	0	TAB610F
	1	0.8	C	TAB611F
2	1	0.8	0	TAB620F
	1	0.8	A	TAB621F
	1	0.8	C	TAB622F
	1	0.8	D	TAB623F
	1	0.8	E	TAB624F
3	1	0.8	0	TAB630F
	1	0.8	A	TAB631F
	1	0.8	B	TAB632F
	1	0.8	C	TAB633F
	1	0.8	D	TAB634F
	1	0.8	E	TAB635F
4	1	0.8	0	TAB640F
	1	0.8	A	TAB641F
	1	0.8	B	TAB642F
	1	0.8	C	TAB643F
	1	0.8	D	TAB644F
5	1	0.8	0	TAB650F
	1	0.8	A	TAB651F
	1	0.8	C	TAB652F
	1	0.8	D	TAB653F
	1	0.8	E	TAB654F
7	1	0.8	0	TAB670F
	1	0.8	D	TAB671F
	1	0.8	E	TAB672F
	1	0.8	A	TAB673F
9	1	0.8	0	TAB690F
	1	0.8	D	TAB691F
	1	0.8	E	TAB692F
	1	0.8	F	TAB693F
11	1	0.8	0	TAB600F
	1	0.8	A	TAB601F
	1	0.8	D	TAB602F
	1	0.8	E	TAB603F

Figure B.1. Baseline and mixing modification for unheated subsonic jets.

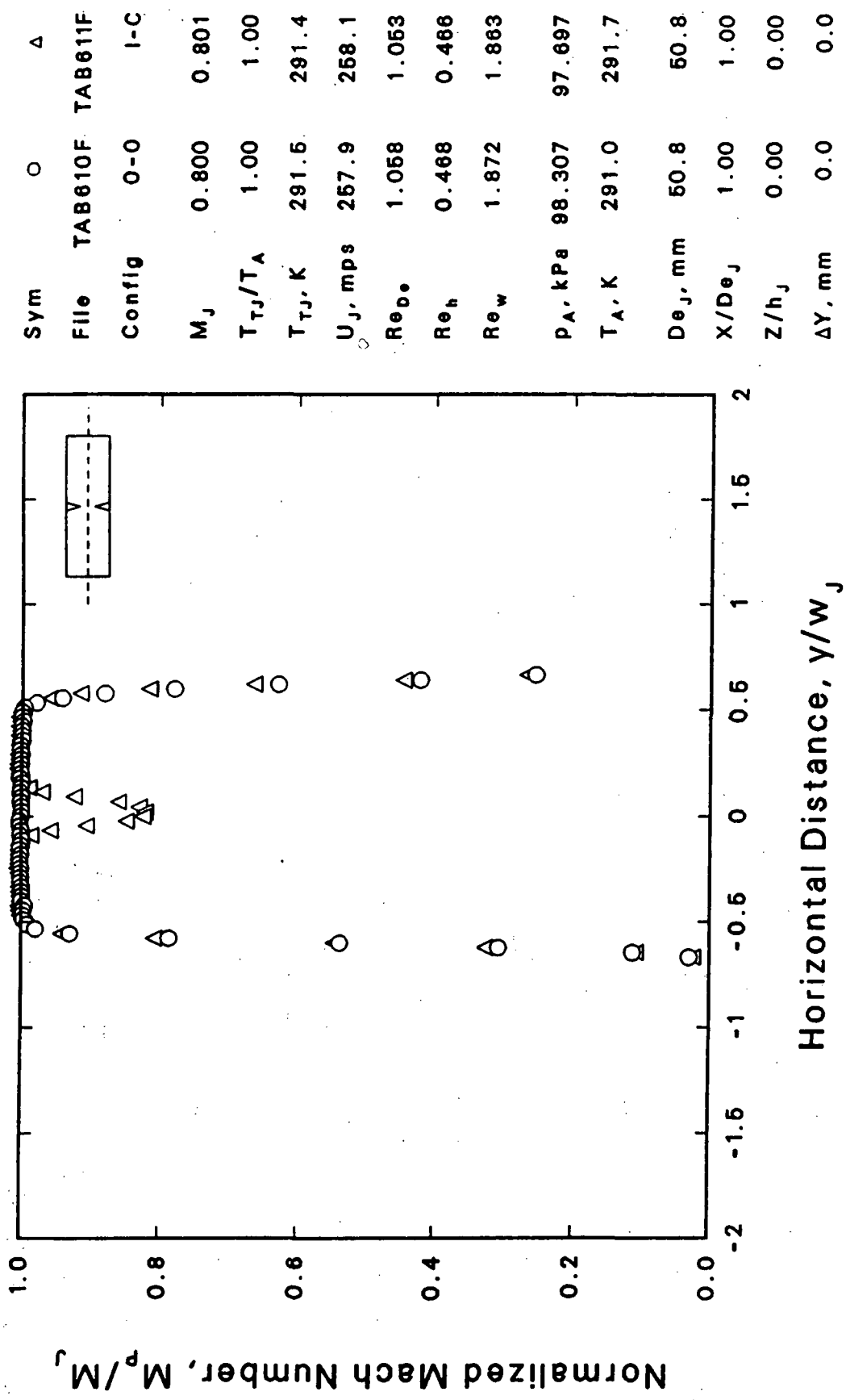


Figure B-2 Horizontal Mach Number Profile, Tab C
 $M_j = 0.8$, $T_j/T_0 = 1$, $X/D\theta = 1$

Normalized Mach Number, M_p/M_j

Horizontal Distance, y/w_j

Horizontal Distance (y/w_j)	M_p/M_j (Open Circles)	M_p/M_j (Open Squares)
-1.8	0.95	0.90
-1.6	0.90	0.85
-1.4	0.85	0.80
-1.2	0.80	0.75
-1.0	0.75	0.70
-0.8	0.70	0.65
-0.6	0.65	0.60
-0.4	0.60	0.55
-0.2	0.55	0.50
0.0	0.50	0.45
0.2	0.45	0.40
0.4	0.40	0.35
0.6	0.35	0.30
0.8	0.30	0.25
1.0	0.25	0.20
1.2	0.20	0.15
1.4	0.15	0.10
1.6	0.10	0.05
1.8	0.05	0.00
2.0	0.00	0.00

Figure B-3 Horizontal Mach Number Profile, Tab A
 $M_j = 0.8$, $T_j/T_0 = 1$, $X/De = 2$

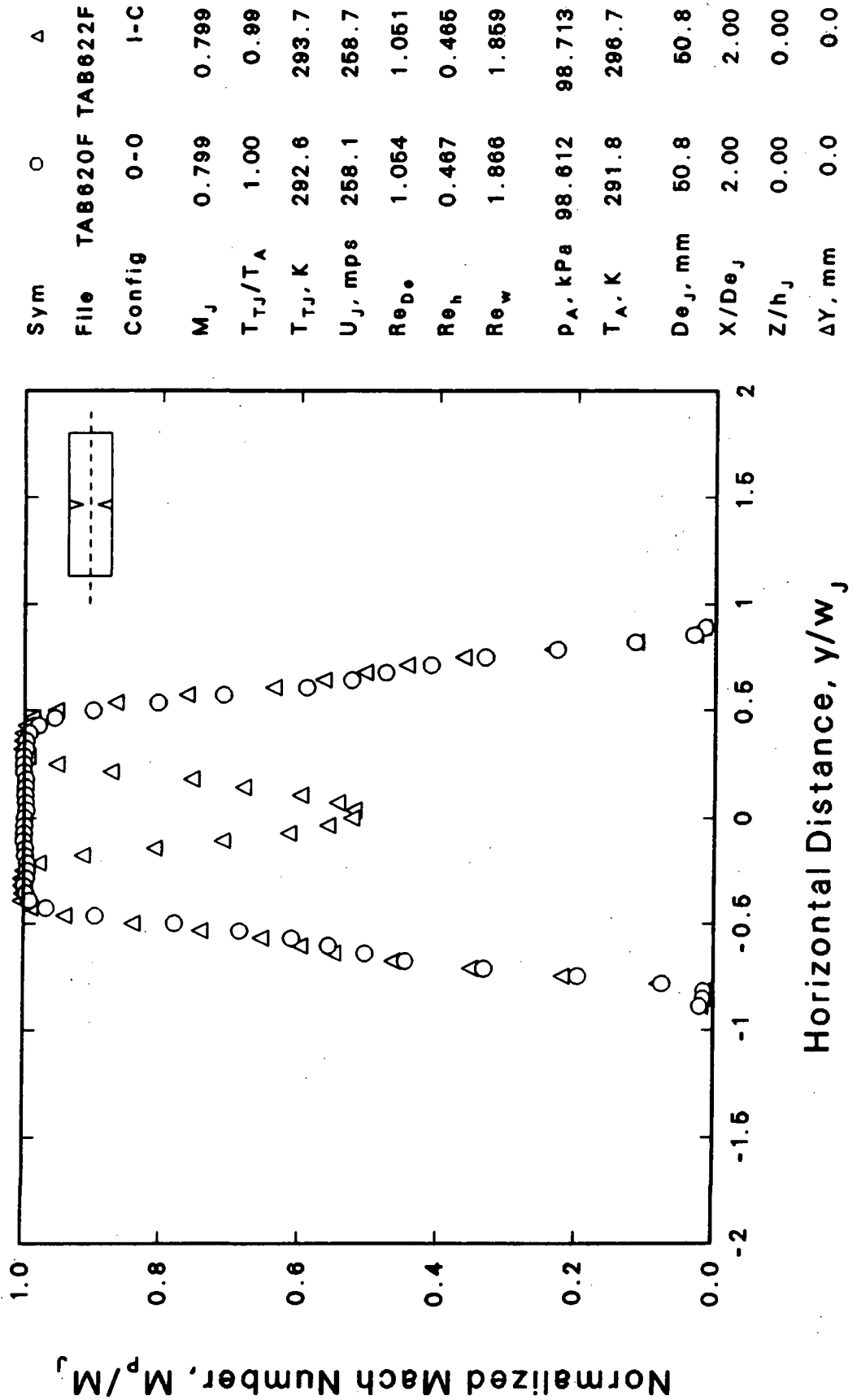


Figure B-4 Horizontal Mach Number Profile, Tab C
 $M_j = 0.8$, $T_j/T_0 = 1$, $X/De = 2$

Sym	O	Δ
File	TAB620F TAB623F	
Config	0-0	I-D
M_J	0.799	0.799
T_{TJ}/T_A	1.00	1.01
T_{TJ}, K	292.6	290.9
U_J, mps	268.1	267.6
Re_{D_0}	1.064	1.061
Re_h	0.467	0.470
Re_w	1.866	1.878
p_A, kPa	98.612	98.476
T_A, K	291.8	288.3
D_{ej}, mm	60.8	60.8
X/D_{ej}	2.00	2.00
Z/h_j	0.00	0.00
$\Delta Y, mm$	0.0	0.0

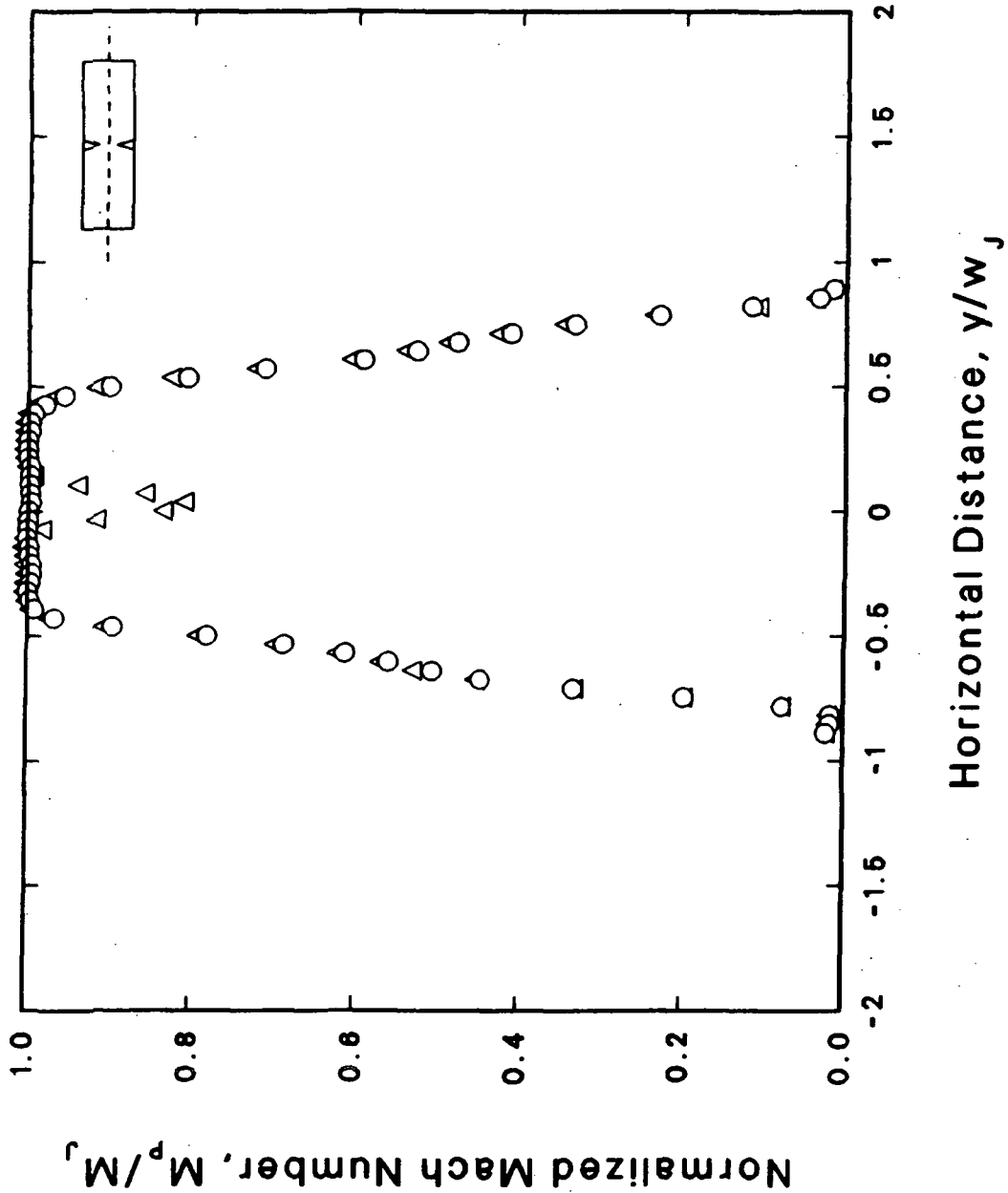


Figure B-5 Horizontal Mach Number Profile, Tab D
 $M_j = 0.8$, $T_j/T_0 = 1$, $X/D_0 = 2$

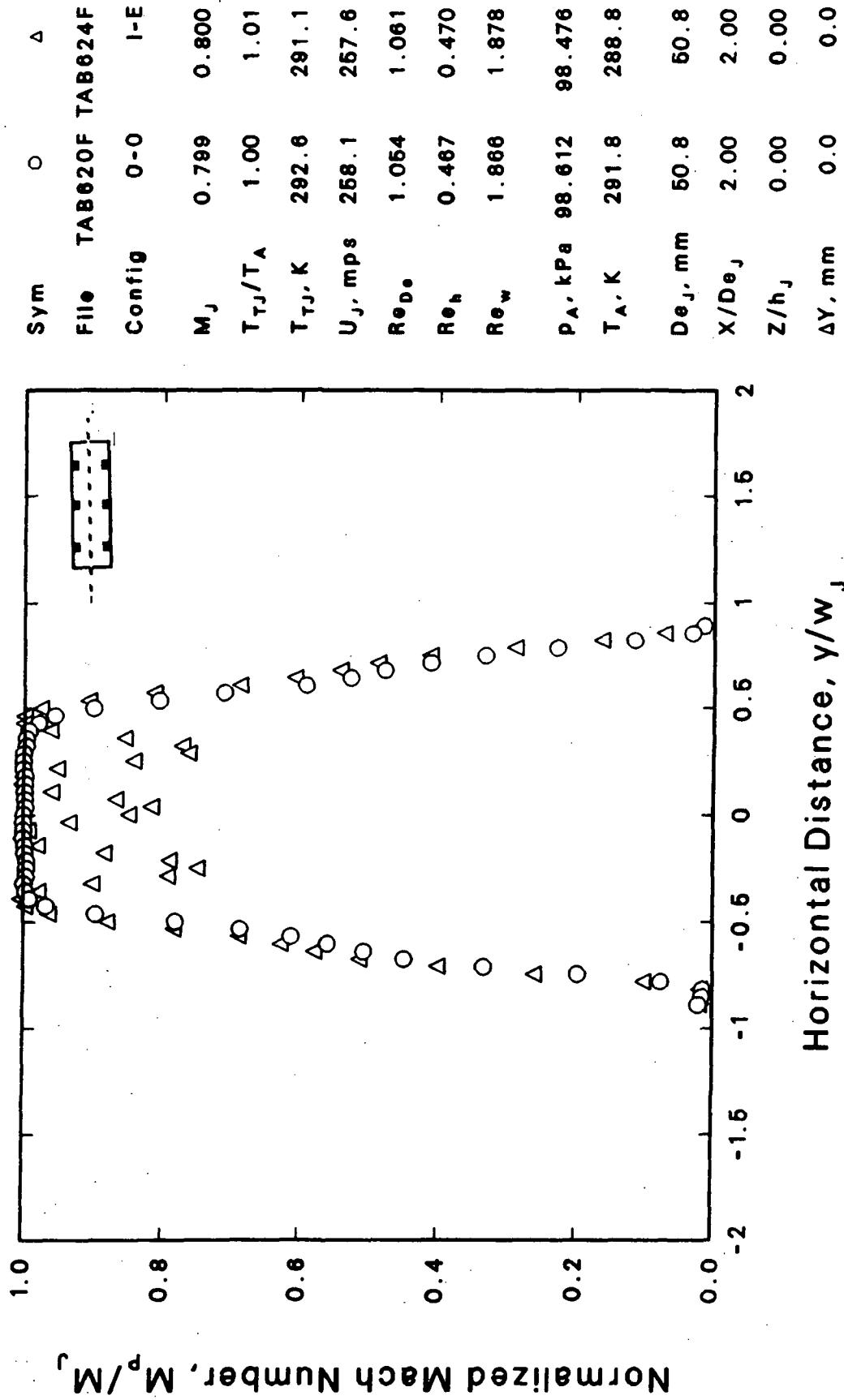


Figure B-6 Horizontal Mach Number Profile, Tab E
 $M_J = 0.8$, $T_j/T_0 = 1$, $X/D\epsilon_J = 2$

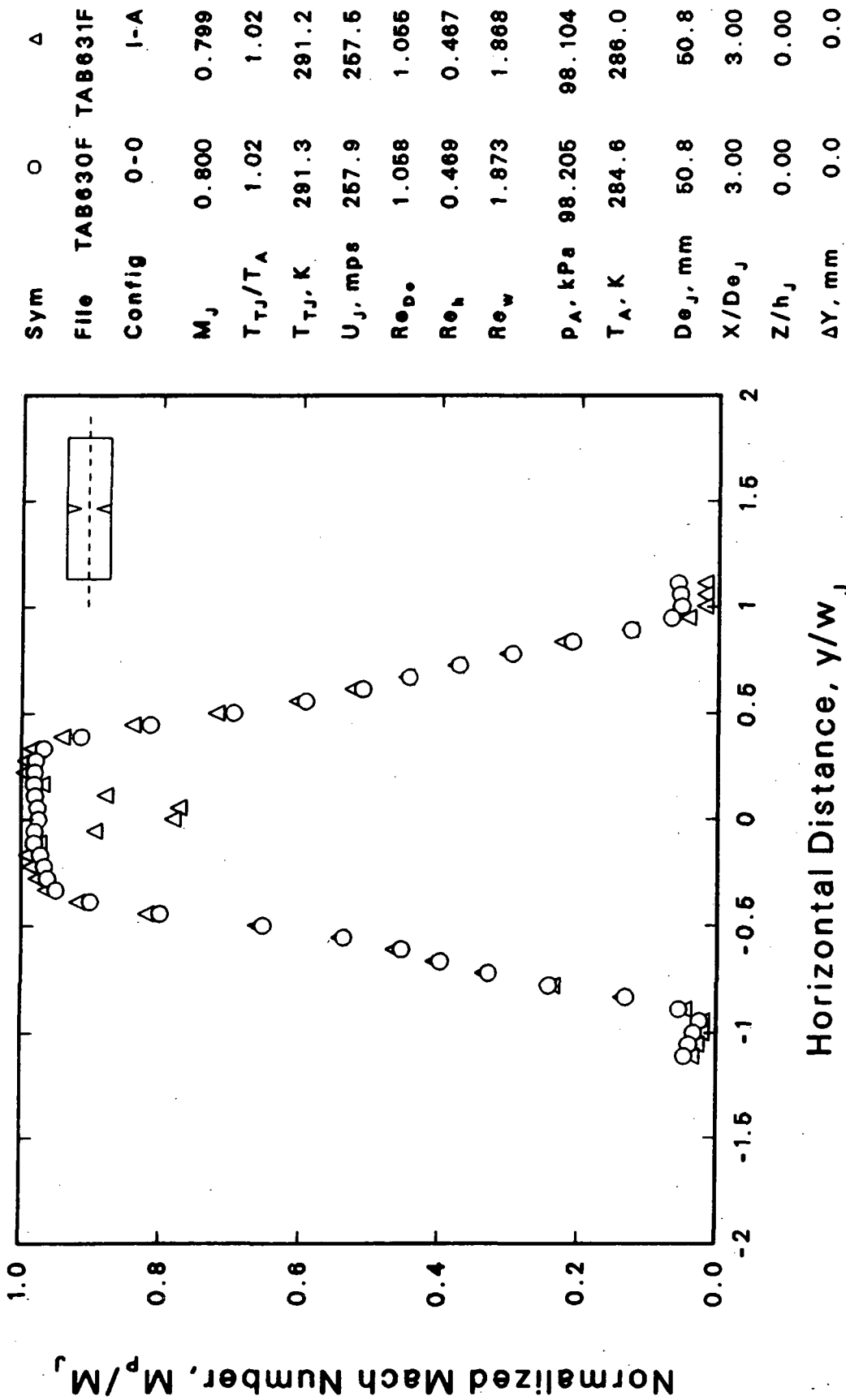


Figure B-7 Horizontal Mach Number Profile, Tab A
 $M_J = 0.8$, $T_J/T_0 = 1$, $X/D\epsilon = 3$

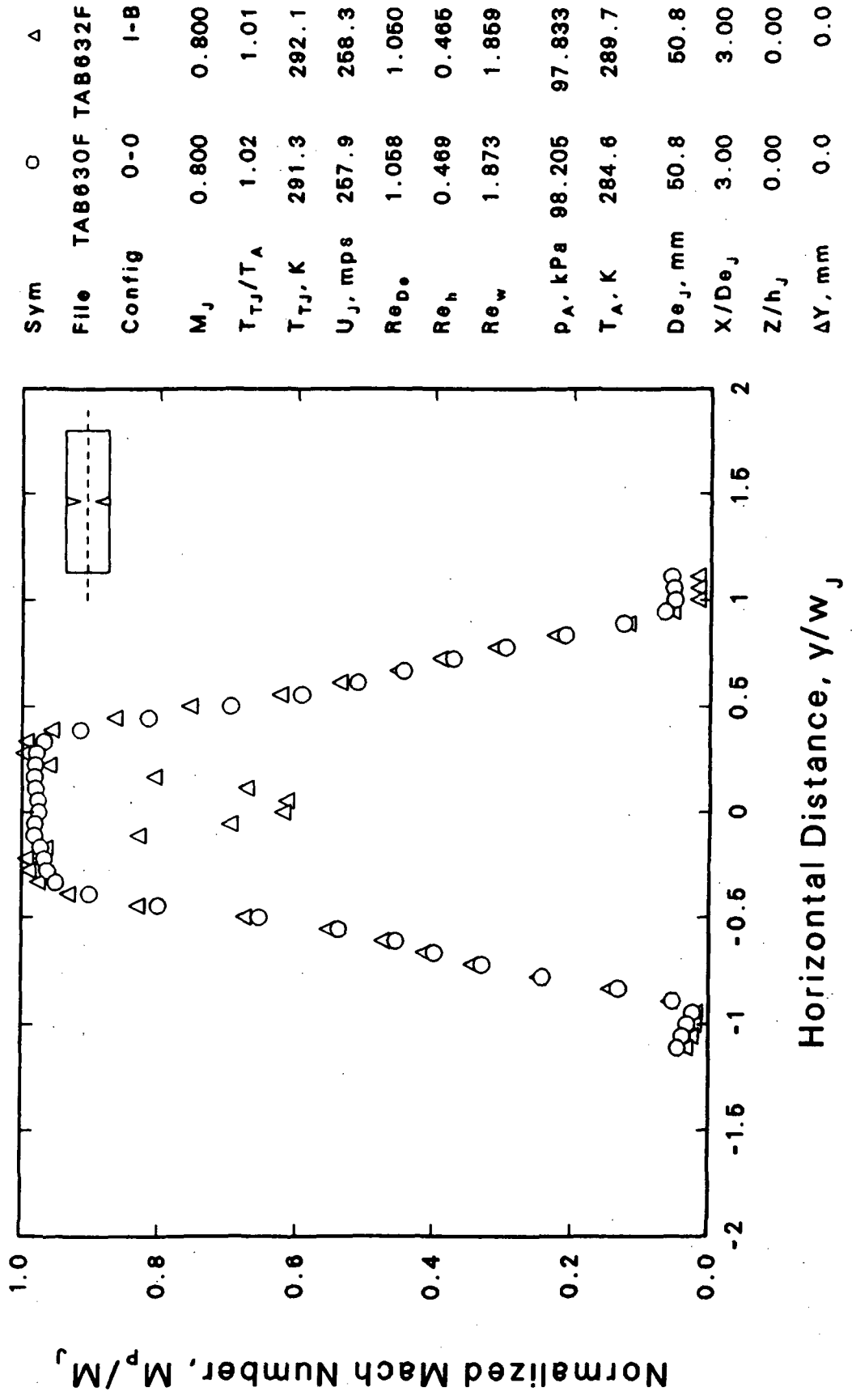


Figure B-8 Horizontal Mach Number Profile, Tab B
 $M_J = 0.8$, $T_J/T_0 = 1$, $X/De = 3$

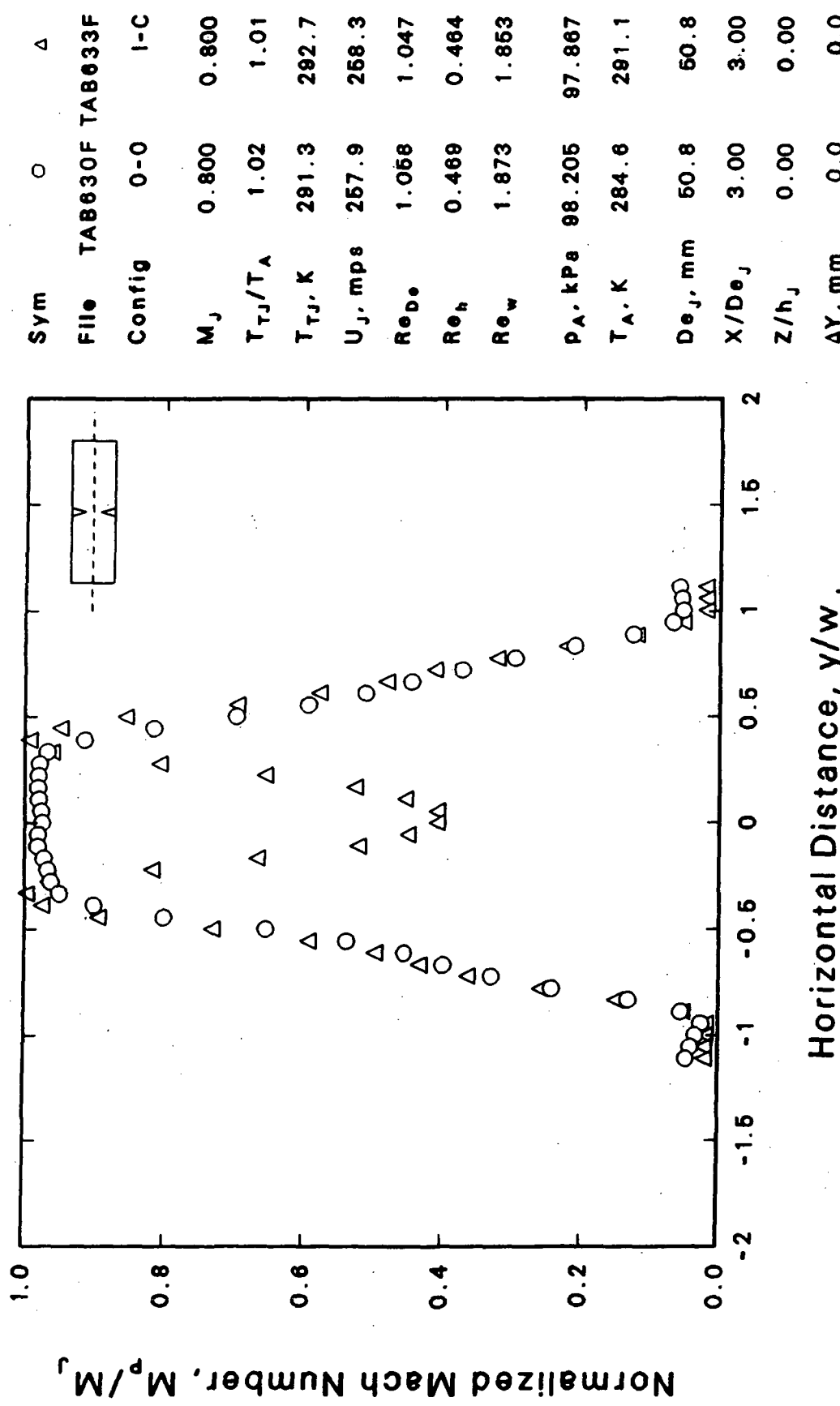


Figure B-9 Horizontal Mach Number Profile, Tab C
 $M_J = 0.8$, $T_J/T_0 = 1$, $X/De = 3$

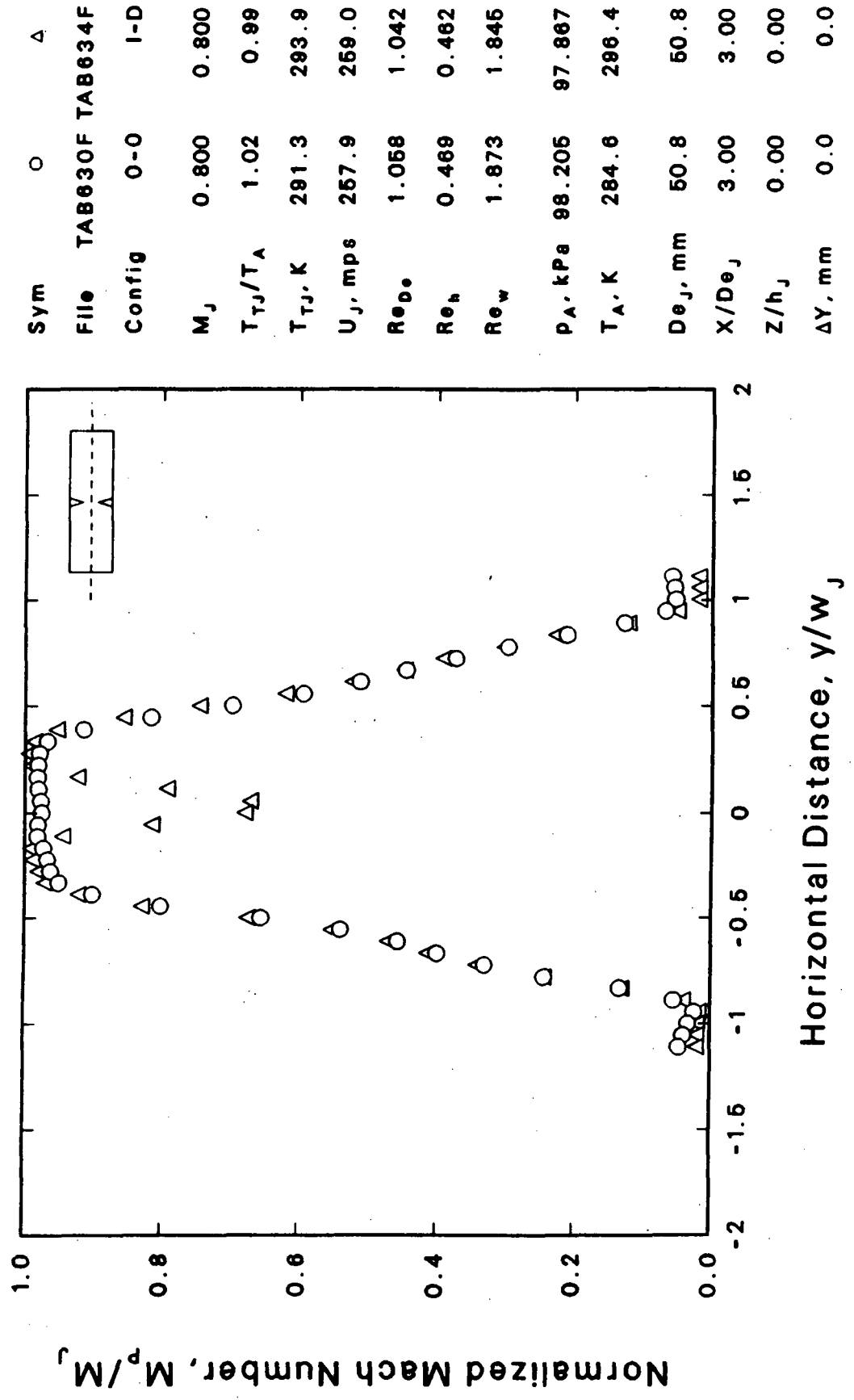


Figure B-10 Horizontal Mach Number Profile, Tab D
 $M_j = 0.8$, $T_j/T_0 = 1$, $X/D\epsilon = 3$

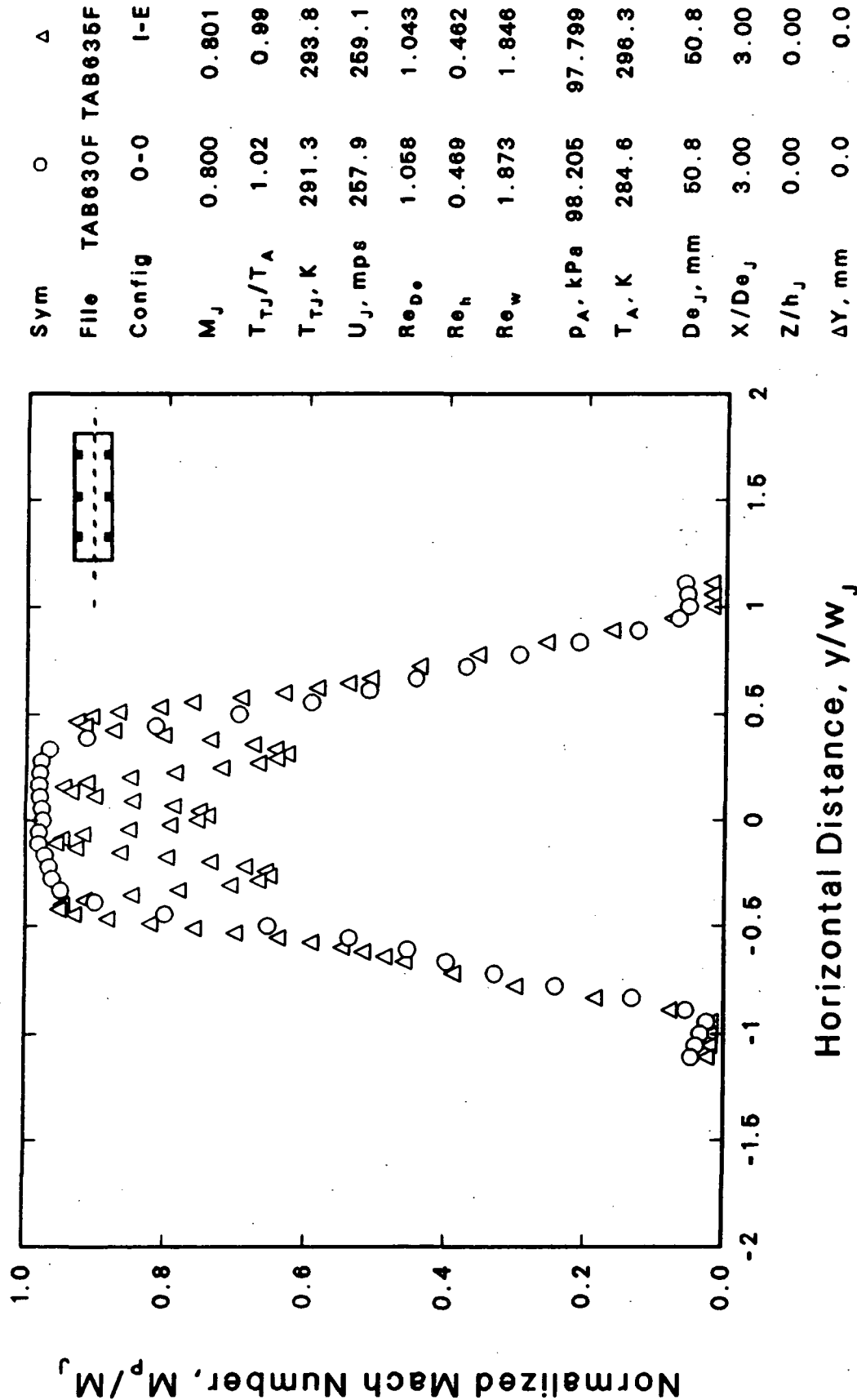


Figure B-11 Horizontal Mach Number Profile, Tab E
 $M_j = 0.8$, $T_j/T_0 = 1$, $X/De = 3$

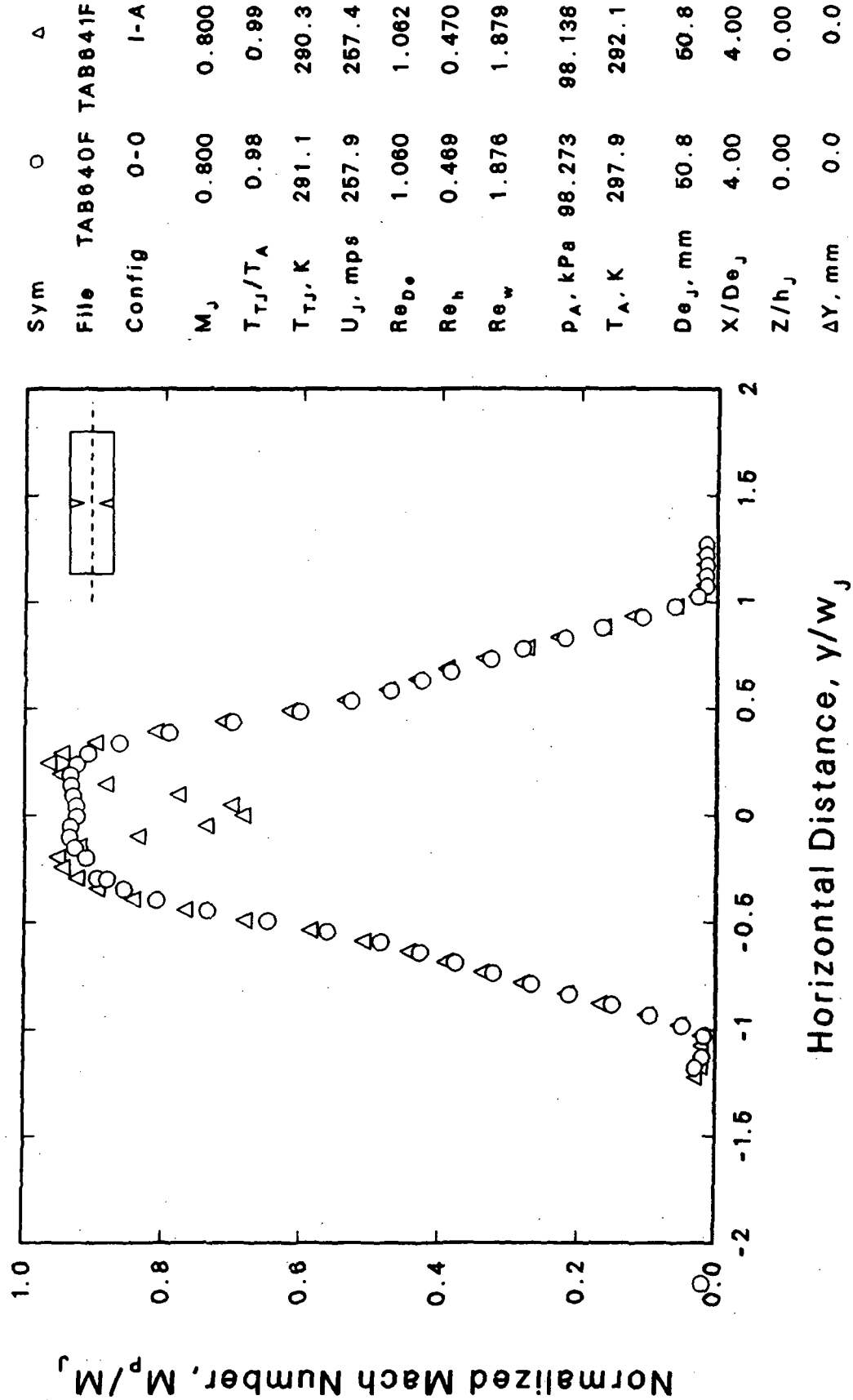


Figure B-12 Horizontal Mach Number Profile, Tab A
 $M_j = 0.8$, $T_j/T_0 = 1$, $X/D\epsilon = 4$

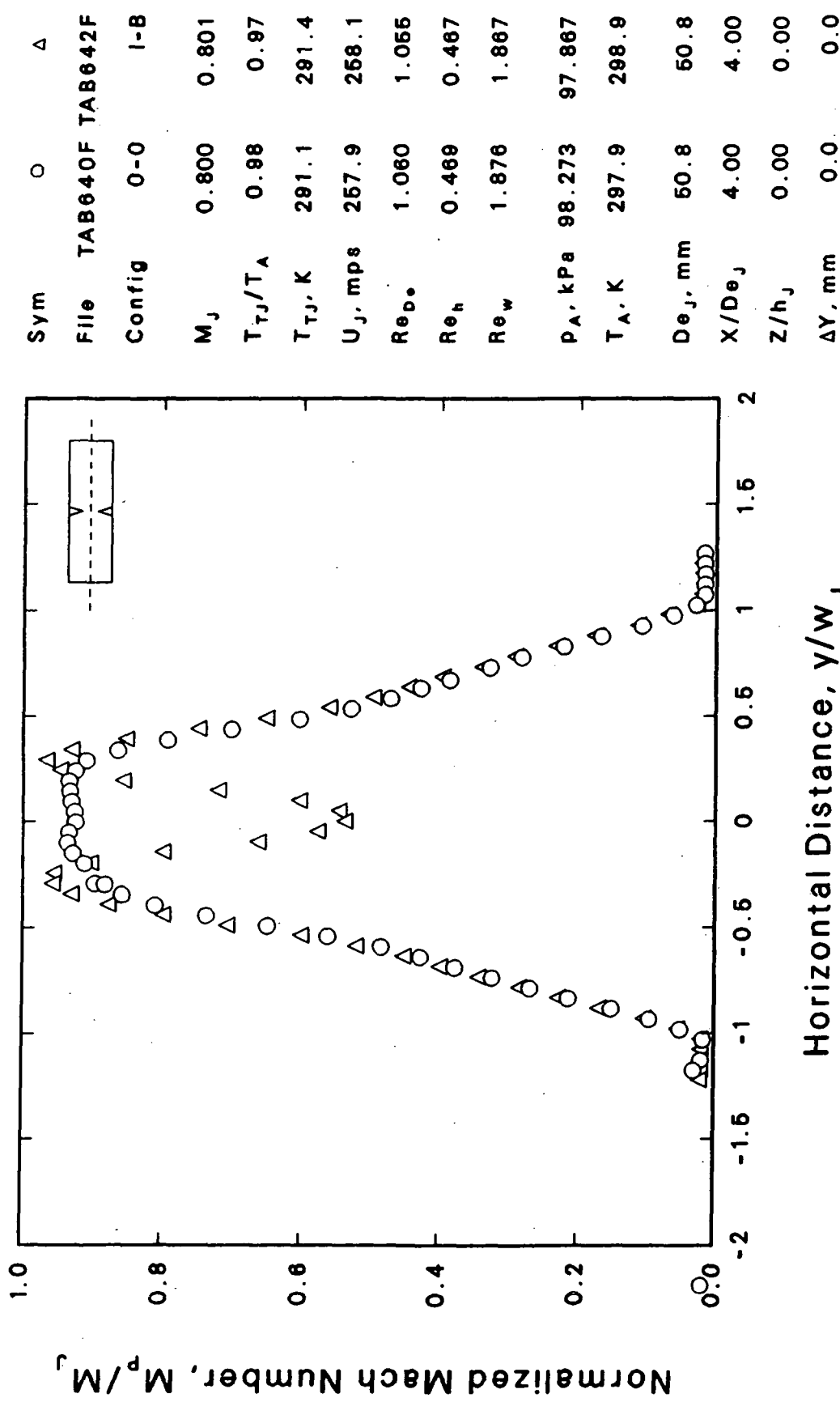


Figure B-13 Horizontal Mach Number Profile, Tab B
 $M_j = 0.8$, $T_j/T_0 = 1$, $X/De = 4$

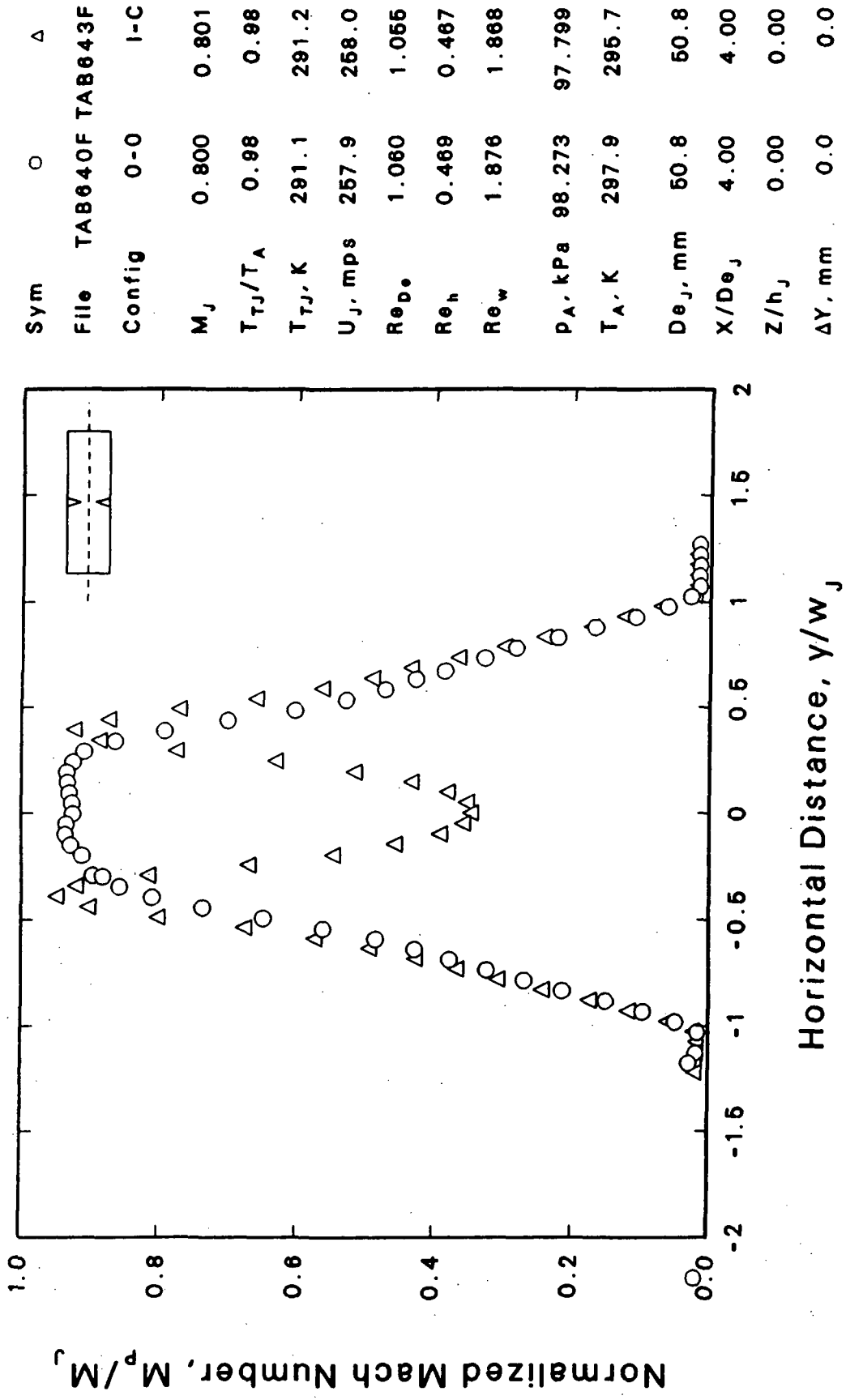


Figure B-14 Horizontal Mach Number Profile, Tab C
 $M_j = 0.8$, $T_j/T_0 = 1$, $X/De = 4$

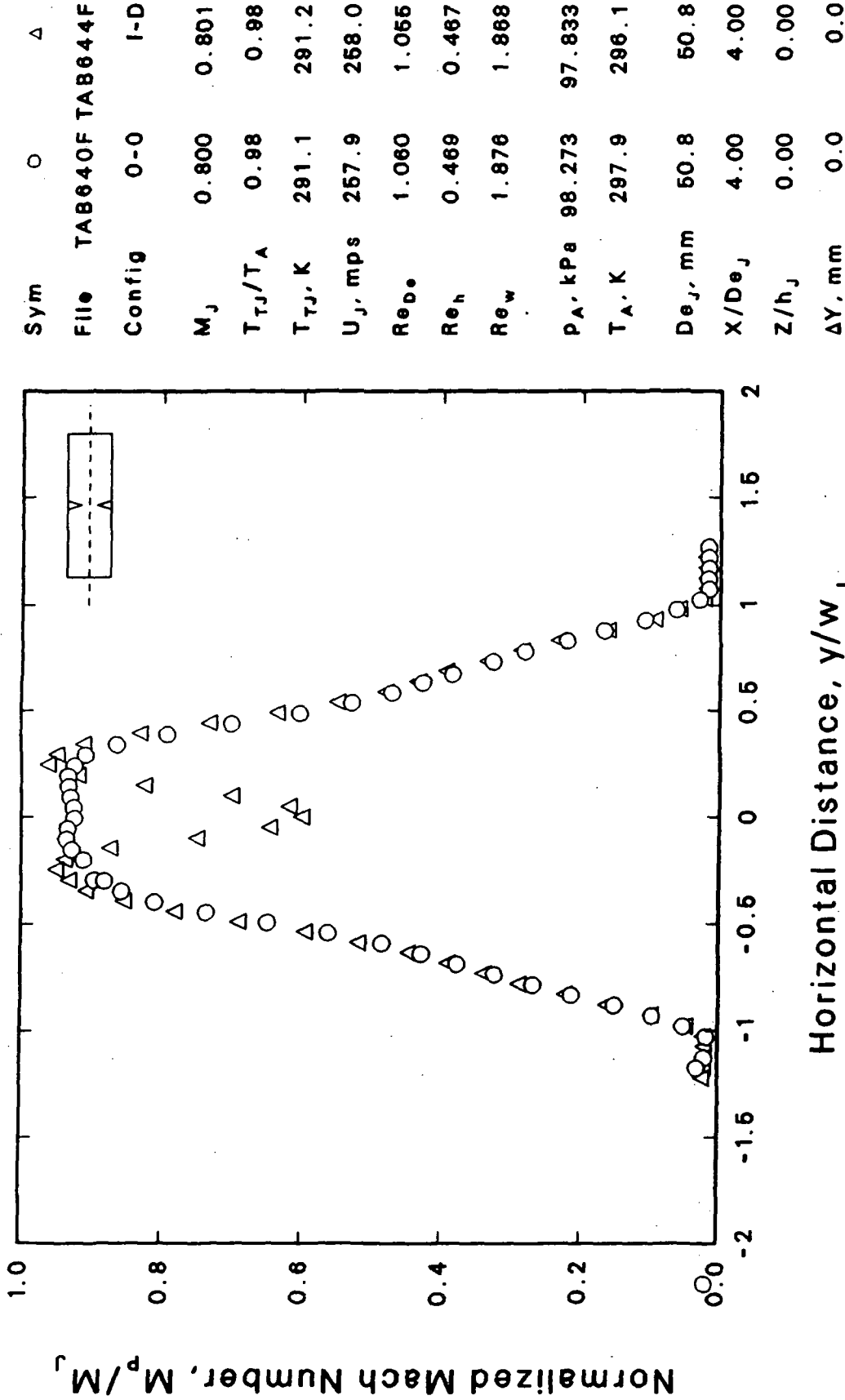


Figure B-15 Horizontal Mach Number Profile, Tab D
 $M_J = 0.8, T_J/T_0 = 1, X/D\epsilon = 4$

Sym	O	Δ
File	TAB660F TAB661F	
Config	0-0	I-A
M_J	0.800	0.800
T_{TJ}/T_A	1.00	1.00
T_{TJ}, K	294.6	294.2
$U_J, \text{ mps}$	269.3	269.1
Re_D	1.028	1.042
Re_h	0.466	0.461
Re_w	1.820	1.844
$p_A, \text{ kPa}$	96.918	98.002
T_A, K	296.1	295.4
$D_{ej}, \text{ mm}$	60.8	60.8
X/De_j	5.00	5.00
Z/h_J	0.00	0.00
$\Delta Y, \text{ mm}$	0.0	0.0

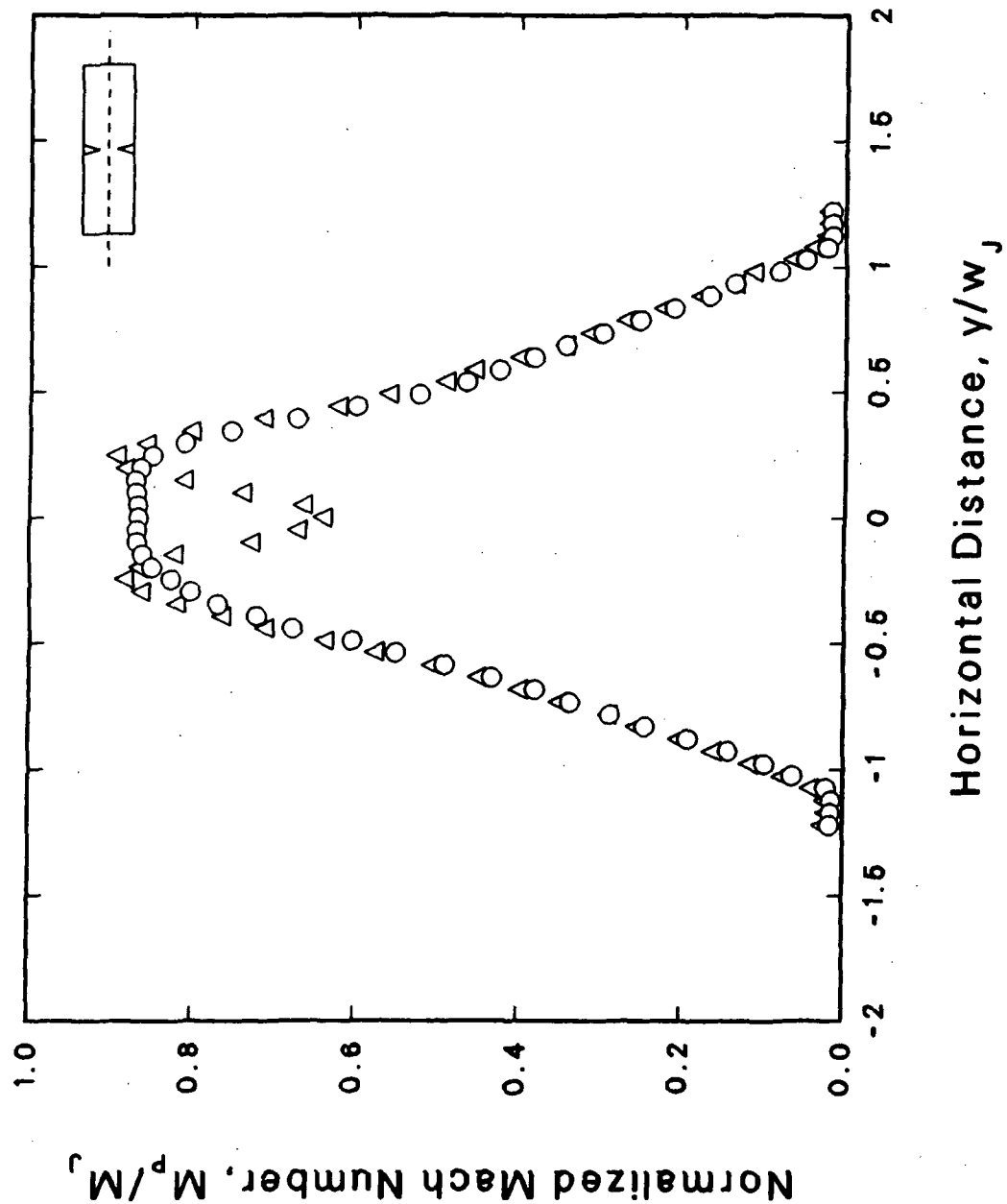


Figure B-16 Horizontal Mach Number Profile, Tab A
 $M_J = 0.8$, $T_J/T_0 = 1$, $X/De = 5$

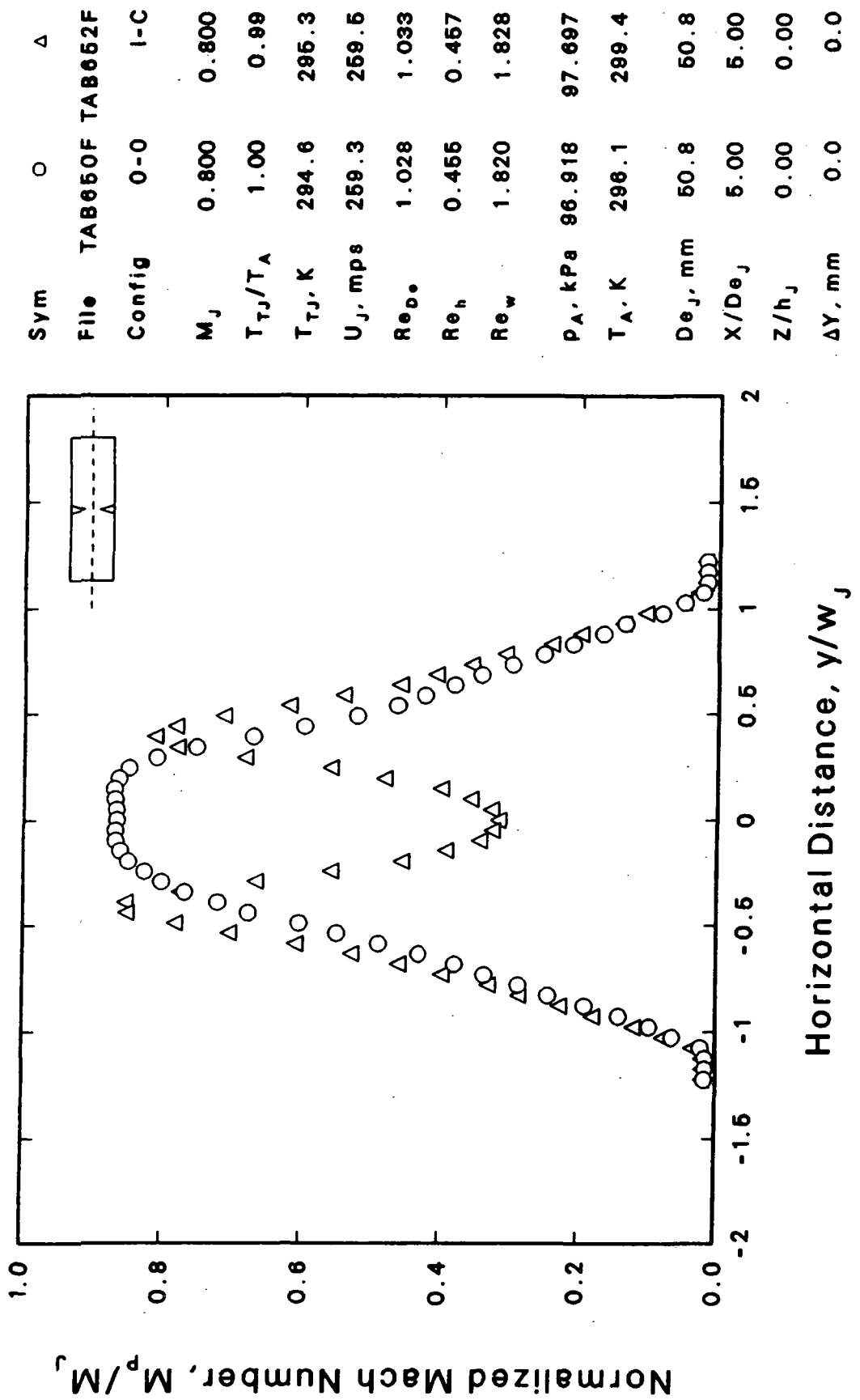


Figure B-17 Horizontal Mach Number Profile Tab C
 $M_j = 0.8$, $T_j/T_0 = 1$, $X/D\theta = 5$

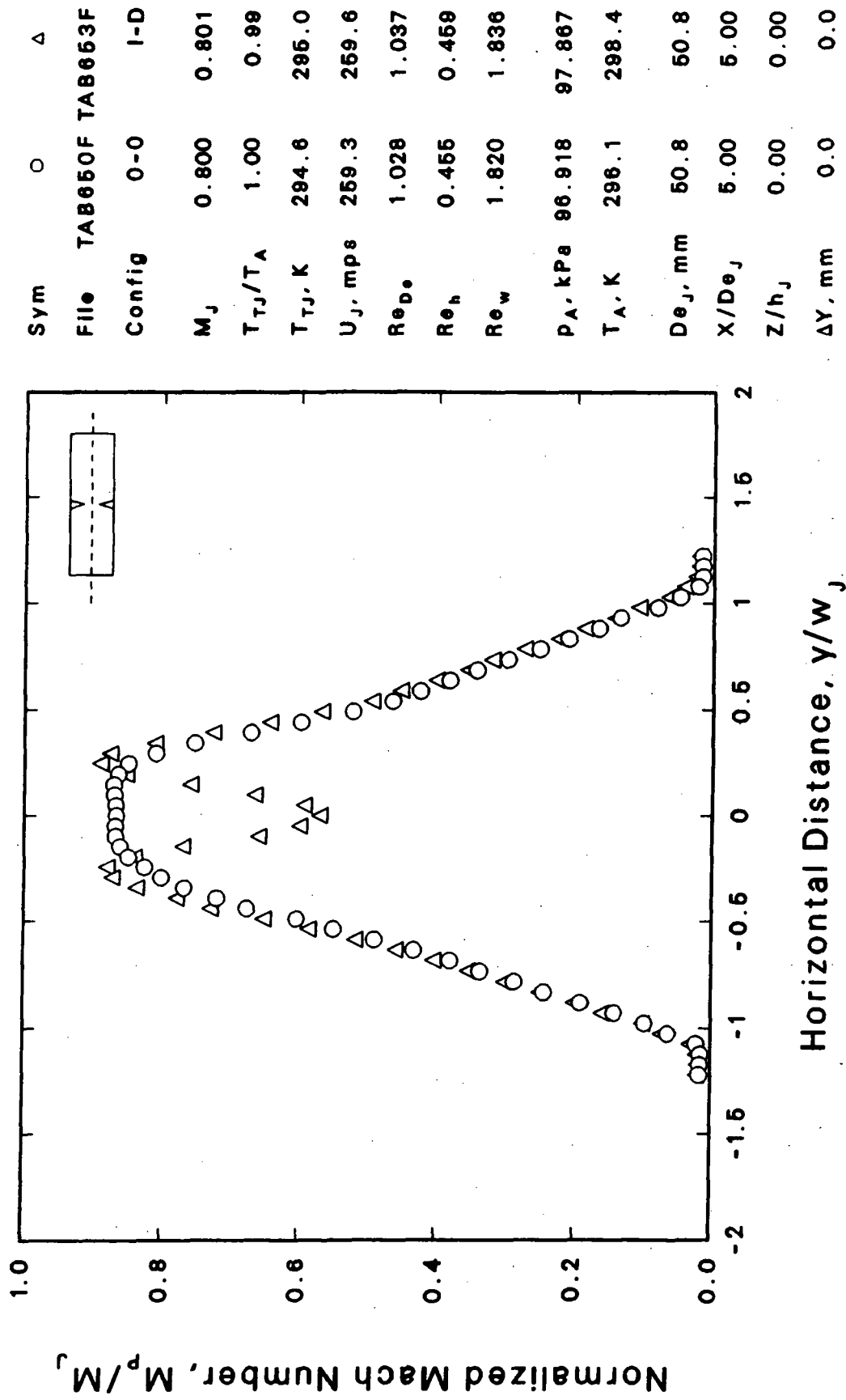


Figure B-18 Horizontal Mach Number Profile, Tab D
 $M_j = 0.8$, $T_j/T_0 = 1$, $X/De = 5$

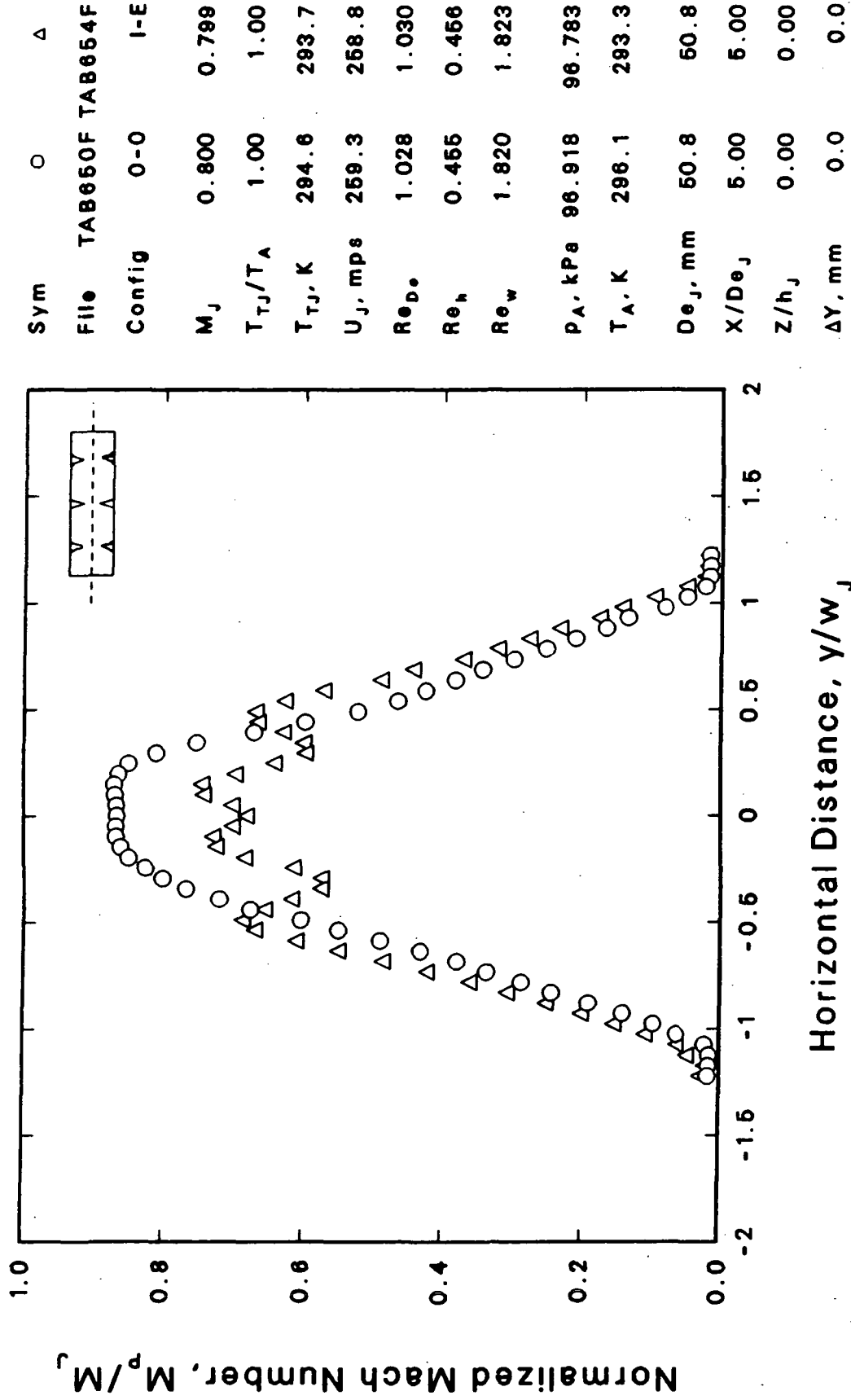


Figure B-19 Horizontal Mach Number Profile, Tab E
 $M_j = 0.8$, $T_j/T_0 = 1$, $X/D_\theta = 5$

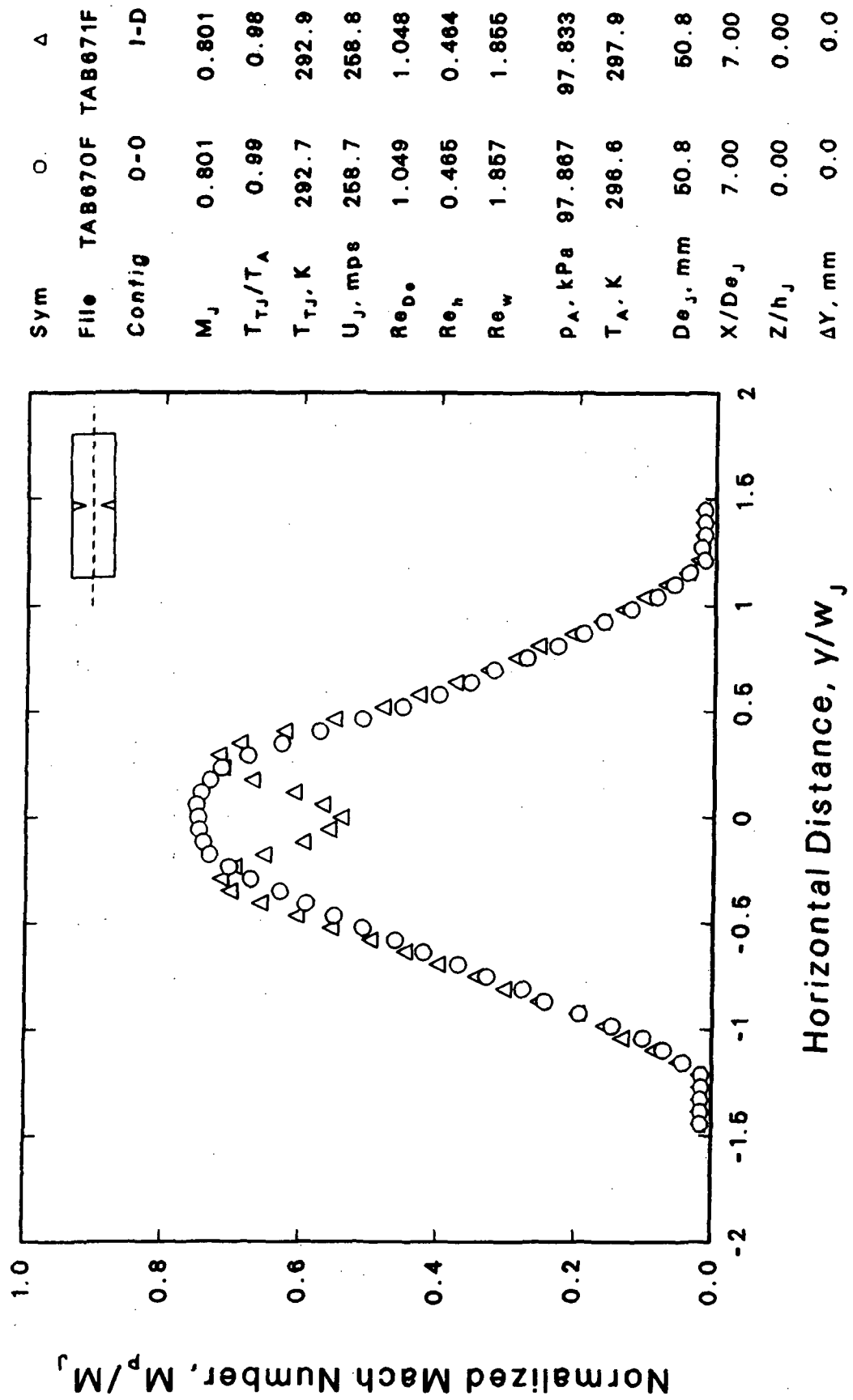


Figure B-20 Horizontal Mach Number Profile, Tab D
 $M_j = 0.8$, $T_j/T_0 = 1$, $X/D\epsilon = 7$

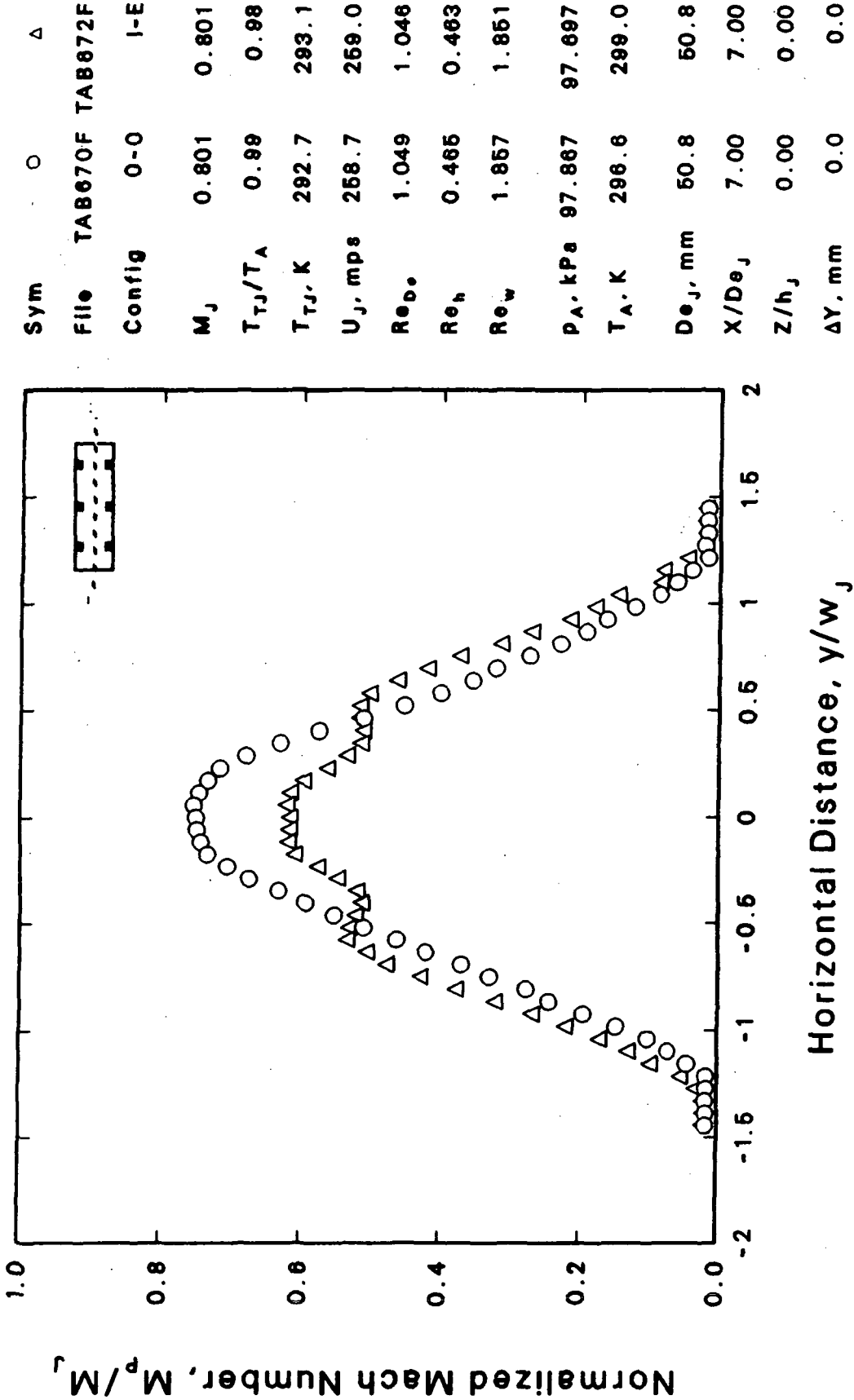


Figure B-21 Horizontal Mach Number Profile, Tab E
 $M_J = 0.8$, $T_J/T_0 = 1$, $X/D_{\bullet} = 7$

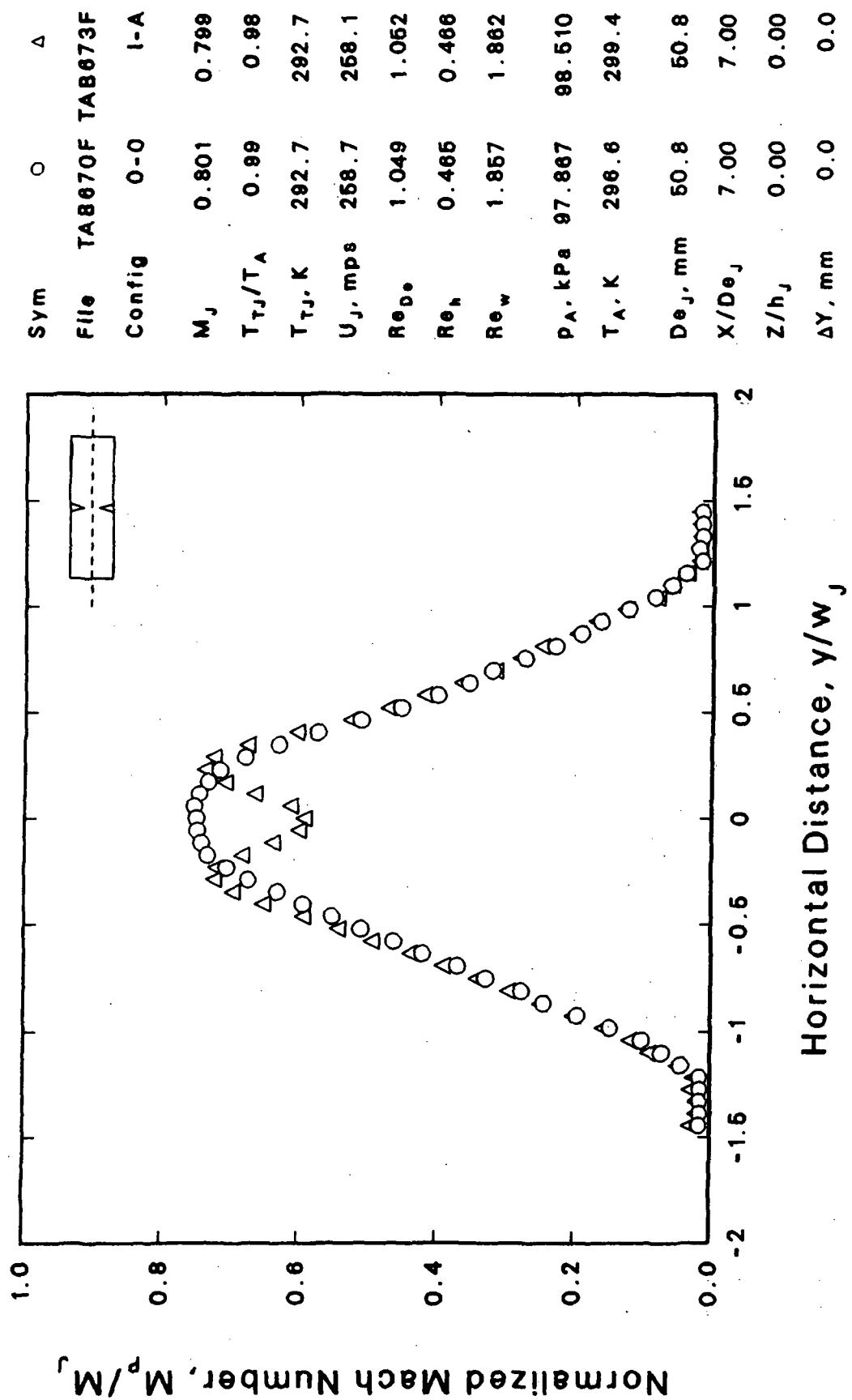


Figure B-22 Horizontal Mach Number Profile, Tab A
 $M_j = 0.8$, $T_{j/T_0} = 1$, $X/D\theta = 7$

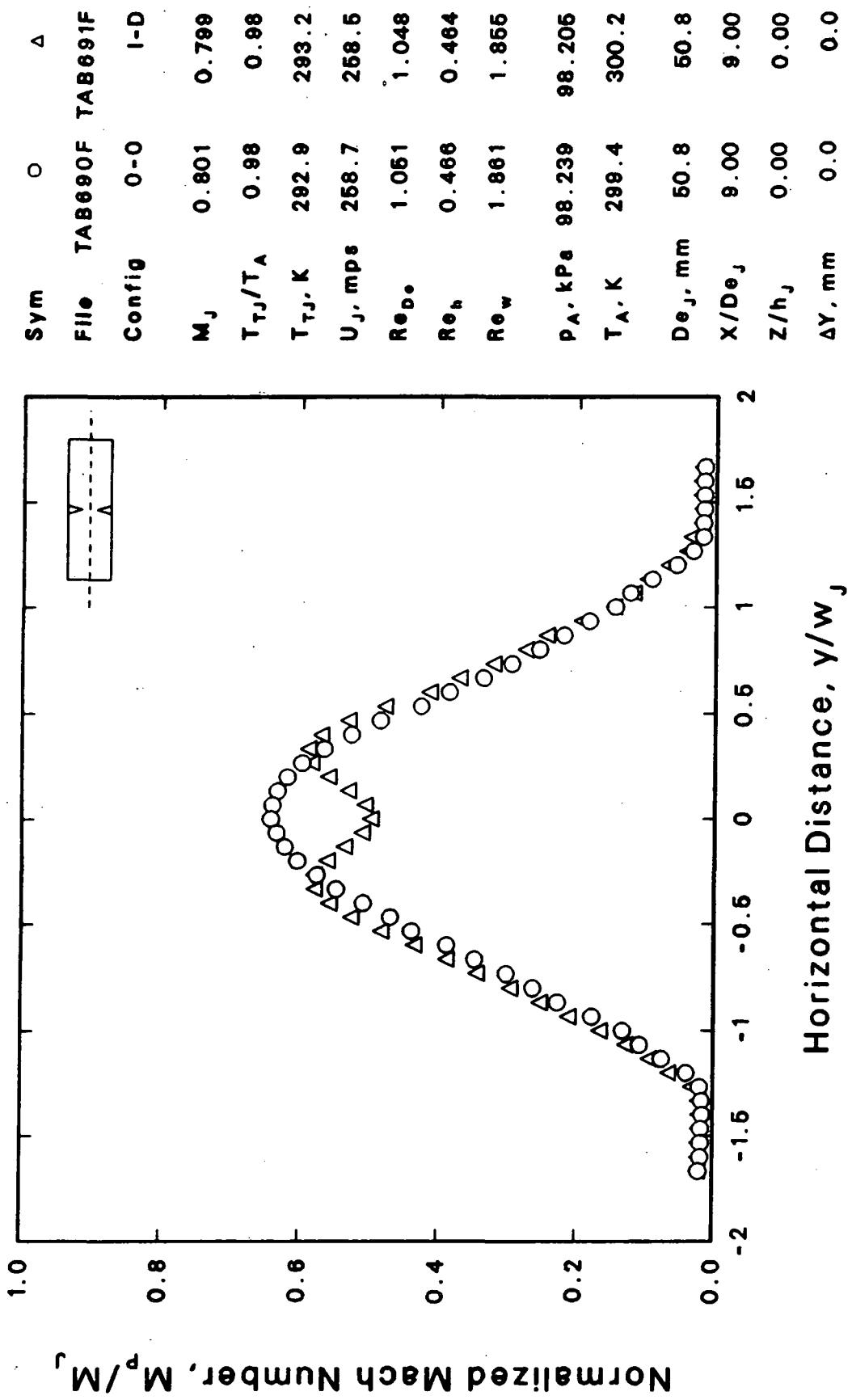


Figure B-23 Horizontal Mach Number Profile, Tab D
 $M_j = 0.8$, $T_j/T_0 = 1$, $X/De = 9$

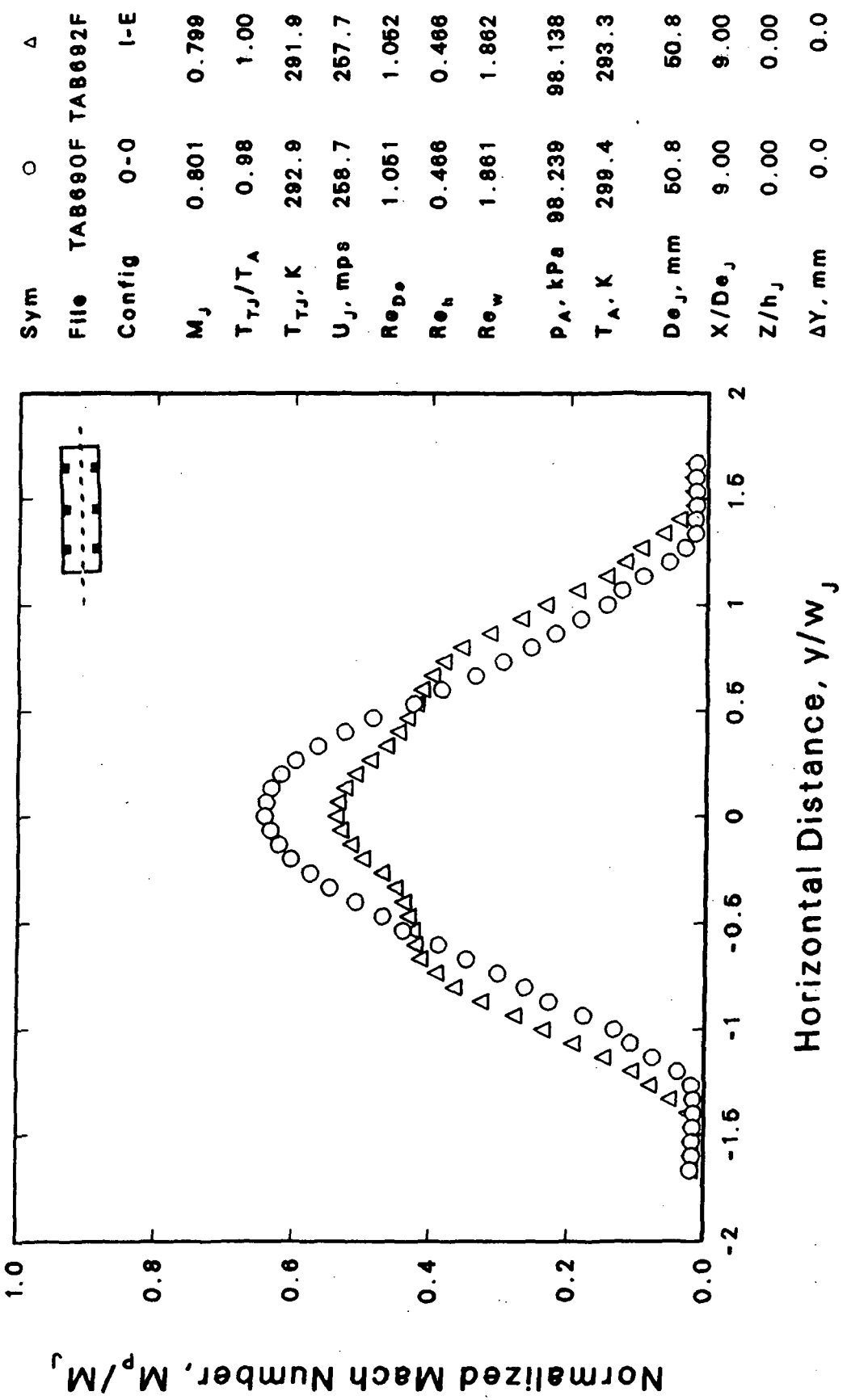


Figure B-24 Horizontal Mach Number Profile, Tab E
 $M_i = 0.8$, $T_{rj}/T_0 = 1$, $X/De = 9$

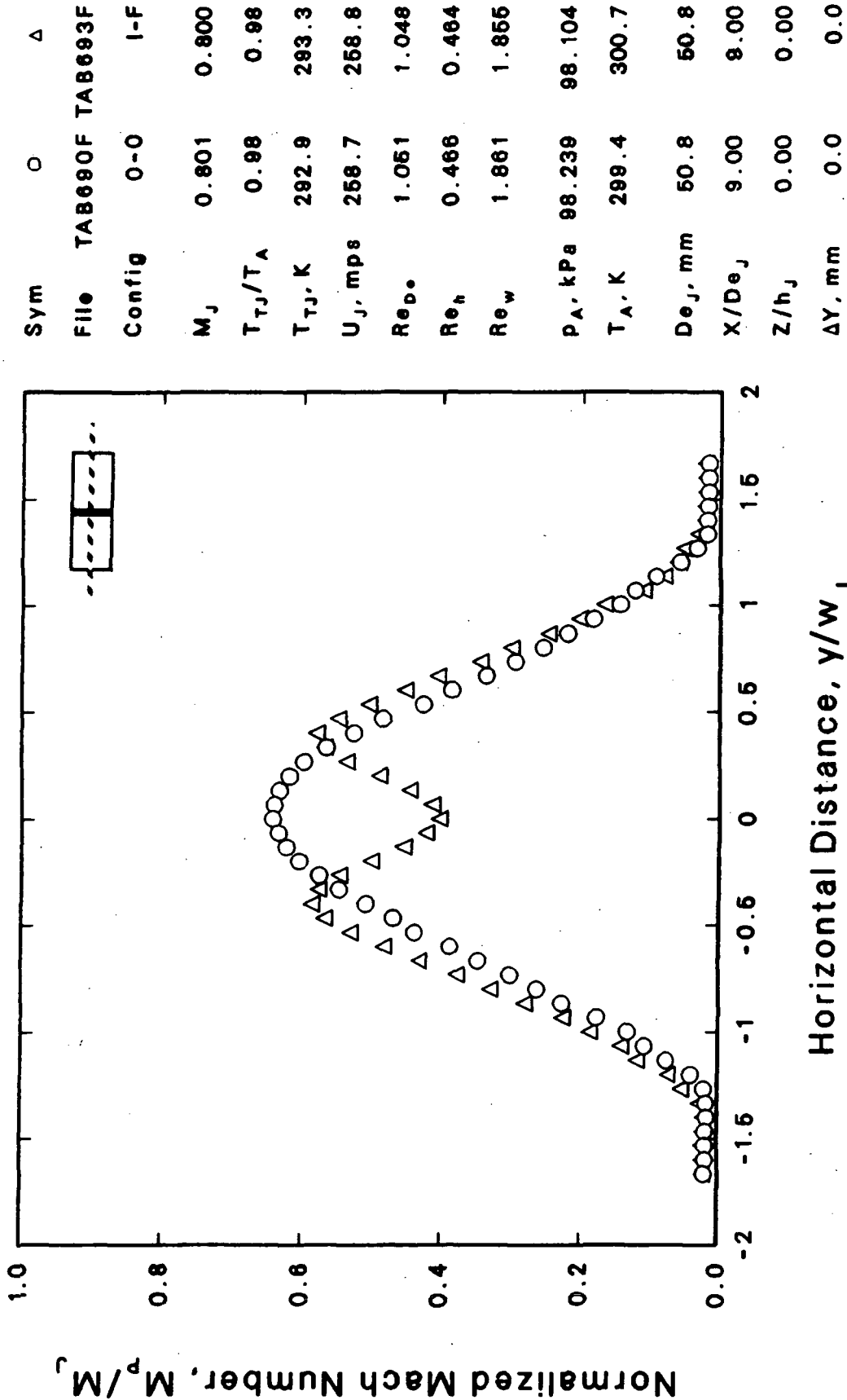


Figure B-25 Horizontal Mach Number Profile, Tab F
 $M_j = 0.8$, $T_j/T_0 = 1$, $X/De = 9$

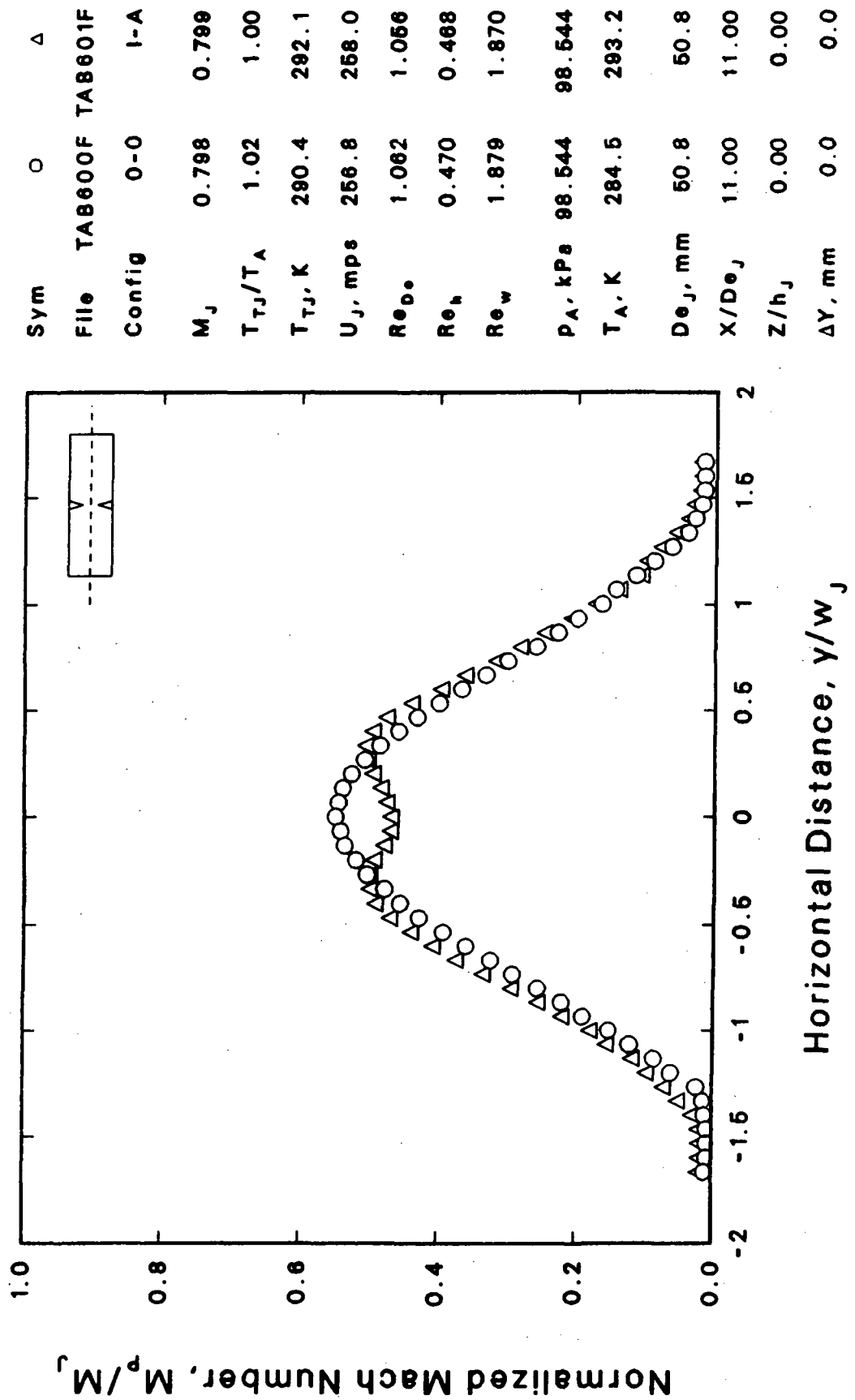


Figure B-26 Horizontal Mach Number Profile, Tab A
 $M_j = 0.8$, $T_j/T_0 = 1$, $X/D_{ej} = 11$

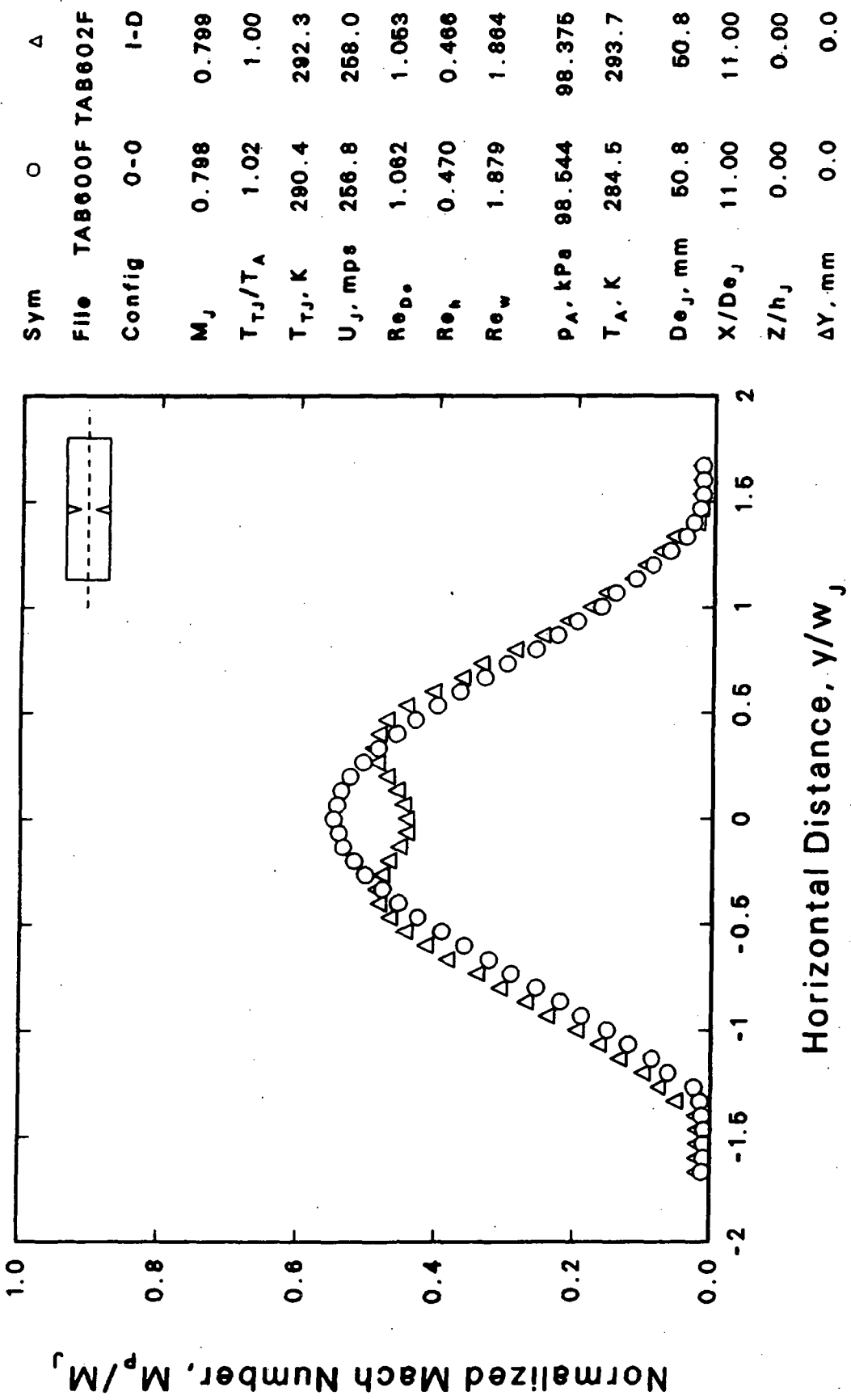


Figure B-27 Horizontal Mach Number Profile, Tab D
 $M_j = 0.8$, $T_j/T_0 = 1$, $X/De = 11$

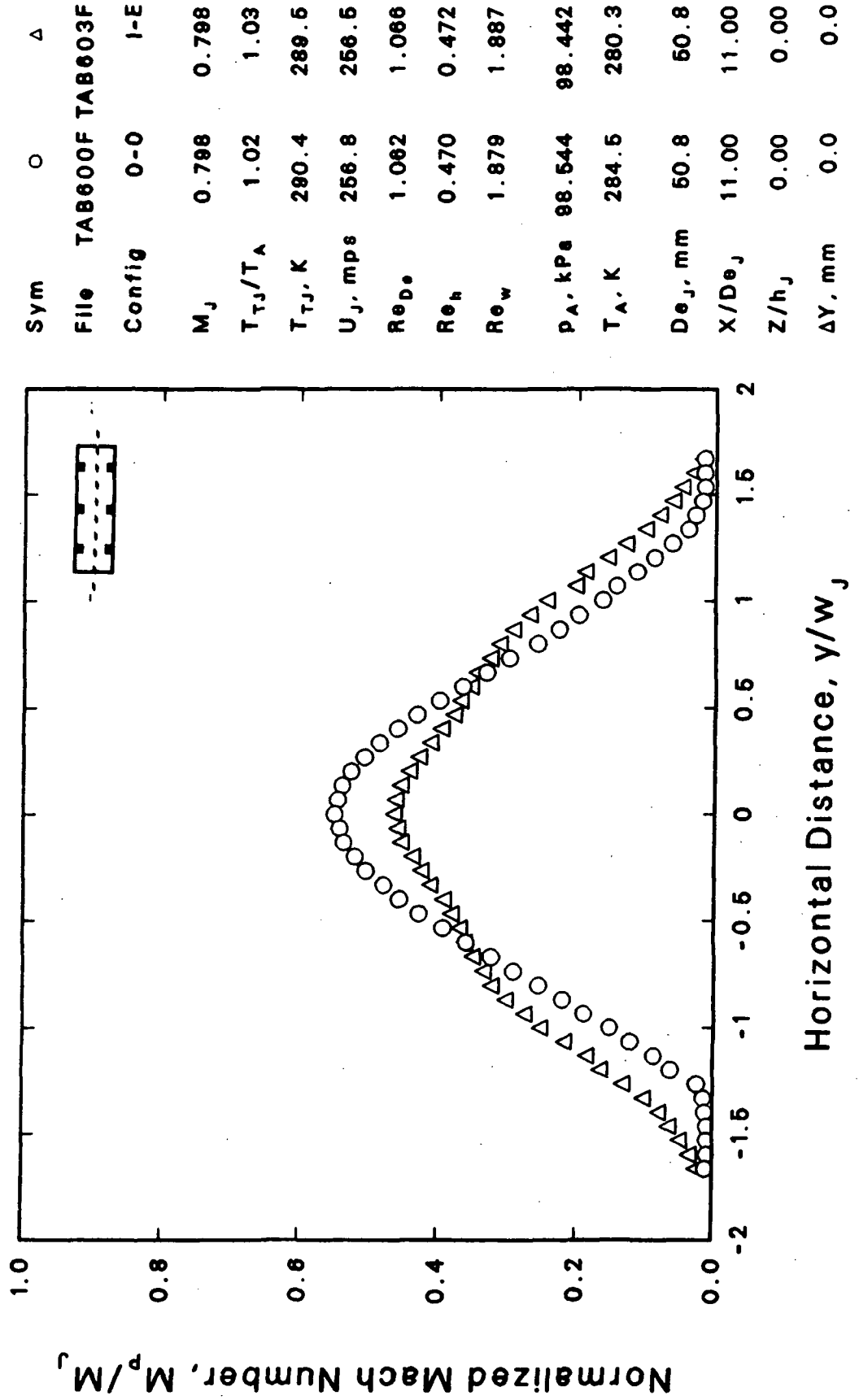


Figure B-28 Horizontal Mach Number Profile, Tab E
 $M_j = 0.8$, $T_j/T_0 = 1$, $X/De = 11$



National Aeronautics and
Space Administration

Report Documentation Page

1. Report No. NASA CR-185207	2. Government Accession No.	3. Recipient's Catalog No.	
4. Title and Subtitle Enhancement of Mixing in a Rectangular Jet by Mechanical Tabs		5. Report Date	
		6. Performing Organization Code A-8402	
7. Author(s) W.H. Brown and K.K. Ahuja		8. Performing Organization Report No.	
		10. Work Unit No. 505-62	
9. Performing Organization Name and Address Georgia Tech Research Institute Georgia Institute of Technology Atlanta, Georgia 30332		11. Contract or Grant No. NAG3-1062	
12. Sponsoring Agency Name and Address National Aeronautics and Space Administration Lewis Research Center 21000 Brookpark Road Cleveland, Ohio 44135		13. Type of Report and Period Covered Grant Report	
15. Supplementary Notes Project Manager, Michael R. Vanco, Propulsion Systems Division, NASA Lewis Research Center.			
16. Abstract This effort was conducted to obtain additional test data/configurations required to better understand the effects of tab length and width on jet mixing enhancement for a rectangular nozzle. The configurations tested were a six-tab configuration defined by NASA, a full-height tab configuration, and two-tab configurations with selected tab lengths and widths. Additional test data were also required for all candidate configurations to better interpret the data. This report presents test data from this effort. On the basis of these data, the following general observations were noted: <i>ARR PRELIMINARY</i> <ol style="list-style-type: none">1. The six-tab rectangular nozzle configuration provided a lower peak velocity than either the two-tab or four-tab configuration; <i>AND</i>2. The rectangular nozzle with a full-height tab had about the same peak velocity as the two-tab configuration; however, the full-height tab configuration had a somewhat lower centerline velocity.			
17. Key Words (Suggested by Author(s)) Jet mixing Shear flow Nozzle flow			
		Date for general release <u>March 1994</u> Subject Category <u>02</u>	
19. Security Classif. (of this report) Unclassified	20. Security Classif. (of this page) Unclassified	21. No. of pages 80	22. Price* A05

National Aeronautics and
Space Administration

Lewis Research Center
Cleveland, Ohio 44135

FOURTH CLASS MAIL

ADDRESS CORRECTION REQUESTED

Official Business
Penalty for Private Use \$300



Postage and Fees Paid
National Aeronautics and
Space Administration
NASA-451

NASA
